Simple and robust ion-selective electrodes for bio/environmental analysis

Tolulope Andrew Fayose

Thesis submitted for the degree of Doctor of Philosophy

Keele University

December 2018

Thesis summary

Chemical sensors have gone through a lot of optimisation renaissance over the years to have come from a typical bench-top tool for measurements of ions in standard solutions, to a more promising analytical technique capable of measuring the activities of free un-complexed nutrients in environmentally and biologically important samples. With various health issues arising due to the increasing anthropogenic contributions of man to the environment amongst other factors, and due to the need for more routine analysis especially do-it-yourself (DIY) of several analytes in physiological samples for clinical purposes, it is therefore imperative that simple, cheap, but robust sensors are developed, and optimised to meet these emerging needs.

First part of this work involved fabricating solid-contact ion selective electrodes (SC-ISEs) based on the mechanical abrasion of graphite on easily modified acetate paper. Similarly results from the impedance spectra and the water layer test for electrodes with or without a conducting polymer (CP) layer indicated the suitability of the procedure. The fabricated paper electrodes importantly showed fast response time and great potential stability over the course of fourteen days. The same fabrication methodology was used to produce stable and functional solid-state paper reference electrode, and then, combined with other graphite-based paper ISEs to yield a single-strip solid contact electrode for simultaneous measurements of nitrate and ammonium in environmental samples. Satisfactory results from the comparison of measured concentrations by potentiometry and standard reference methods indicated this simplified electrode platform, designed from household materials can be used as a cheaper alternative to other solid contact electrodes.

Subsequent works in this thesis involved the application of the fabricated SC-ISEs in optimization of measurement procedures of environmentally important nutrients and biologically important analytes.

Routine monitoring of reactive nitrogen Nr (majorly NH_4^+ and NO_3^-) in environmental samples including soils from major land types is important to soil management system. In achieving a relatively rapid turn-around time of analysis, inorganic N species were extracted from various soil types using a single extracting solution (0.1 M $MgSO_4$). Extractable-NH_4^+ and -NO_3^- in soils, and bioavailable NH_4^+ and NO_3^- in water samples measured concurrently using paper ISEs showed similar results to standard analytical methods.

The analysis of urinary iodine (UI) is important to the public health due to serious health issues attached to its deficiency. As a result, iodide-selective electrodes based on [9] Mercuracarborand-3 (MC3) and [12] Mercuracarborand-4 (MC4) as ionophores, and NPOE and DOS as plasticizers were developed with a view to evaluate the concentration of iodide in urine.

However, ion-selective electrodes (ISEs) are one of the very few experimental techniques whose limit of detection (LOD) is not defined as signal-to-noise ratio. As a result, the Bayesian model was applied to estimate the activities of nitrate and ammonium in soil and water samples, and iodide in urine samples. While the Bayesian estimates for nitrate and ammonium ions were satisfactory, significant discrepancy of estimated results for iodide in urine shows more work needs to be done in relation to designing more selective ionophores to complement non-linear approaches.

Dedicated to the Glory of God

Acknowledgements

I am most grateful to my supervisors, Dr. Aleksandar Radu and Dr. Sami Ullah, for their tremendous help and guidance throughout my doctoral research. I have enjoyed every moment right from my first interview day till post-submission. The trainings and supports I have learnt from working with you will forever remain part of me. I definitely would not have made it without you.

I also would like to thank staff from the School of Chemical and Physical Sciences, and the School of Geography, Geology and the Environment, Keele University, especially the laboratory staff who always made sure I got my orders without any hassle. I really owe it to you.

I personally would love to thank every member of Dr. Karin Chumbimuni-Torres' team from the University of Central Florida, Orlando, you all made my secondment really interesting. It was nice working with you all.

Importantly, I reserve special gratitude to my parents (Engr and Mrs Fayose), who have been extremely supportive since this dream started. I hope I will, one day be able to repay that kindness.

I would like to specially thank my lovely and caring wife, Folashade Fayose who has been very generous and patient in understanding the demands of the programme. She definitely deserves this Ph.D. as much as I do for her sacrifice. I love you so much.

My unreserved gratitude goes to my cute little jewels (Nathaniel and Daniel). Hopefully someday you would realise you enormously counted towards this project. Daddy loves you.

I cannot thank enough my adorable sisters (Oluwatosin Akinduyite, Oluwakemi Fasomoyin and Oluwafunmilayo Fayose) for being there to support countlessly.

To my inspirational uncle (Dr. Sola Fayose), whom I get so much motivation from, my nephews and niece, numerous uncles, aunts and cousins, who I really can't mention here because of space. Thanks all for your supports.

Also my appreciation goes to the family of Mr and Mrs Aloba, you really made this possible, God bless you all.

I finally thank all my friends for being there when the going was tough, God bless you all.

Papers published in the course of this project include:

1. Mendecki, L.; **Fayose, T**.; Stockmal, K. A.; Wei, J.; Granados-Focil, S.; McGraw, C. M.; Radu, A. *Anal*. *Chem*. 2015, 87 (15), 7515−7518.
2. **Fayose, T**.; Mendecki, L.; Ullah, S.; Radu, A. *Anal*. *Methods*, 2017, (9), 1213-1220.

Table of Contents

List of Figures

List of Tables

Chapter 1 Introduction

1.1 An overview of chemical sensors

A system interacts, in other words, senses its environment through a sensing medium. Such system – environment relationships can be likened to our earth - ecosystems link, whereby activities existing on various ecosystems can be felt, and responded to by the earth. A closer, but rather fairly-less complex sensing profile is how the human body responds to various parameters like: noise, taste, temperature, pressure, stress, emotion, knowledge etc.

Therefore chemical sensing will involve the transfer of chemical information between different phases, for example, from within an environment into a chemical system.

Any device involved in such transfer of chemical species from a sample solution (the environment) into an analytically useful signal (the information) being processed by an analytical instrument like an electrochemical cell (the system), is referred to as a chemical sensor.[1] The four main types of electrochemical techniques include: potentiometry, ion-sensitive field-effect transition (ISFET), voltammetry and coulometry.

Potentiometric measurement which is the most commonly used of these techniques, involves the measurement of a potential (voltage) generated by a cell under essentially equilibrium condition.[2]

1.2 Ion-selective electrodes

Ion-selective electrodes (ISEs) belong to a group of chemical sensors primarily based on potentiometry, which estimates the activity of a specific ion dissolved in a solution by converting it into an electrical potential. This signal is then read by a voltmeter or pH meter. Figure 1.1 shows a schematic representative of an electrochemical set up which usually measures activities of un-complexed analyte from a given sample solution.

Typically, a suitable reference electrode is linked together with a working electrode either separately, or as a combined reference / working electrode to form a cell.

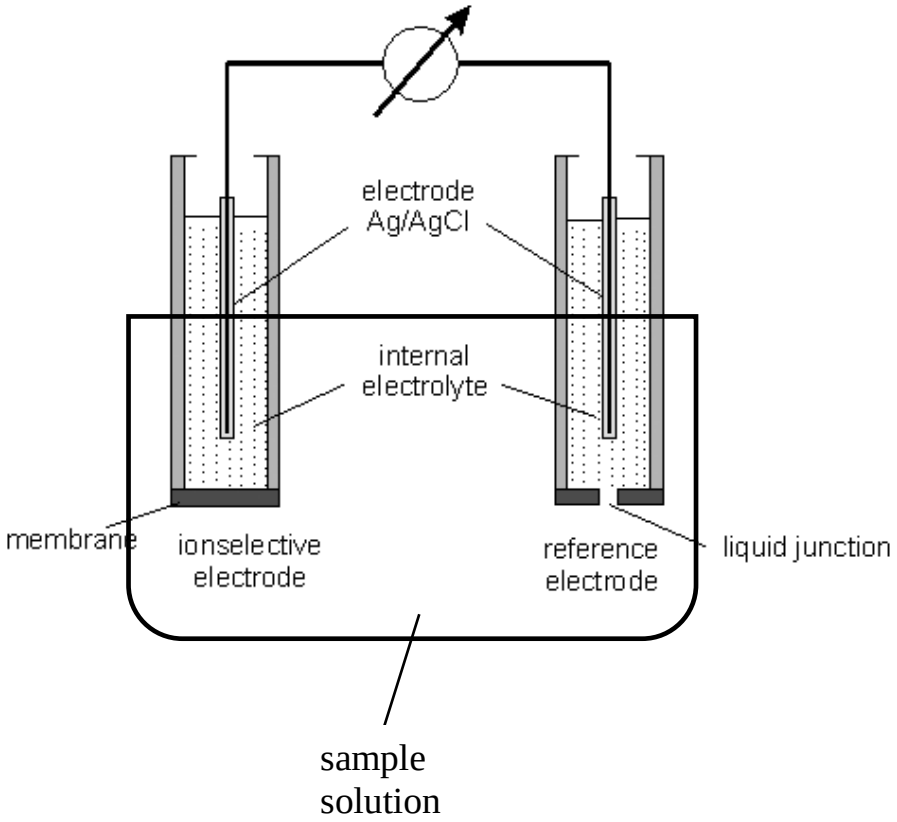

Figure 2.1 A schematic diagram of a typical liquid membrane ion-selective electrode.

1.2.1 Parts of an ion-selective electrode

An ion-selective electrode consists mainly of the membrane, the reference electrode, working electrode, reference solution and sample solution.

ISEs have been known to be classified based on the membrane types. Such membranes which could be glass, crystalline or polymeric, allow for the partitioning and diffusion of ions between different phases of the electrode system, and contains components specifically designed according to the ion of interest.[3] The reference electrode can either be a single-junction or double junction form of electrode system containing high concentration of stable salt solution which ensures constant potential change is attained. Common examples of such salt solutions are high concentration of KCl or LiOAc. The working electrode, also called the indicator electrode is a set-up that ensures adequate contact between an internal reference material (inner solution or solid contact) and ISE membrane. For polymeric ISEs, the working electrode is classified as either liquid-contact or solid-contact electrode depending on the internal reference material. And since the potential of the reference electrode is constant, it is the potential developed across the working electrode that dictates a measurement.

Historically, ion-selective electrode dates back to the original work of Max Cremer in 1906 when he reported the existence of an electrical potential (also known as electromotive force, EMF) developed across a glass membrane, and proportional to the pH difference across that membrane. This was followed by Walter Nernst's finding in the early 20th century where he found that at room temperature, a 10-fold increase in the activity of measured monovalent hydrogen ion of a glass electrode corresponded to 59.2mV change in EMF.[3] Analogously, as a result of chemical equilibrium also taking place across the surface of ion-selective membrane, ISE produce electrode

potential change against suitable reference electrode, and generally, the relationship known as the Nernst equation can be written as follows:

$$EMF = E° + \frac{RT}{ZiF} \ln ai \qquad (1.1)$$

Where *EMF* represents the electrical potential (in volts) developed across the reference electrode and the reference electrode, E° represents the cell standard potential (also in volts) at standard temperature T = 273 K. The activity and charge of ion primary ion i = a_i, and Z_i respectively. R and F represent the gas rate and Faraday's constants respectively.

1.2.2 Types of ISE

Ion selective electrodes can be classified into glass, crystalline or polymeric membrane based on their membrane type. The glass ISEs have been utilised for species like H^+, Na^+, Li^+ and NH_3.[3] Solid-state ISEs like the crystalline sensors have been proposed and applied for the determination of crystalline compounds like AgCl, LaF_3 or Ag_2S.[3] However, it is the polymeric types that have seen much popularity in majority of analytical applications.[4] This led to the discovery and now much-researched study of active binding sites rather called ionophores (neutral receptors), and ion-exchangers for electrically charged ion-binders. Early days ionophores were basically large molecule natural antibiotics. The ionophore-based polymer membrane ISEs - which happens to be the most versatile and the focus of many research groups - hold the most promise for expansion into environmental analysis,[4] and it is based on their construction through further advances in research that they are further sub-divided into liquid- and solid-contact electrodes.

1.2.3 Components of a polymeric ISE

Polymeric-membranes for ISEs are generally designed based on highly selective binding sites embedded in water-immiscible viscous liquid which convert chemical information into electrical signal through contact with aqueous electrolytes or conductive wire and an internal or external reference. Such compositions are generally a combination of an ionophore, an ionic site/ ion-exchanger, a plasticizer, and the polymeric matrix. Recent advances in the field of sensors have seen various materials tested and used in formulating sensing membranes for improved performances, which include; ionic liquids,[5,6] conductive polymers,[7] and alternative plasticizer/polymer system.[8,9]

1.2.3.1 The polymeric matrix

The polymeric matrix functions as the backbone to provide adequate mechanical strength to the membrane. Typically inert and chemically stable, the matrix houses other important species required for functioning of the electrode.[10] This requirement, coupled with its necessary compatibility with large number of plasticizers,[11] has led to the wide use of poly (vinyl chloride), PVC in fabricating membrane-based ISEs.[12] However, caveats surrounding PVC like the presence of small amount of impurities,[13] or non-biocompatibility with physiological materials as a result of possible leaching of other membrane components,[8] have opened the door to the emergence of several polymer alternatives like silicon rubber,[14] polyurethane,[15] methacrylic and acrylic resins.[16]

1.2.3.2 Plasticizers

Crystalline polymers and amorphous polymers that form hard and brittle glasses at room temperature are not suitable as polymeric matrixes for a rubber-like homogenous hydrophobic condition, in which the ionophore, ionophore complexes, and ionic sites can move freely, as well as the target ion's movement back and forth between the aqueous sample and the membrane phase.[3] The reason for this is due to the formation of polymeric membrane with high glass transition temperature. Therefore, low-vapour pressure liquids also known as plasticizers are generally added to most polymers like PVC to lower the transition temperature resulting in a more flexible elastomer. Examples of common plasticizers used for ISEs as shown in figure 1.2 are dioctyl phthalate (DOP), dibutyl phthalate (DBP), dioctyl sebacate (DOS) and 2-nitrophenyl octyl ether (NPOE).

In an extensive report on plasticizers, Zareh reported that the polarities and dielectric constants of plasticizers can have significant impacts on the selectivity of a polymeric ISE.[17] However, the major shortcoming of plasticizer roles within a polymeric membrane is leaching of the plasticizer components, which in turn tend to pull along other sensing components of the membrane, causing major problems like: loss of sensitivity, reduction of sensors lifetime, and even the possibility of causing unsteady responses resulting from contamination of the sample.[18] Due to these shortcomings, there has been a growing interest to develop polymers that are plasticizer-free.[9,16,19]

DOP

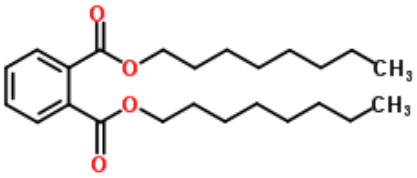

DBP

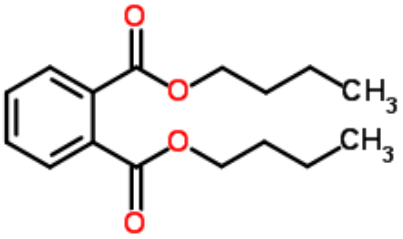

DOS

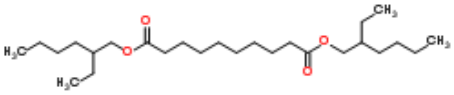

σ-NPOE

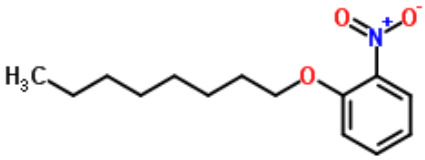

Figure 1.2 Common plasticizers used for preparation of ISE membranes.

1.2.3.3 Lipophilic ion exchanger

An ion exchanger or ionic site is key towards effectively reversible partitioning of target ion to and from the sample into the polymeric membrane. In principle, an ionic site contains a bulky lipophilic site, balanced by a more hydrophilic counter ion. Even it was thought in earlier studies in ISE field that the addition of ionic sites to membrane

components protect the electro-neutrality of common naturally-occurring binding sites,[20] recent investigations have shown adding ionic sites to charged ionophores can also be used to optimise electrode characteristics like selectivity and lifetime (later discussed in this thesis).[21,22]

In addition, the sensitivity of an ISE normally depends on the percentage of ion-exchanger added to the membrane by defining the ion-ionophore to free ionophore ratio in the membrane. This percentage in turn, greatly depends on the stoichiometric formation type the active binding site has towards the ion of interest. It is worth noting that ion-exchanging of interfering ions from samples,[23] or from small impurities from other components in the membrane,[24] can also influence the response of the electrode. Therefore, addition of adequate ionic sites to the ion-selective membrane will ensure it maintains its perm-selectivity, therefore ensuring Nernstian responses.

Some common ionic sites used in polymeric ion-selective electrodes include; the derivatives of tetrakis[3,5-bis(trifluoromethyl)phenyl]borate for cation-selective electrodes and tetraalkylammonium salts for anion-selective electrodes as shown in figure 1.3.

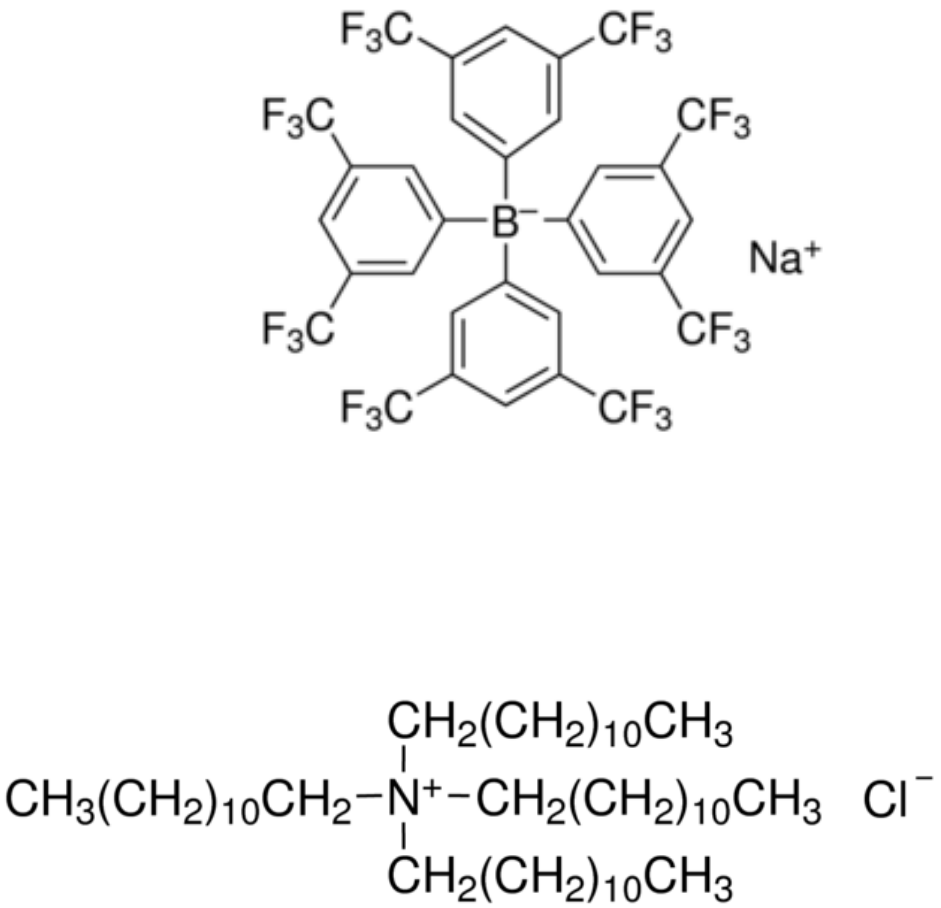

Figure 1.3 Some common ion-exchangers used for ISE membranes. Top) Sodium tetrakis[3,5-bis(trifluoromethyl)phenyl]borate. Bottom) Tetradodecylammonium chloride.

1.2.3.4 Ionophores or ion binder

The response of a typical polymeric ion-selective electrode containing only an ion exchanger together with polymer and plasticizers, will tend to follow the Hofmeister series, which is a phenomenon where ISE responds to ionic species according to their solvation energy or lipophilicity.[25] The response then follow this order; $F^- > SO_4^{2-} > HPO_4^{2-} > OAc^- > Cl^- > NO_3^- > Br^- > I^- > ClO_4^- > SCN^-$ for anions, and $NH_4^+ > Cs^+ > Rb^+ > K^+ > Na^+ > Li^+ > Mg^{2+} > Ca^{2+}$.

Additionally, since samples in most analytical applications of ISE contain several ions, it is therefore important that the membrane, for preferential uptake and binding of the specific ion of interest, is doped i.e. loaded with adequate complexing agents. This complexing agent called the ionophore typically binds with the primary ion through the formation of reversible complexes, and as such, shows specific selectivity towards the ion of interest.[26,27] The ionophore can either be electrically-neutral receptors or charged ligands, capable of forming large formation constant strong enough to keep the ion of interest bound within the membrane.

Antibiotics, like nonactin and valinomycin shown in figure 1.4, were the first set ion receptors reported to exhibit chelating properties towards monovalent ions NH_4^+ and K^+, with valinomycin getting better recognition for its application in measuring K ions in biological fluids.[3] Urea-containing compounds like di-urea calix[4]arenes 1 and 2 have been tested for binding anions like nitrate and chloride.[28] While most ionophores are based on complexation, it has been reported by Bakker et al that any reversible reaction involving covalent bond formation can be used if the equilibrium is established sufficiently fast.[29] Also lipophilic acids and bases have been reported for H^+ electrodes.[30]

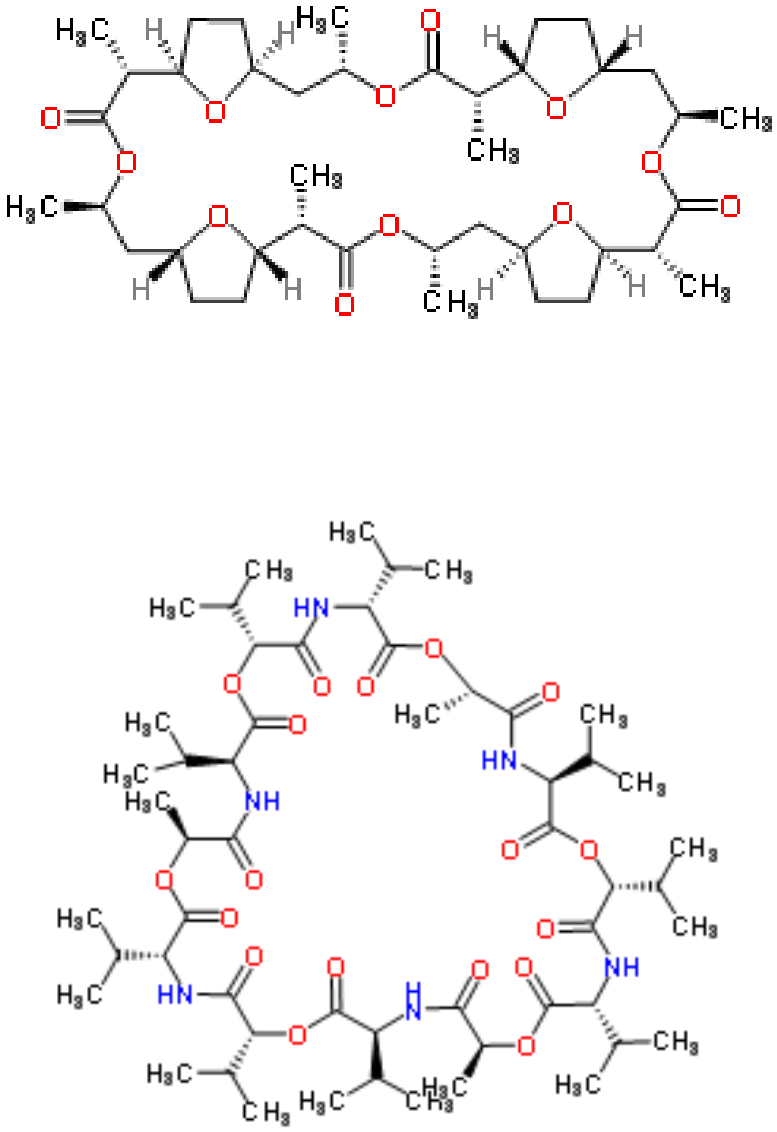

Figure 1.4 Structures of nonactin and valinomycin which have served as a model for polyethers (crown ethers) widely used in detecting NH_4^+ and K^+ activities.

1.2.3.5 Inert lipophilic additive

For polymeric membranes with high resistance, highly lipophilic salts with no ion-exchanging properties are usually added to reduce resistance by increasing membrane

conductivity. Its addition also increases the ionic strength of the membrane, therefore making it more selective for divalent ions over monovalent ions.[31]

1.3 Response mechanism of ion-selective electrode

1.3.1 Basic theory of ISE measurement

Several explanations of the theories guiding the response of potentiometry have been debated and suggested in the literature.[32] However, the phase boundary model and the ion dynamic models remain the two most prominently adopted. A simplified equation for the total potential difference (*EMF)* for an ion-selective electrode has been stated earlier in equation 1.1, and considering that only the membrane potential E_{mem}, and the liquid junction potential of the reference electrode $E_{D.ref}$, are sample dependent, the other terms can be expressed as a constant contribution, giving the total potential to be:

$$EMF = E_{const} + E_{mem} + E_{D.ref} \qquad (1.2)$$

The reference electrode potential $E_{D.ref}$ is as a result of difference in mobilities of ions at the phase boundary between the sample solution and the bridge electrolyte of the reference electrolyte. This is kept at a minimum and constant by using salts of high concentration as bridge electrolytes. Commonly used salt-bridge solutions include high concentration of KCl, NH_4NO_3 or LiOAc. Additionally, variations at the junction potentials can be minimised by keeping the ionic strength of the sample constant.

The ionic strength which is used as a measure of the total ionic contributions from all the reactive entities within the solution can be expressed as follows:

$$I = \frac{1}{2}\sum_i z_i^2 c_i \qquad (1.3)$$

Where c (mol/ L) is concentration and z is the charge on ion i.

Equation 1.3 above can be used to calculate the necessary activity coefficients to convert concentrations to the required activities through the Debye-Hückel equation as shown in equation 1.4.

$$\log \gamma_i = -Az_i^2 \frac{\sqrt{I}}{1 + B\text{å}\sqrt{I}} \qquad (1.4)$$

According to the phase-boundary potential model, it is assumed that there exists a chemical equilibrium between the organic phase and aqueous solution interface, and that the junction potential, E_{JP} across the sample/organic interface dictates the membrane response.[29] Although, the diffusion potential, which is related to the kinetics of ionic species for example, charge separations within the membrane due to different mobilities, is neglected.[32]

Since other liquid junction potentials (E_{const}) including the reference electrode potential $E_{D.ref}$ can be kept minimal and constant, these assumptions therefore lead to a more generalised equation for the total potential (*EMF*) which can be expressed in equation 1.5 as:

$$EMF = E_{const} + E_{JP} \qquad (1.5)$$

Likewise, according to a concept by Guggenheim (see equation 1.6), the electrochemical potential between two phases in contact, $\mu_I\tilde{}$ of an ion I in equilibrium, must be equal.[32]

$$\mu_I\tilde{} = \mu^o_I + RT \ln a_I + z_I F\varphi \qquad (1.6)$$

Where, μ_I is the chemical potential (μ^o_I under standard conditions), z_I the valency and a_I the activity of the un-complexed ion I^{zI+}, φ the electrical potential, and R, T and F are the universal gas constant, the absolute temperature and the Faraday constant.

However, in a more general form, the phase-boundary potential, E_{PB} can be written as follows:

$$E_{\mathrm{PB}} = \frac{RT}{z_I F} \ln k_I + \frac{RT}{z_I F} \ln \frac{a_I(\mathrm{aq})}{a_I(\mathrm{org})} \qquad (1.7)$$

Where α_I (aq) and α_I (org) are the activity of the un-complexed primary ion (with charge z_I) in the aqueous sample and the contacting organic phase boundary, respectively, and k_I is a function of the relative free energies of solvation in both the sample and the membrane phase. Note: k_I denotes standard potential which is constant to ion I, and represents its lipophilicity. ($k_I = \exp(\{\mu^o_I(\mathrm{aq}) - \mu^o_I(\mathrm{org})\}/RT)$, where μ^o_I (aq) and μ^o_I (org) are the chemical standard potentials of the ion I^{zI+} in the respective phase).

With an assumption that the primary ion activity within the membrane is usually constant in the absence of interfering ions, combining all the constant terms, including

k_I, into a single term E_{const}, and represented as the intercept of the linear response of the ISE, the electromotive force (*EMF*) may be re-written in the form of equation 1.5 as the sum of E_{const} and E_{PB} to yield the familiar form of the Nernst equation in equation 1.8, that can accurately describe the electrode response in the absence of interfering ions with a slope (s) = ±59.16/ z_I mV at 25°C over a linear range.

$$E = E_{const} + \frac{RT}{z_i F} \ln a_{i,} \quad \ln \alpha_i(aq) \qquad (1.8)$$

By extending the phase-boundary model to accommodate the presence of interfering ion within a sample, it is also possible to model the electrode response, by considering the formation constant of the complex between an ionophore and such ion.[32] This is further helped by the added or inherent lipophilic ionic sites, *Q*, within the membrane, whose free counter-ion governs the maximum total activity of all exchangeable ions of opposite charge within the membrane.

1.3.2 Electrode characteristics

1.3.2.1 Selectivity

The actual performance of an ion-selective electrode is importantly based on its affinity to bind ions.[25] In other words, the ratio at which the sensor binds a primary ion, preferentially, in any given sample solution, relative to other co-existing un-complexed ions.[29]

This term is simply referred to as selectivity and the co-existing ions are referred to as interfering ions. A quantitative measure of the response of polymeric sensors to

different activities of ions in a solution is termed as the selectivity coefficient, $logK_{I,J}^{pot}$.

While equation 1.1 clearly dictates the potentiometric response of an ISE in a standard solution with only one primary ion, the same can't be said of a solution containing mixed ions. Virtually all selectivity considerations in the past were based on the semi-empirical Nicolskii-Eisenman equation,[33] which accounts for the influence of interfering ions on the total EMF of the cell, as seen here in equation 1.9.

$$EMF = E_I^0 + \frac{RT}{z_I F} ln\left(a_I(IJ) + \sum_{I \neq J} K_{IJ}^{POT} \times a_J(IJ)^{z_I/z_J}\right) \quad (1.9)$$

The two well-studied methods for the determination of selectivity coefficients of ion-selective electrode are the fixed interference method (FIM) and separate solution method (SSM).

To calculate selectivity coefficient using the FIM, a known concentration of an interfering ion *J* is fixed, while that of primary ion *I* is varied until no further response of change in the activity of *I* is observed. The relationship can be given in equation 1.10;

$$K_{IJ}^{pot} = \frac{a_I}{a_J^{z_I/z_J}} \quad (1.10)$$

Where a_I and a_J are the activities of the primary ion and interfering ions respectively. z_I and z_J are the charges of ions *I* and *J*.

The widely used separate solution method firstly proposed by Bakker et al for calculating unbiased selectivity coefficient involves a modified version of the traditional SSM.[30] Briefly, the responses of the ISE in a solution of the interfering ions are recorded first, while making sure the electrode potential of the primary ion is recorded last. The selectivity coefficient value for each ion using the SSM can then be calculated from Equation 1.11 as follows;

$$logK_{I,J}^{pot} = \frac{(Ej - Ei)ziF}{RT \ln 10} + \left(1 - \frac{zi}{zj}\right) \log ai \qquad (1.11)$$

However, near-Nernstian slopes for ISEs in foreign ion solutions - which is the main prerequisite for correct determination of the selectivity coefficients by SSM (according to IUPAC recommendations) - often cannot be practically fulfilled for the strongest interfering ions.

Therefore, the matched potential method (MPM) is seen as an alternative way of measuring selectivity coefficients.[34] This involves measurement of potential of a solution with a known activity of the primary ion *I*. The activity of the primary ion is then increased by a known amount and the potential change is recorded. To the same initial solution with the known primary ion activity, an interfering ion, *J*, is added to match the potential change previously observed. The expression can be written as:

$$K_{IJ}^{pot} = \frac{\Delta a_I}{a_J}. \qquad (1.12)$$

It is worth noting that the selectivity coefficients obtained by MPM often strongly depend on the measurement conditions, and are also biased, therefore, making its accurate determination actually very topical.[35]

1.3.2.2 Limit of detection

Fundamentally, the electrode response of an ISE deviates from the Nernstian theoretical behaviour at low and high primary ion activities resulting in a corresponding low detection limit (LDL) and high detection limit (UDL) respectively. This phenomenon as can be seen from figure 1.5 greatly summarises the sensitivity of a typical polymeric ISE in a practical sense. According to IUPAC, the corresponding upper and lower detection limits are defined by the cross-section of the two extrapolated linear segments of the calibration curve.[36,37] The upper detection limit (UDL) results in loss of membrane perm-selectivity from the co-extraction of primary ions together with counter-ions - coming from samples containing high concentrations of primary ions or containing very lipophilic counter-ions - thereby in the process causing an increase in the concentration of primary ions inside the membrane. This is also referred to as the Donnan exclusion failure.[21]

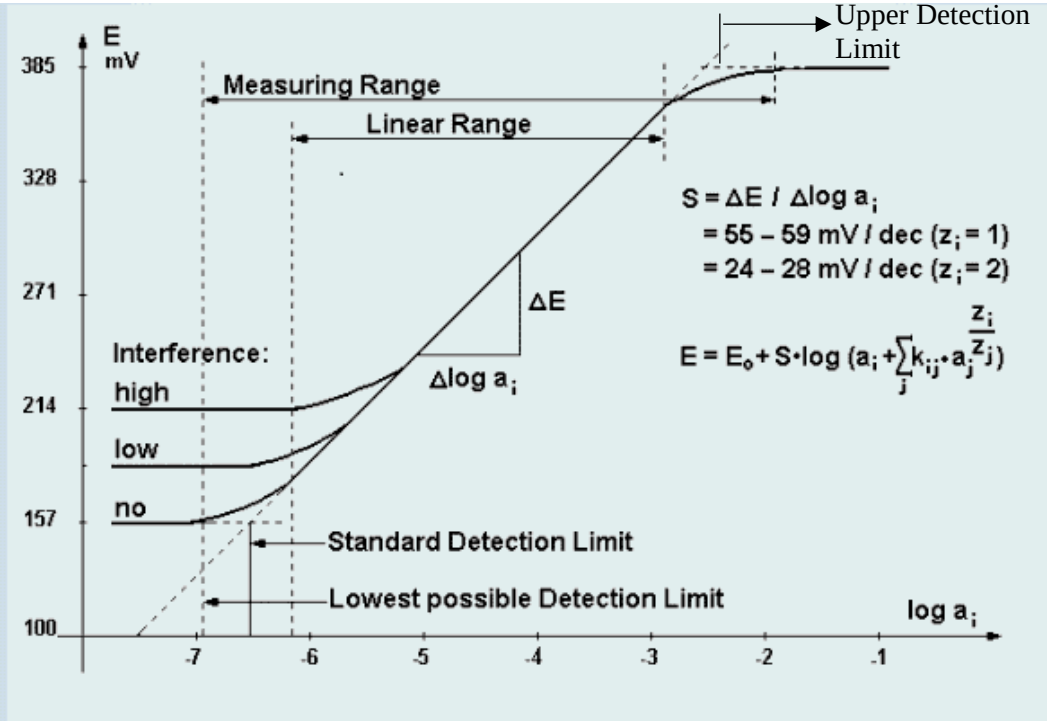

Figure 1.5 Representation of upper and lower detection limits according to IUPAC, and adapted from http://www.nico2000.net.[38]

Also shown in figure 1.5 above, is the lower detection limit (LDL) which is as a result of interferences which could either arise from other ions present in the sample solution (in the absence of ion fluxes from the membrane into the sample), or induced by the transmembrane ionic fluxes resulting from the constant release of primary ions either from the membrane bulk and/or inner solution (for liquid contact electrodes) into the sample.[39] Malon et al already stated that in the absence of fluxes, a well-defined part (50% for $z_I = z_J$) of the primary ion I is replaced by interfering ion J in the organic phase,[40] which means the slope S, which is equivalent to the sensitivity of the electrode, suffers from the influence of an increased level of interfering ions. This also emphasises the influence of the selectivity of a membrane towards a given interfering

ion on the detection limit. Later sub-sections highlighted several approaches to eliminate or reduce the ionic fluxes within an ISE, hence improve detection limits.

1.3.2.3 Response time

The response time of an ion-selective electrodes is a very important property that defines how suitable they are for different applications for example, in routine analysis.[41] It indicates the time interval that must elapse after the first contact of the electrode with the measured solution, or after a sudden change in concentration of ion measured with a relative error not larger than a fixed value.[42]

The response time of ISE is an important characteristic of the electrode since it is essentially linked to the stability and equilibrium state of electrode. It can be improved by modifying experimental procedures like: conditioning step, stirring speed, or membrane components and thickness.[43]

1.3.2.4 Life-span

The life span or lifetime of an ion-selective electrode indicates its functionalities after exposure to sample solutions. The leaching of membrane components influence the lifetime of a polymeric electrode, for example, the choice and use of membrane components like plasticizer as explained above in section 1.2.3.2.[18] Since ion-exchanging at sample/ membrane interface are influenced by the type and concentration of ions within a sample concentration, the stoichiometry and stability of ionophore-analyte complexes formed subsequently, affects the rate of ionophore leaching,[21] except for ionophores covalently to polymeric matrix.[44]

1.4 Recent advances in ion-selective electrodes used in bio/ environmental analysis

Ion-selective electrodes have been widely utilized in the laboratories for study of different analytes. In addition, because they measure the activities of bioavailable species as compared to total concentration, they have been successfully applied as a suitable technique for routine study/ monitoring of various important species,[4] in various fields including medicine, agricultural sciences and environmental analysis.[45–47]

This unique property has been exploited in the determination of several analytes and more routinely, in the analyses of important trace contaminant species like I^-,[48] NO_3^-,[45,49,50] NO_2^-,[51,52] NH_4^+,[53] Pb^{2+},[54] Cd^{2+},[5] Cu^{x+},[55] in complex environmental media even at less than parts per millions (ppm) range with little sample pre-treatment.

Additionally, their biological or biomedical application in the measurement of bioavailable activities in physiological samples species like (iodide, potassium, sodium, magnesium,[49]) is attributed to numerous advantages they offer such as fast response time, relatively small size, low production and running cost, simplicity of operation, minimal exposure to toxic chemicals and ease of operation by semi-skilled users.[4]

All these qualities make polymeric ion-selective electrodes a suitable clinical instrument,[56] or even part of a wireless monitoring system.[57]

The reviews to discuss advances in ISE always focus on the same goal, which are mainly to showcase to audience that several approaches have been taken to ensure ISE's practical usefulness that is, from being a typical bench-top tool to a more robust analytical technique for routine testing of important species in real applications.

The key studies and approaches to extend the scope of the application of polymeric ISEs have majorly focused on improving the detection limits, selectivity, cost-effectiveness and robustness.[36,58,59] These can be grouped into methodologies and materials as shown in figure 1.6.

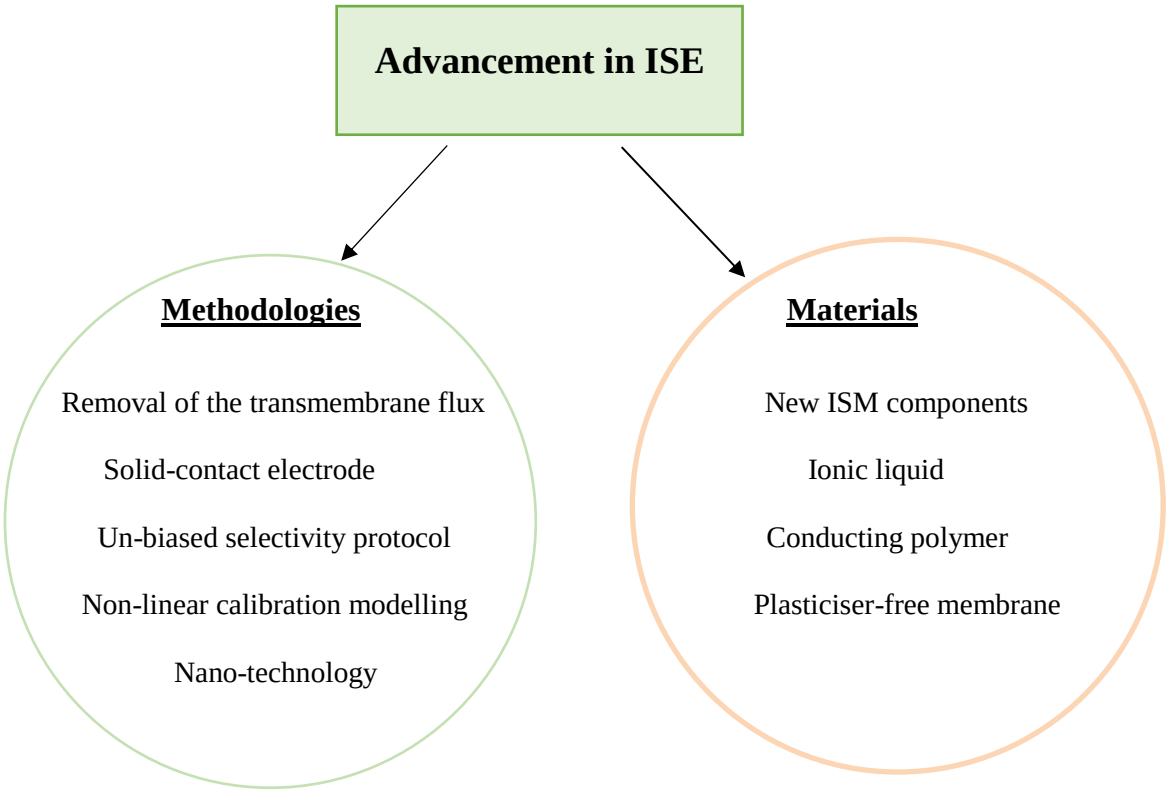

Figure 1.6 Scheme showing some of the approaches to improve ISE's application.

1.4.1 Trends in methodologies and materials development

With so much quest for new applications of analytical tools, the importance of low-detection limit mode of analysis of analytes using ion-selective electrode has been well stated.[60] In the late 90s/ early 2000s, several groups made significant efforts to push

the limit of detection below the "mediocre" level – a traditionally acceptable range in the early days of chemical sensors.[36]

It was reported that with a membrane thickness of about 200 microns and a radius of 3 mm, a typical ion-selective membrane contains about 30 nmol of the primary ions.[60] A release of even small percentage of that by any means, into a surrounding environment can compromise the primary ion activity at the membrane/ sample interface, thereby increasing limit of detection.

Additionally, with the inner part of a traditional liquid-contact ISE constantly in contact with a high concentration solution of primary ion, zero-current transmembrane fluxes due to the exchange of primary ions at both interfaces by interfering ions leading to counter-diffusion fluxes across the membrane can result into increased level of primary ions in the sample phase.[8,61,62]

A significant approach to limit the effect of transmembrane flux by optimizing the inner filling solution of ISE was evaluated by replacing primary ions with interfering ions. This protocol, tested for perchlorate and iodide, however, showed improved detection limit, although less significant when compared to cation-selective membrane.[40]

In addition, it is widely known that reducing the ion exchange composition of an ionophore-based cation-selective membrane improves lower detection limit.[43,60] However, an opposite effect was observed in the case of iodide-selective membrane containing mercuracarborane ionophore and TDMACl.[40]

Bedlechowicz et al and Zareh reported that the type of plasticizer used to fabricate ISE can also influence the detection limit, hence selectivity.[17,37]

Another breakthrough in minimising the transmembrane flux was by using rotating disk electrodes, which uses stirring effect to evaluate whether an electrode is properly optimised for low detection limit measurements.[43]

Similar effects of minimising activities of primary ions in the inner filling solution of a liquid-contact electrodes have been achieved by using resins and chelators.[24,63]

The work by Radu et al summarised key parameters like; stir rate, inner filling solution, ion-exchanger concentration and covalently-bounded ionophore-polymer system, as guidelines improving the detection limit of polymeric ion-selective electrode.[61]

In general, Bakker and Pretsch highlighted notable steps to reduce the limit of detection which include using lower plasticiser content, membrane components that are covalently attached within the membrane phase, using inert lipophilic micro particles.[36] These all led to a dramatic improvement in the detection limit of liquid-contact ISEs, and subsequently, measurements of several analytes at trace levels.

Clearly, choosing an optimal protocol designed to minimise the effect of the composition of the inner filling solution led to improvement in the detection limits of liquid-contact ISEs.[43,62] However, the need for robust electrodes adaptable for the expanding practical applications of ISEs, like routine measurement of various contaminants in environmental media or on-site continuous monitoring of dangerous chemical species gave rise to the emergence of solid-contact ISEs (SC-ISEs).[64]

The first generation SC-ISEs like coated-wire, glassy carbon or screen-printed electrode, for example, generally displayed poor limit of detection as a result of the formation of water pockets between the ion-selective membrane (ISM) and the underlying conducting support, or extreme O_2 partial pressures in the sample, subsequently leading to potential drifts.[65] This quickly led to several attempts to

minimise the water layer formation by introducing conducting polymers (CPs) as ion-to-electron transducers, at the interface between the ISM and the sensor platform.[66]

While early-day ISEs utilized several polymers like; poly(pyrrole),[65] poly(3-octylthiophene),[67] poly(aniline),[7] poly(3,4-ethylenedioxythiophene doped with poly(styrenesulfonate),[67] as ion-to-electron transducers,[63] the application of carbon materials for transduction mechanism in solid-contact ISEs shown in figure 1.7 has seen significant recognition for its ability to provide great potential stability.[68,69] This is due to their extraordinary properties like fast electron transportation, a high surface area, a high thermal conductivity and an excellent mechanical properties.[70]

Upon their applications as ion-electron transducers, these carbon materials including graphene,[71,72] carbon nanotubes,[68,73] 3-dimensionally ordered macroporous (3DOM) carbon,[74,75] colloid imprinted mesoporous (CIM) carbon,[76] and graphite,[77] have displayed improved electrode response.

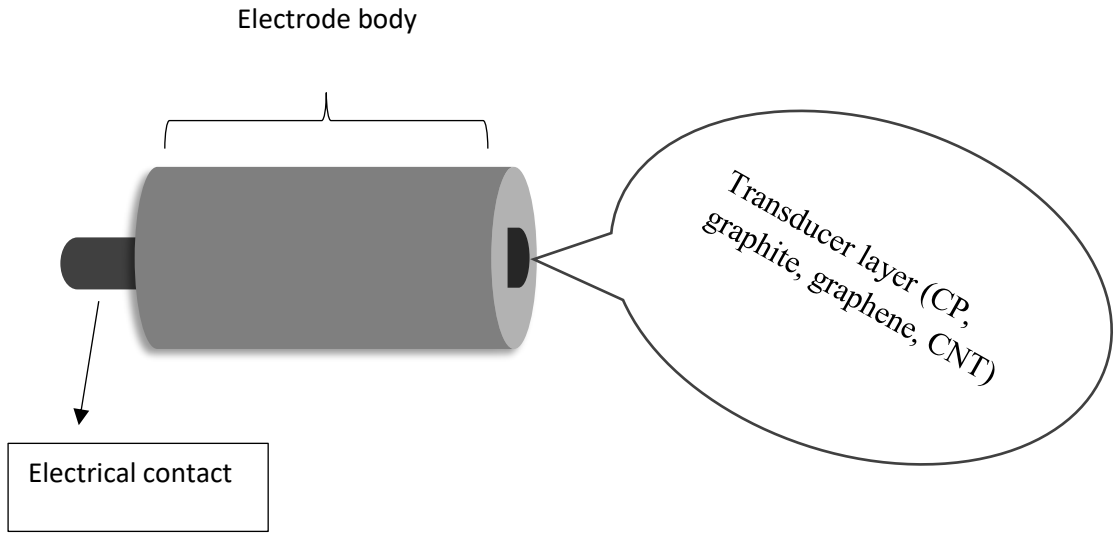

Figure 1.7 Scheme of a solid-contact ISE showing the area of transduction.

Crucially, the drive to source cheaper and simple materials for an overall cost-effective analysis in the field has opened the door for several opportunities of using papers as sensing platforms for routine measurements of important analytes using potentiometry.[73,77,78]

The all-round approach towards advancement of solid-contact ion-selective electrode has opened the door of opportunity for continuous research to improve experimental protocols previously suggested.[79,80]

Essentially, improved electrode characteristics have widened the use of solid-contact ISEs in various practical applications where simplicity, yet stability and robustness are important, and such, ultimately kicking off the approaches for miniaturisation of sensors for procedures like in-situ deployment in real life application.[58,81]

1.5 Statistical modelling of potentiometric analysis by the Bayesian method

The cross-sectional area of two lines of an ISE graph corresponds to the limit of detection according to IUPAC (LOD_{IUPAC}) as opposed to the general definition of LOD (three times the standard deviation of noise, $LOD_{S/N=3}$) in general analytical chemistry, while the limit of quantification (LOC) is indicated as the lowest expected level where the target analyte is about one order of magnitude higher than the LOD_{IUPAC}.[4] For ISE measurements, an estimated noise value of ~ 0.1 mV is frequently observed due to random variations in the potentiometric signal (instrumental noise). This is in addition to the more significant noise value as a result of random process of ion diffusing through membrane, leaching of membrane components, temperature change etc (simply called ISE noise), which generally cause variations in measurements near the LOD_{IUPAC}.[82]

The concentration of primary ions in physiological and environmental samples usually contains a varying level of several interfering ions, whose amount may be too significant to subdue even highly selective ISEs. This effect, which is greatly observed more closely at the curvilinear region of the ISE as shown in figure 1.8, poses a degree of uncertainty for the analysis of ions in physiological and environmental samples, which normally require a high level of accuracy and precision, therefore stressing the importance of the utilization of the entire response curve and need for improvement of the precision for measurements of ions near the LOD. Efforts to utilize the entire response curve of the potentiometric analysis by introducing the $LOD_{S/N=3}$ have been explored by comparing results of Pb^{2+} in digested soil samples.[54] The commonly expected bias was removed by utilizing non-linear regression, and the concentrations obtained approached the reference values measured with standard analytical method.

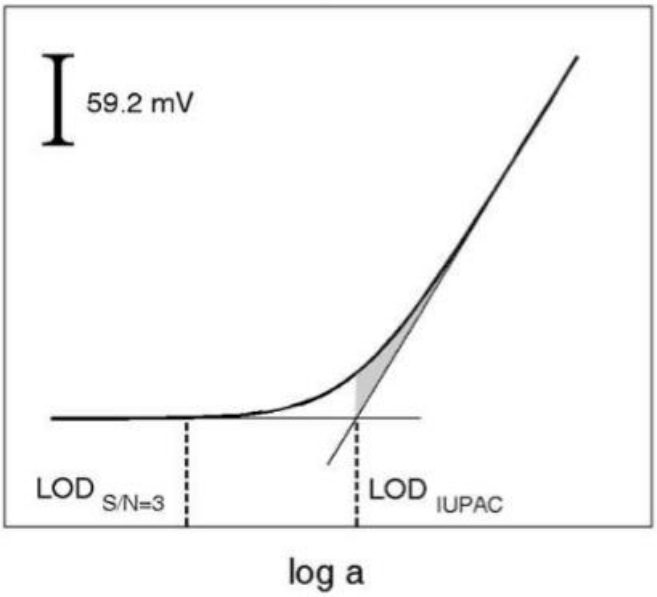

Figure 1.8 ISE response curve showing the classical LOD_{IUPAC} and the $LOD_{S/N = 3}$. The shaded area indicates bias introduced by the IUPAC definition as the electrode response deviates from the linear segment near the detection limit.

For ISEs to be more practically relevant in routine measurements of important analytes and as early warning indicator for contamination, variations observed during measurements need to show a level or value of estimates of uncertainty, in other words, display a level of precision. Since this is not often the case with most ISE measurements, developing a statistical approach to model the non-linear response of ISEs' calibrations, and estimate measurement uncertainty by using the Bayesian methods is crucial in achieving improved precision.[82] The significance of this non-linear model is that realistic estimates of measurement uncertainty are returned like in most other methods of chemical analysis, to easily improve measurement precision by using a prior understanding of important information from functioning ISEs, thereby subsequently discarding data from failing electrodes and incorporating asymmetry in calibration intervals into the final calibration interval.[4,83,84]

Practical application of the Bayesian statistical approach was performed by Dillingham et al using the standard addition method for measurement of lead in soil samples with the single-ISE model and multiple-ISE model separately. It was concluded that while the standard addition method minimized bias by reducing electrode drifts, short tail, long tails, asymmetry, and extreme variability in the width of calibration intervals considerably decreases in the multiple-ISEs model.[82] Since the individual single ISE has different properties, improvement in the final estimated values shows that the final precision of the multiple ISE model was not driven by one ISE of high quality, but took advantage of information from each electrode.[4]

1.6 Nitrogen as an environmentally important ion

1.6.1 Nitrogen in the environment

Over the last decade there has been a major rise in the inputs of nitrogen (N) species from anthropogenic activities like septic tanks, industrial effluents from polymers, clothing, beef and milk productions and fertiliser application to soil.[85,86] However, nitrogen-based organic fertilisers like farm yard manures or slurries from livestock have proved to boost crop growth by improving the soil qualities, especially in rapidly developing countries.[87–89] In the UK alone, about 90 million tonnes of livestock manure (47 million tonnes of slurry and 43 million tonnes of solid manure) supplying 450,000 tonnes of nitrogen are applied to agricultural lands in the UK each year.[90]

As a result of the geometric rise in the use of organic fertilisers, pressure coming from input of N supplements on the environment has to be monitored to avoid environmental and public health issues caused by pollution from its excessive application to soils, as well as to account for its inputs from other sources.[91–93]

Inorganic nitrogen - majorly ammonium ion (NH_4^+) and nitrate ion (NO_3^-) - are two important forms through which plants utilize nitrogen, which typically, come from the mineralization of organic matters through bacterial and fungal decomposition of dead matters within the soil or from applied nutrients. Depending on ambient conditions, nitrogen in environmental samples transforms from one form to another - processes which include nitrification, denitrification, mineralization, immobilization, as shown through the nitrogen cycle in figure 1.9.

Upon application of nitrogen to soils, these transformations are generally dependent on microbial activities and facilitated by various biogeochemical parameters, for

example, moisture content, pH, ambient temperature, C/N ratio, dry matter, organic content, oxygen condition and cation exchange capacity (CEC) of soil.[94–96]

Consequently, nitrogen is lost from fertilizers and animal manures in various pathways including leaching, denitrification, and ammonia volatilization.[97] These processes are governed by fertilizer type (animal manure, chemical fertilizer), climate, soil-hydrological conditions, and N loss mitigation measures.

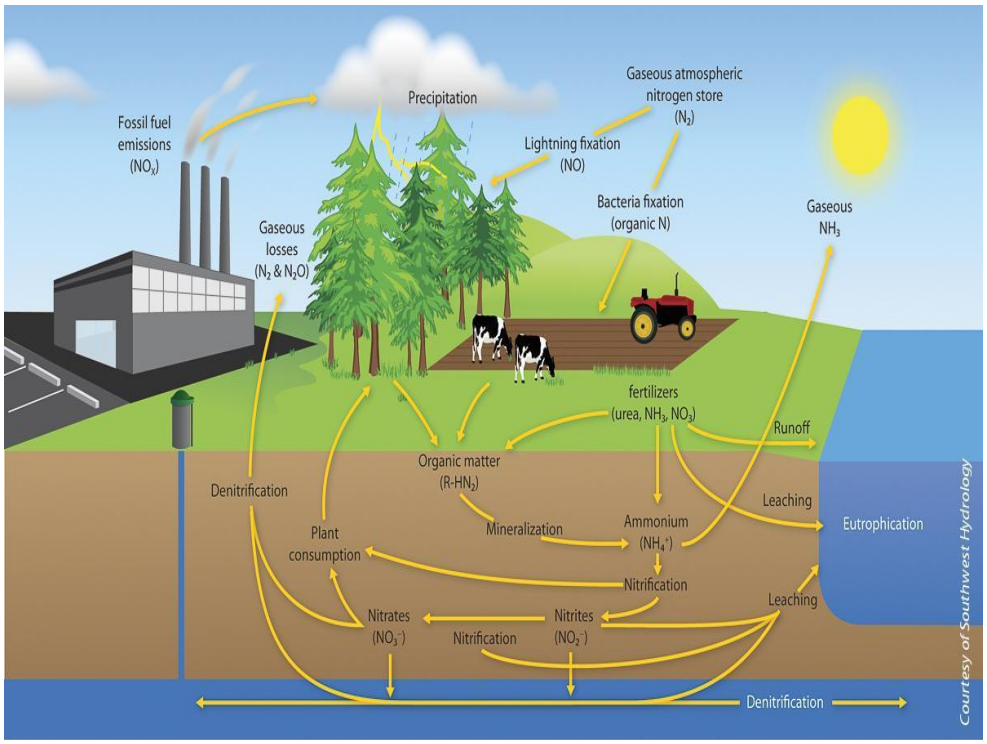

Figure 1.9 The nitrogen cycle showing major transformations in the environment.[98]

Denitrification is the loss of gaseous nitrogen (N_2 and N_2O) from stored organic fertilizers, or from surfaces of soils and water bodies. Although it tends to be the least form of toxic nitrogen loss to the atmosphere as N gas released is not harmful, nitrous oxide (N_2O) is a potent greenhouse gas that can combine with rain water to form acid rain.[91] Ammonia volatization is the conversion of ammonium to ammonia at a pKa of

9.25 - a process which depends on pH, moisture content and ambient temperature. It is also a form of N loss peculiar to open-vessel slurry storage facility. Rotz, et al reported that high loss of N through volatization during the first few hours of application of organic fertiliser onto soil was facilitated by exposed surface area and air movement.[99] High concentrations of ammonia in drinking water and other water resources can lead to adverse effects for man and also cause major environment pollutions.[100]

Pollution of groundwater and surface waters by nitrogen compounds especially through nitrate leached from agricultural activities is a major environmental issue. In the UK, nitrate loss to surface water because of intense fertilization through the use of inorganic fertilizers and organic manures has called for control of the Nitrate Vulnerable Zones (NVZs), which is part of the control measures in soil/ agriculture management system within the European Union (EU). As a guideline within its member states, the EU has set an alert limit, and maximum allowable concentration of 50 mg/ L NO_3^- for groundwater and drinking waters respectively (The Nitrates Directive, 91/676/EEC).[101] The current Nitrate Vulnerable Zones Action Programme (NVZ-AP) in the UK covers about 62%, 14% and 3% of agricultural land in England, Scotland and Wales, respectively, and it restricts the application of high readily available N organic manures in the autumn/winter period.[90]

Hunt et al reported that about 61% of total N being loaded into surface waters in England and Wales are from lands with agricultural activities, with a slightly smaller value (59%) when considering England alone, leading to the possibility of nutrient deposition into water bodies.[102] While also in the Netherlands, more than 60% of agricultural land is used for dairy farming - increasing the possibility of pollution as result of loss of N species.

Eutrophication is the enrichment of the water bodies by excessive nutrients, mainly nitrogen and phosphorus that stimulate the growth of aquatic plant life usually leading to the depletion of dissolved oxygen resulting in algal bloom and an unpleasant aquatic environment. This is a major concern in the UK's inland and coastal water with a large part of this enrichment as a result of agricultural activities, mainly fertilization.[103–105]

Song et al reported high concentration of nitrate leachate between 152 to 347 kg N ha^{-1} from agricultural practices as a result of applied N fertilizer greatly exceeding the capacity of crop uptake (33% of applied N), which was evident in seepage water from drainable lysimeters during a growing reason, inevitably leading to massive nitrate getting into groundwater during intensive vegetable production.[106]

Excessive nitrate intake which has been linked to methemoglobinemia, or rather called blue baby syndrome, was reported to have been experienced by young infants less than 6 months, through poor water quality as evident from water used to prepare infant formula.[107] This syndrome is as a result of Fe^{2+} being oxidised to Fe^{3+} in the haemoglobin to form methemoglobin – which has stronger binding capacity to oxygen causing less oxygen transport to the tissues, resulting in hypoxia. Nitrite (an intermediate specie of the conversion of ammonium to nitrate), on the other hand, can react with secondary amines present in the body thereby resulting in the formation of carcinogenic nitrosamines.[108]

Therefore, due to these alarming health issues resulting from reactive nitrogen (Nr) within environmental habitats, simple robust measurements that can accurately predict and routinely monitor nitrogen in samples are very important.

1.6.2 Measurement of nitrogen

Due to its vast importance in the environment, various analytical techniques have been proposed to measure N species in different samples like soil, vegetables, dairy products and water. These methods include spectrophotometry, reflectometry, capillary electrophoresis, wet chemistry, ion chromatography, and potentiometry.[49,100,109,110] Note, the last two techniques will be covered later in details in the course of this thesis.

1.6.2.1 Spectrophotometry

Ultraviolet-visible (UV-VIS), infra-red (IR) and near infrared (NIR) reflectance spectroscopy are common spectroscopic techniques used in environmental analysis. The (UV-VIS) covers the range between 190 nm to 790 nm of the electromagnetic spectrum, while the infrared region is between 0.78 and 1000 mm. The light source (a combination of tungsten/halogen and deuterium lamps) provides the visible and near ultraviolet radiation covering the 200 – 800 nm band. The output of the incoming light source from samples is split into component colours of different wavelength after passing through a diffracting grating. When sample molecules are exposed to light having an energy that matches a possible electronic transition within the molecule, some of the light energy will be absorbed as the electron is promoted to a higher energy orbital. An optical spectrometer records the wavelengths at which absorption occurs, together with the degree of absorption at each wavelength. The resulting spectrum is presented as a graph of absorbance versus wavelength. The relationship can be derived from the Beer-Lambert law which states that the absorbance of a solution is directly proportional to the concentration of the absorbing species in the solution and the path length.

The direct measurement of nitrogen species like nitrate and nitrite by UV-VIS spectrophotometer is a rapid, easy and accurate method that involves the absorption of light between 200-210 nm region. However the presence of some saline constituents which may cause interference, as well as the strong absorption of light by dissolved organic matters at around the same wavelength cause major setback.[111]

The infrared (IR) radiation covers the range of the electromagnetic spectrum between 0.78 mm and 1 mm. Vibrational energy transitions in molecules typically require energy of a frequency that corresponds to the IR region of the electromagnetic spectrum. Hence IR radiation will activate molecular interatomic vibrations, and this provides the basis of the IR spectroscopy technique. For a compound to be IR active, it is required to have covalent bonding. Absorptions of IR radiations are due to vibrations of molecular bonds such as O-H, C-H, N-H, C=O, C-N, or N-O. The NIR spectrophotometry which is a non-destructive, rapid, reproducible and low-cost method that characterizes materials according to their reflectance in the wavelength range between 800 and 2500 nm band has been widely used for the analysis of nitrogen contents. Although for heterogeneous samples like soils, the effect of sample properties, hence sample pre-treatment process is still debatable.[112]

1.6.2.2 Reflectometry

Measurement using the time domain reflectometry (TDR) in medium like soil or pore water involves applying a very fast rise time step voltage increase to a coaxial cable that carries the pulse to a probe that is placed in the sample examined. A combination of cable tester and oscilloscope is commonly used to provide the voltage step and capture the reflected waveform.[113] Sample properties like water content and bulk electrical conductivity can be obtained from the applied pulse, which can then be

correlated and used to monitor the change in nitrate composition in a sample. Alternatively, a nitrate-containing platform like a filter paper can be used to determine nitrate using an automated reflectometer.[114]

1.6.2.3 Capillary electrophoresis

Electrophoresis is a method used to separate charged particles from one another based on differences in their migration speed. It is a rapid, high-resolution analytical technique for the separation of a wide variety of charged and uncharged species. In Capillary Electrophoresis, separations are based on the differential migration rates of species through a solution or gel in the presence of an electric field. Capillary electrophoresis has been used to measure several nitrogen-containing species like nitrate, nitrite and ammonium in different important samples. However, Martínková et al reported an improved limit of detection was achieved for nitrate and nitrite by the addition of a cationic surfactant to the background electrolyte of Tris–HCl buffer to suppress the electro-osmotic flow (EOF) or changes its direction.[115] A fast capillary electrophoresis method for a single-run direct (NO_3^-, NO_2^-) and indirect (NH_4^+) UV detection at 214 nm showed some improvement in sensitivity following the addition of anionic internal standard for cationic analytes and vice versa. This method was successfully applied to test for Nr in rainwater samples.[116]

1.6.3 Advantages of potentiometric analysis using ISE

Since water samples and some soil samples having relatively low N compositions, most researches have been channelled towards improving the sensitivity of current techniques. Typical example of this was the approach proposed by Moliner-Martínez et

al for an improved Berthelot method based on the extraction of indothylmol blue into solid-phase extraction membranes.[117]

While some of these aforementioned methods are often known for their accuracy and sensitivity, they are generally too tedious to be conducted, thereby resulting in data with notable irregularities and biases, especially in analysis involving complex environmental samples. Furthermore, these methods often suffer few common setbacks for example, the use of chemicals which are expensive and sometimes toxic, stressful preparation/ storage of chemicals, the use of catalysts and derivatives, lack of portability or suitability for in-situ measurements, time consuming reaction processes as well as highly technical and very expensive equipment.

It is also noteworthy to mention the laborious pre-treatment steps involved in the clarification of samples, whose complex and turbid nature can either impair the resolution of a highly sensitive technique due to matrix interferences, or whose colours can affect detection of analyte by techniques like colorimetric method.

As discussed earlier, measurement of free bioavailable analyte ions by ion selective electrodes not only offer a cheaper alternative relative to expensive standard techniques,[45] it also reduces the inconveniencies and sometimes the impossibilities associated with very a thorough sample pre-treatment required for most standard analytical techniques - a major challenge in some under-developed or developing nations.[49,50] Therefore, potentiometric measurements of Nr using ISE will be evaluated.

1.7 Iodide as a biologically important ion

1.7.1 Iodide deficiency

Iodine is used by the thyroid gland to produce thyroid hormones which are of great physiological importance to humans and other animals.[118] Iodine is also actively involved in other biological activities like; cell growth, brain development, body metabolism, and neurological functions. As a result of these significance, deficiency of iodine can lead to iodine deficiency disorders (IDD) such as; mental retardation, deafness, stunted growth, neurological problems and goiter.[119] About 1.6 billion people (mostly in developing countries) are at risk of IDD.[120]

Typically, urinary iodide (UI) is a useful indicator for iodine nutrition status of an individual in a population, and as a recommendation, the UI levels within a population are categorized into; < 20 μg/ L (severely deficient), 20 – 49 μg/ L (moderately deficient), 50 -100 μg/ L (mildly deficient), 100 200 μg/ L (adequate) and > 300 (excessive intake). The risks of excessive iodine intake include hyperthyroidism and thyroid autoimmune diseases; however whether this occurs at a UI level of 300 μg/ L is debatable.[121]

Due to the insignificant of faecal excretion of iodine, and since close to almost all of the ingested iodine is excreted in the urine as urinary iodide,[122] the UI can therefore be used as a tool to evaluate the status of iodine nutrition of a population.[123]

The analysis of UI is important in physiological studies and to public health. Several methods developed for measurement of UI have been discussed by,[124] however they are either still deemed lengthy or rather too expensive for routine measurements of UI

especially in countries where there are limited technology resources. Potentiometry is a viable and simpler alternative technique to rival the standard methods.[48]

Other general advantages of polymeric ISEs discussed earlier apply herein to the analysis of UI. However, due to the strict accuracy and precision required for clinical analysis, a limit of detection (LOD) lower than previously achieved would be crucial for routine analysis of UI in real-life samples.

1.7.2 Measurement of iodide

Common analytical methods for the determination of iodine are differential pulse polarography, ion chromatography, capillary electrophoresis, flame atomic absorbance spectrometry, the Sandell and Kolthoff (S-K) kinetic–catalytic method, inductively coupled plasma mass spectrometry (ICP-MS) and ion-selective electrodes. Majority of these standard methods are either too tedious, highly specialized and complicated, or deemed too expensive (with exception of potentiometric measurement), for routine/ DIY analysis of iodide in physiological sample like urine.

Presently, urinary iodine measurement is carried out almost exclusively by one of the Sandell and Kolthoff spectrophotometric method or the inductively coupled plasma mass spectrometry (ICP-MS).[121]

1.7.2.1 The Sandell and Kolthoff (s-k) spectrophotometric method

The method is a kinetic-catalytic colourimetric method that involves the reduction of yellow Ce (IV) by As (III) to colourless Ce (III). This reaction is catalyzed by trace amounts of iodide. The reaction follows the following scheme:

$$\left.\begin{aligned} 2\,Ce^{4+} + 2\,I^{-} &\rightarrow 2\,Ce^{3+} + I_2 \\ As^{3+} + I_2 &\rightarrow As^{5+} + 2\,I^{-} \end{aligned}\right\} \qquad (1.13)$$

The decreasing rate of absorbance is directly proportional to the amount of iodine in the sample. A setback for this method is the interference that could result from the UV-absorbing organic matters present in the samples by chelating Ce (IV) or Ce (III) or otherwise directly affecting the reaction rate. This therefore means there is a need for complete mineralization of samples to digest the organics.[125]

1.7.2.2 Inductively coupled plasma mass spectrometry (ICP-MS)

ICP-MS has become predominant in ultra-trace and multi-element. Its attractive features like high selectivity, sensitivity, accuracy, low detection limits and its ability to discriminate the isotopes of the same element according to their mass, make it a gold standard technique for analysing urinary iodine (UI).[126] The operation follows the introduction of microwave or radio frequency power through an induction coil to generate high temperature argon plasmas, 4500 – 8000 K, with an electron temperature of 8000 –10,000 K. The plasma then atomizes the sample and strips the atoms of one or more valence electrons. The resulting positive ions then typically enter a single quadrupole mass analyzer for sorting out ions of different m/z and are then detected. An important factor to consider before testing for UI using ICP-MS is the effect of sample matrix on the ionization process. This is because the presence of other ionizable materials present in the samples could affect the plasma. Because urine samples contains high compositions of salts and dissolved solid contents, sample pretreatment is usually required before analysis. However, UI analysis without a prior digestion or oxidation still produced some results slightly comparable to the S-K method as reported by Macours et al.[127] It was concluded that even though lower urinary iodine

values with ICP-MS were observed at iodine concentrations below 250 mg/L, values for urinary iodine were lower using the ICP-MS than the values obtained with the S–K method. The lower urinary iodine values could result from the higher specificity of the ICP-MS method compared with the colorimetric S–K method.[127]

1.8 Aims

The overall aim of this inter-disciplinary project was to develop simple, low cost, and easy to fabricate polymeric ion-selective electrodes for routine analysis of nitrate and ammonium in water and soil samples, and iodide activities in urine sample.

Subsequently, the thesis covers three areas, namely:

1) The fabrication of single strip solid contact ion selective electrodes on simple platform prepared using household items. This will aim at driving down cost of analysis important nutrients in environmental and physiological samples.

2) Subsequent upon achieving reasonably robust sensors, paper-based electrodes were then tested for concurrent measurement of inorganic nitrogen in soil and water samples from different areas in the UK.

3) Lastly, non-linear Bayesian modelling was applied to estimate activities of biological and environmental analytes. This was aimed at improving measurement precision and accuracy.

References

(1) Hulanicki, A.; Glab, S.; Ingman, F. Chemical Sensors: Definitions and Classification. *Pure Appl. Chem.* **1991**, *63* (9), 1247–1250.

(2) Dimeski, G.; Badrick, T.; John, A. S. Ion Selective Electrodes (ISEs) and Interferences—A Review. *Clin. Chim. Acta* **2010**, *411* (5), 309–317.

(3) Bühlmann, P.; Chen, L. D. Ion-Selective Electrodes with Ionophore-Doped Sensing Membranes. In *Supramolecular Chemistry*; John Wiley & Sons, Ltd, 2012.

(4) Radu, A.; Radu, T.; McGraw, C.; Dillingham, P.; Anastasova, S.; Diamond, D. Ion Selective Electrodes in Environmental Analysis. *J. Serbian Chem. Soc.* **2013**, *78*, 1729–1761.

(5) Wardak, C. Solid Contact Cadmium Ion-Selective Electrode Based on Ionic Liquid and Carbon Nanotubes. *Sens. Actuators B Chem.* **2015**, *209*, 131–137.

(6) Wardak, C. Solid Contact Nitrate Ion-Selective Electrode Based on Ionic Liquid with Stable and Reproducible Potential. *Electroanalysis* **2014**, *26* (4), 864–872.

(7) Bobacka, J.; Lindfors, T.; McCarrick, M.; Ivaska, A.; Lewenstam, A. Single-Piece All-Solid-State Ion-Selective Electrode. *Anal. Chem.* **1995**, *67* (20), 3819–3823.

(8) Peper, S.; Tsagkatakis, I.; Bakker, E. Cross-Linked Dodecyl Acrylate Microspheres: Novel Matrices for Plasticizer-Free Optical Ion Sensing. *Anal. Chim. Acta* **2001**, *442* (1), 25–33.

(9) Qin, Y.; Peper, S.; Bakker, E. Plasticizer-Free Polymer Membrane Ion-Selective Electrodes Containing a Methacrylic Copolymer Matrix. *Electroanalysis* **2002**, *14* (19–20), 1375–1381.

(10) Thomas, J. D. R. Selective Membrane Electrodes for Analysis. *Analyst* **1994**, *119* (2), 203–208.

(11) Eugster, R.; Rosatzin, T.; Rusterholz, B.; Aebersold, B.; Pedrazza, U.; Rüegg, D.; Schmid, A.; Spichiger, U. E.; Simon, W. Plasticizers for Liquid Polymeric Membranes of Ion-Selective Chemical Sensors. *Anal. Chim. Acta* **1994**, *289* (1), 1–13.

(12) Johnson, R. D.; Bachas, L. G. Ionophore-Based Ion-Selective Potentiometric and Optical Sensors. *Anal. Bioanal. Chem.* **2003**, *376* (3), 328–341.

(13) Paczosa-Bator, B.; Piech, R.; Lewenstam, A. Determination of the Leaching of Polymeric Ion-Selective Membrane Components by Stripping Voltammetry. *Talanta* **2010**, *81* (3), 1003–1009.

(14) Cha, G. S.; Liu, D.; Meyerhoff, M. E.; Cantor, H. C.; Midgley, A. R.; Goldberg, H. D.; Brown, R. B. Electrochemical Performance, Biocompatibility, and Adhesion of New Polymer Matrixes for Solid-State Ion Sensors. *Anal. Chem.* **1991**, *63* (17), 1666–1672.

(15) Yun, S. Y.; Hong, Y. K.; Oh, B. K.; Cha, G. S.; Nam, H.; Lee, S. B.; Jin, J. I. Potentiometric Properties of Ion-Selective Electrode Membranes Based on Segmented Polyether Urethane Matrices. *Anal. Chem.* **1997**, *69* (5), 868–873.

(16) Heng, L. Y.; Hall, E. A. H. Producing "Self-Plasticizing" Ion-Selective Membranes. *Anal. Chem.* **2000**, *72* (1), 42–51.

(17) Zareh, M. M. Plasticizers and Their Role in Membrane Selective Electrodes. **2012**.

(18) Dinten, O.; Spichiger, U. E.; Chaniotakis, N.; Gehrig, P.; Rusterholz, B.; Morf, W. E.; Simon, W. Lifetime of Neutral-Carrier-Based Liquid Membranes in

Aqueous Samples and Blood and the Lipophilicity of Membrane Components. *Anal. Chem.* **1991**, *63* (6), 596–603.

(19) Mendecki, L.; Chen, X.; Callan, N.; Thompson, D. F.; Schazmann, B.; Granados-Focil, S.; Radu, A. Simple, Robust, and Plasticizer-Free Iodide-Selective Sensor Based on Copolymerized Triazole-Based Ionic Liquid. *Anal. Chem.* **2016**, *88* (8), 4311–4317.

(20) Schaller, U.; Bakker, E.; Spichiger, U. E.; Pretsch, E. Ionic Additives for Ion-Selective Electrodes Based on Electrically Charged Carriers. *Anal. Chem.* **1994**, *66* (3), 391–398.

(21) Buhlmann, P.; Umezawa, Y.; Rondinini, S.; Vertova, A.; Pigliucci, A.; Bertesago, L. Lifetime of Ion-Selective Electrodes Based on Charged Ionophores. *Anal. Chem.* **2000**, *72* (8), 1843–1852.

(22) Amemiya, S.; Buhlmann, P.; Pretsch, E.; Rusterholz, B.; Umezawa, Y. Cationic or Anionic Sites? Selectivity Optimization of Ion-Selective Electrodes Based on Charged Ionophores. *Anal. Chem.* **2000**, *72* (7), 1618–1631.

(23) Miyake, M.; Chen, L. D.; Pozzi, G.; Bühlmann, P. Ion-Selective Electrodes with Unusual Response Functions: Simultaneous Formation of Ionophore–Primary Ion Complexes with Different Stoichiometries. *Anal. Chem.* **2012**, *84* (2), 1104–1111.

(24) Qin, W.; Zwickl, T.; Pretsch, E. Improved Detection Limits and Unbiased Selectivity Coefficients Obtained by Using Ion-Exchange Resins in the Inner Reference Solution of Ion-Selective Polymeric Membrane Electrodes. *Anal. Chem.* **2000**, *72* (14), 3236–3240.

(25) Bakker, E.; Meruva, R.; Pretsch, E.; E. Meyerhoff, M. Selectivity of Polymer Membrane-Based IonSelective Electrodes: Self-Consistent Model Describing the Potentiometric Response in Mixed Ion Solutions of Different Charge. *Anal. Chem. - ANAL CHEM* **1994**, *66*, 3021–3030.

(26) Schaller, U.; Bakker, E.; Pretsch, E. Carrier Mechanism of Acidic Ionophores in Solvent Polymeric Membrane Ion-Selective Electrodes. *Anal. Chem.* **1995**, *67* (18), 3123–3132.

(27) Luboch, E.; Jeszke, M.; Szarmach, M.; Łukasik, N. New Bis(Azobenzocrown)s with Dodecylmethylmalonyl Linkers as Ionophores for Sodium Selective Potentiometric Sensors. *J. Incl. Phenom. Macrocycl. Chem.* **2016**, *86* (3–4), 323–335.

(28) Schazmann, B.; Diamond, D. Improved Nitrate Sensing Using Ion Selective Electrodes Based on Urea–Calixarene Ionophores. *New J. Chem.* **2007**, *31* (4), 587–592.

(29) Bakker, E. Determination of Unbiased Selectivity Coefficients of Neutral Carrier-Based Cation-Selective Electrodes. *Anal. Chem.* **1997**, *69* (6), 1061–1069.

(30) Bakker, E.; Pretsch, E.; Bühlmann, P. Selectivity of Potentiometric Ion Sensors. *Anal. Chem.* **2000**, *72* (6), 1127–1133.

(31) Nägele, M.; Mi, Y.; Bakker, E.; Pretsch, E. Influence of Lipophilic Inert Electrolytes on the Selectivity of Polymer Membrane Electrodes. *Anal. Chem.* **1998**, *70* (9), 1686–1691.

(32) Bakker, E.; Bühlmann, P.; Pretsch, E. The Phase-Boundary Potential Model. *Talanta* **2004**, *63* (1), 3–20.

(33) Umezawa, Y.; Umezawa, K.; Sato, H. Selectivity Coefficients for Ion-Selective Electrodes: Recommended Methods for Reporting $K_{A,B}^{Pot}$ Values (Technical Report). *Pure Appl. Chem.* **1995**, *67* (3), 507–518.

(34) Tohda, K.; Dragoe, D.; Shibata, M.; Umezawa, Y. Studies on the Matched Potential Method for Determining the Selectivity Coefficients of Ion-Selective Electrodes Based on Neutral Ionophores: Experimental and Theoretical Verification. *Anal. Sci. Int. J. Jpn. Soc. Anal. Chem.* **2001**, *17* (6), 733–743.

(35) Egorov, V. V.; Zdrachek, E. A.; Nazarov, V. A. Improved Separate Solution Method for Determination of Low Selectivity Coefficients. *Anal. Chem.* **2014**, *86* (8), 3693–3696.

(36) Bakker, E.; Pretsch, E. Potentiometric Sensors for Trace-Level Analysis. *Trends Anal. Chem. TRAC* **2005**, *24* (3), 199–207.

(37) Bedlechowicz, I.; Maj-Żurawska, M.; Sokalski, T.; Hulanicki, A. Effect of a Plasticizer on the Detection Limit of Calcium-Selective Electrodes. *J. Electroanal. Chem.* **2002**, *537* (1), 111–118.

(38) Guide to ISE Measurements, Chap. 7) CALIBRATION THEORY http://www.nico2000.net/Book/Guide8.html (accessed Nov 28, 2017).

(39) Gyurcsányi, R. E.; Pergel, É.; Nagy, R.; Kapui, I.; Thu Lan, B. T.; Tóth, K.; Bitter, I.; Lindner, E. Direct Evidence of Ionic Fluxes Across Ion-Selective Membranes: A Scanning Electrochemical Microscopic and Potentiometric Study. *Anal. Chem.* **2001**, *73* (9), 2104–2111.

(40) Malon, A.; Radu, A.; Qin, W.; Qin, Y.; Ceresa, A.; Maj-Zurawska, M.; Bakker, E.; Pretsch, E. Improving the Detection Limit of Anion-Selective Electrodes: An Iodide-Selective Membrane with a Nanomolar Detection Limit. *Anal. Chem.* **2003**, *75* (15), 3865–3871.

(41) Lindner, E.; Toth, K.; Pungor, E. Definition of the Response Time of Ion-Selective Electrodes and Potentiometric Cells. *Anal. Chem.* **1984**, *56* (4), 808–810.

(42) Buck, R. P.; Lindner, E. Recommendations for Nomenclature of Ionselective Electrodes (IUPAC Recommendations 1994). *Pure Appl. Chem.* **1994**, *66* (12), 2527–2536.

(43) Radu, A.; Telting-Diaz, M.; Bakker, E. Rotating Disk Potentiometry for Inner Solution Optimization of Low-Detection-Limit Ion-Selective Electrodes. *Anal. Chem.* **2003**, *75* (24), 6922–6931.

(44) Bakker, E.; Bühlmann, P.; Pretsch, E. Carrier-Based Ion-Selective Electrodes and Bulk Optodes. 1. General Characteristics. *Chem. Rev.* **1997**, *97* (8), 3083–3132.

(45) Ardakani, M. M.; Dastanpour, A.; Salavati-Niasari, M. A Highly Selective Nitrate Electrode Based on a Tetramethyl Cyclotetra-Decanato-Nickel(II) Complex. *J. Electroanal. Chem.* **2004**, *Complete* (568), 1–6.

(46) Covington, A. K.; Kataky, R. Calibration Solutions for the Simultaneous Potentiometric Measurement of Sodium, Potassium and Calcium in Blood Plasma: Examination of the Electrochemical Factors Affecting Precision and Accuracy in Direct Potentiometric Clinical Analysers. *J. Chem. Soc. Faraday Trans.* **1993**, *89* (2), 369–376.

(47) Ortuño, J. A.; Expósito, R.; Sánchez-Pedreño, C.; Albero, M. I.; Espinosa, A. A Nitrate-Selective Electrode Based on a Tris(2-Aminoethyl)Amine Triamide Derivative Receptor. *Anal. Chim. Acta* **2004**, *525* (2), 231–237.

(48) Ibupoto, Z. H.; Khun, K.; Willander, M. A Selective Iodide Ion Sensor Electrode Based on Functionalized ZnO Nanotubes. *Sensors* **2013**, *13* (2), 1984–1997.

(49) Shaw, R.; Williams, A. P.; Miller, A.; Jones, D. L. Assessing the Potential for Ion Selective Electrodes and Dual Wavelength UV Spectroscopy as a Rapid On-Farm Measurement of Soil Nitrate Concentration. *Agriculture* **2013**, *3* (3), 327–341.

(50) Tully, K. L.; Weil, R. Ion-Selective Electrode Offers Accurate, Inexpensive Method for Analyzing Soil Solution Nitrate in Remote Regions. *Commun. Soil Sci. Plant Anal.* **2014**, *45* (14), 1974–1980.

(51) Ibrahim, H. Determination of Nitrite in Environmental Samples Using Chemically Modified Carbon Paste Electrode Based on New Co(III)-Benzopyran-4-One Schiff Base Complex. *Sens. Electroanal.* **2012**.

(52) Pasquali, C. E. L.; Gallego-Picó, A.; Hernando, P. F.; Velasco, M.; Alegría, J. S. D. Two Rapid and Sensitive Automated Methods for the Determination of Nitrite and Nitrate in Soil Samples. *Microchem. J.* **2010**, *94* (1), 79–82.

(53) Guenat, O. T.; Generelli, S.; de Rooij, N. F.; Koudelka-Hep, M.; Berthiaume, F.; Yarmush, M. L. Development of an Array of Ion-Selective Microelectrodes Aimed for the Monitoring of Extracellular Ionic Activities. *Anal. Chem.* **2006**, *78* (21), 7453–7460.

(54) McGraw, C. M.; Radu, T.; Radu, A.; Diamond, D. Evaluation of Liquid- and Solid-Contact, Pb2+-Selective Polymer-Membrane Electrodes for Soil Analysis. *Electroanalysis* **2008**, *20* (3), 340–346.

(55) Wardak, C.; Grabarczyk, M. Analytical Application of Solid Contact Ion-Selective Electrodes for Determination of Copper and Nitrate in Various Food

Products and Drinking Water. *J. Environ. Sci. Health Part B* **2016**, *51* (8), 519–524.

(56) Darwish, A.; Hassanien, A. E. Wearable and Implantable Wireless Sensor Network Solutions for Healthcare Monitoring. *Sensors* **2011**, *11* (6), 5561–5595.

(57) Fay, C.; Anastasova, S.; Slater, C.; Buda, S. T.; Shepherd, R.; Corcoran, B.; O'Connor, N. E.; Wallace, G. G.; Radu, A.; Diamond, D. Wireless Ion-Selective Electrode Autonomous Sensing System. *IEEE Sens. J.* **2011**, *11* (10), 2374–2382.

(58) Crespo, G. A. Recent Advances in Ion-Selective Membrane Electrodes for in Situ Environmental Water Analysis. *Electrochimica Acta* **2017**, *245* (Supplement C), 1023–1034.

(59) Bakker, E.; Bühlmann, P.; Pretsch, E. Polymer Membrane Ion-Selective Electrodes–What Are the Limits? *Electroanalysis* **1999**, *11* (13), 915–933.

(60) Ceresa, A.; Sokalski, T.; Pretsch, E. Influence of Key Parameters on the Lower Detection Limit and Response Function of Solvent Polymeric Membrane Ion-Selective Electrodes. *J. Electroanal. Chem.* **2001**, *501* (1), 70–76.

(61) Radu, A.; Peper, S.; Bakker, E.; Diamond, D. Guidelines for Improving the Lower Detection Limit of Ion-Selective Electrodes: A Systematic Approach. *Electroanalysis* **2007**, *19* (2–3), 144–154.

(62) Telting-Diaz, M.; Bakker, E. Effect of Lipophilic Ion-Exchanger Leaching on the Detection Limit of Carrier-Based Ion-Selective Electrodes. *Anal. Chem.* **2001**, *73* (22), 5582–5589.

(63) Fibbioli, M.; Morf, W. E.; Badertscher, M.; de Rooij, N. F.; Pretsch, E. Potential Drifts of Solid-Contacted Ion-Selective Electrodes Due to Zero-

Current Ion Fluxes Through the Sensor Membrane. *Electroanalysis* **2000**, *12* (16), 1286–1292.

(64) Chumbimuni-Torres, K. Y.; Rubinova, N.; Radu, A.; Kubota, L. T.; Bakker, E. Solid Contact Potentiometric Sensors for Trace Level Measurements. *Anal. Chem.* **2006**, *78* (4), 1318–1322.

(65) Cadogan, A.; Gao, Z.; Lewenstam, A.; Ivaska, A.; Diamond, D. All-Solid-State Sodium-Selective Electrode Based on a Calixarene Ionophore in a Poly(Vinyl Chloride) Membrane with a Polypyrrole Solid Contact. *Anal. Chem.* **1992**, *64* (21), 2496–2501.

(66) Sutter, J.; Lindner, E.; Gyurcsányi, R. E.; Pretsch, E. A Polypyrrole-Based Solid-Contact Pb2+-Selective PVC-Membrane Electrode with a Nanomolar Detection Limit. *Anal. Bioanal. Chem.* **2004**, *380* (1), 7–14.

(67) Bobacka, J.; McCarrick, M.; Lewenstam, A.; Ivaska, A. All-Solid-State Poly(Vinyl Chloride) Membrane Ion-Selective Electrodes with Poly(3-Octylthiophene) Solid Internal Contact. *Analyst* **1994**, *119*.

(68) Crespo, G. A.; Macho, S.; Rius, F. X. Ion-Selective Electrodes Using Carbon Nanotubes as Ion-to-Electron Transducers. *Anal. Chem.* **2008**, *80* (4), 1316–1322.

(69) Crespo, G. A.; Macho, S.; Bobacka, J.; Rius, F. X. Transduction Mechanism of Carbon Nanotubes in Solid-Contact Ion-Selective Electrodes. *Anal. Chem.* **2009**, *81* (2), 676–681.

(70) Paczosa-Bator, B. Ion-Selective Electrodes with Superhydrophobic Polymer/Carbon Nanocomposites as Solid Contact. *Carbon* **2015**, *95* (Supplement C), 879–887.

(71) Yan, R.; Qiu, S.; Tong, L.; Qian, Y. Review of Progresses on Clinical Applications of Ion Selective Electrodes for Electrolytic Ion Tests: From Conventional ISEs to Graphene-Based ISEs. *Chem. Speciat. Bioavailab.* **2016**, *28* (1–4), 72–77.

(72) Hernández, R.; Riu, J.; Bobacka, J.; Vallés, C.; Jiménez, P.; Benito, A. M.; Maser, W. K.; Rius, F. X. Reduced Graphene Oxide Films as Solid Transducers in Potentiometric All-Solid-State Ion-Selective Electrodes. *J. Phys. Chem. C* **2012**, *116* (42), 22570–22578.

(73) Mensah, S. T.; Gonzalez, Y.; Calvo-Marzal, P.; Chumbimuni-Torres, K. Y. Nanomolar Detection Limits of Cd2+, Ag+, and K+ Using Paper-Strip Ion-Selective Electrodes. *Anal. Chem.* **2014**, *86* (15), 7269–7273.

(74) Lai, C.-Z.; Fierke, M. A.; Stein, A.; Bühlmann, P. Ion-Selective Electrodes with Three-Dimensionally Ordered Macroporous Carbon as the Solid Contact. *Anal. Chem.* **2007**, *79* (12), 4621–4626.

(75) Szűcs, J.; Lindfors, T.; Bobacka, J.; Gyurcsányi, R. E. Ion-Selective Electrodes with 3D Nanostructured Conducting Polymer Solid Contact. *Electroanalysis* **2016**, *28* (4), 778–786.

(76) Hu, J.; Zou, X. U.; Stein, A.; Bühlmann, P. Ion-Selective Electrodes with Colloid-Imprinted Mesoporous Carbon as Solid Contact. *Anal. Chem.* **2014**, *86* (14), 7111–7118.

(77) Fayose, T.; Mendecki, L.; Ullah, S.; Radu, A. Single Strip Solid Contact Ion Selective Electrodes on a Pencil-Drawn Electrode Substrate. *Anal. Methods* **2017**, *9* (7), 1213–1220.

(78) Novell, M.; Parrilla, M.; Crespo, G. A.; Rius, F. X.; Andrade, F. J. Paper-Based Ion-Selective Potentiometric Sensors. *Anal. Chem.* **2012**, *84* (11), 4695–4702.

(79) Rich, M.; Mendecki, L.; Mensah, S. T.; Blanco-Martinez, E.; Armas, S.; Calvo-Marzal, P.; Radu, A.; Chumbimuni-Torres, K. Y. Circumventing Traditional Conditioning Protocols in Polymer Membrane-Based Ion-Selective Electrodes. *Anal. Chem.* **2016**, *88* (17), 8404–8408.

(80) Mendecki, L.; Fayose, T.; Stockmal, K. A.; Wei, J.; Granados-Focil, S.; McGraw, C. M.; Radu, A. Robust and Ultrasensitive Polymer Membrane-Based Carbonate-Selective Electrodes. *Anal. Chem.* **2015**, *87* (15), 7515–7518.

(81) Hu, J.; Stein, A.; Bühlmann, P. Rational Design of All-Solid-State Ion-Selective Electrodes and Reference Electrodes. *TrAC Trends Anal. Chem.* **2016**, *76* (Supplement C), 102–114.

(82) Dillingham, P. W.; Radu, T.; Diamond, D.; Radu, A.; McGraw, C. M. Bayesian Methods for Ion Selective Electrodes. *Electroanalysis 24*, 316–324.

(83) Duarte, L. T.; Jutten, C.; Moussaoui, S. A Bayesian Nonlinear Source Separation Method for Smart Ion-Selective Electrode Arrays. *IEEE Sens. J.* **2009**, *9*, 1763–1771.

(84) Duarte, L. T.; Jutten, C.; Moussaoui, S. Ion-Selective Electrode Array Based on a Bayesian Nonlinear Source Separation Method. In *Independent Component Analysis and Signal Separation*; Adali, T., Jutten, C., Romano, J. M. T., Barros, A. K., Eds.; Lecture Notes in Computer Science; Springer Berlin Heidelberg, 2009; pp 662–669.

(85) M. Vitousek, P.; A. Mooney, H.; Lubchenco, J.; Melillo, J. Human Domination of Earth's Ecosystems. *Science* **1997**, *277*.

(86) M. Vitousek, P.; D. Aber, J.; Howarth, R.; E. Likens, G.; A. Matson, P.; W. Schindler, D.; Schlesinger, W.; G. Tilman, D. Human Alteration Of The

Global Nitrogen Cycle: Sources And Consequences. *Ecol. Appl.* **1997**, *7*, 737–750.

(87) Díez, J. a.; Hernaiz, P.; Muñoz, M. j.; de la Torre, A.; Vallejo, A. Impact of Pig Slurry on Soil Properties, Water Salinization, Nitrate Leaching and Crop Yield in a Four-Year Experiment in Central Spain. *Soil Use Manag.* **2004**, *20* (4), 444–450.

(88) Smith, K. A.; Jackson, D. R.; Pepper, T. J. Nutrient Losses by Surface Run-off Following the Application of Organic Manures to Arable Land. 1. Nitrogen. *Environ. Pollut. Barking Essex 1987* **2001**, *112* (1), 41–51.

(89) Galloway, J. N.; Townsend, A. R.; Erisman, J. W.; Bekunda, M.; Cai, Z.; Freney, J. R.; Martinelli, L. A.; Seitzinger, S. P.; Sutton, M. A. Transformation of the Nitrogen Cycle: Recent Trends, Questions, and Potential Solutions. *Science* **2008**, *320* (5878), 889–892.

(90) Williams, J. R.; Chambers, B. J.; Nicholson, F.; Thorman, R.; Harris, D.; Chadwick, D. IMPROVING MANURE NITROGEN MANAGEMENT: BENEFITS TO ECOSYSTEM SERVICES; 2012; pp 321–328.

(91) McGeough, K.; Laughlin, R.; Watson, C.; Müller, C.; Ernfors, M.; Cahalan, E.; Richards, K. The Effect of Cattle Slurry in Combination with Nitrate and the Nitrification Inhibitor Dicyandiamide on in Situ Nitrous Oxide and Dinitrogen Emissions. *Biogeosciences* **2012**, *9*, 4909–4919.

(92) Angle, J. S.; Gross, C. M.; Hill, R. L.; McIntosh, M. S. Soil Nitrate Concentrations under Corn as Affected by Tillage, Manure, and Fertilizer Applications. *J. Environ. Qual.* **1993**, *22* (1), 141–147.

(93) Oenema, J.; Burgers, S.; Verloop, K.; Hooijboer, A.; Boumans, L.; Berge, H. ten. Multiscale Effects of Management, Environmental Conditions, and Land

 J. Environ. Qual. **2010**, *39* (6), 2016–2028.

(94) Ruser, R.; Flessa, H.; Russow, R.; Schmidt, G.; Buegger, F.; Munch, J. C. Emission of N2O, N2 and CO2 from Soil Fertilized with Nitrate: Effect of Compaction, Soil Moisture and Rewetting. *Soil Biol. Biochem.* **2006**.

(95) Delon, C.; Mougin, E.; Serça, D.; Manuela, G.; Hiernaux, P.; Diawara, M.; Corinne, G.-L.; Kergoat, L. Modelling the Effect of Soil Moisture and Organic Matter Degradation on Biogenic NO Emissions from Soils in Sahel Rangeland (Mali). *Biogeosciences Discuss.* **2015**, *12*, 1155–1203.

(96) Oenema, O. Nitrogen Budgets and Losses in Livestock Systems. *Int. Congr. Ser.* **2006**, *1293* (Supplement C), 262–271.

(97) Rosenstock, T.; Liptzin, D.; Six, J.; Tomich, T. Nitrogen Fertilizer Use in California: Assessing the Data, Trends and a Way Forward. *Calif. Agric.* **2013**, *67* (1), 68–79.

(98) Palmes, K.; Cabanilla, C.; Canillas, N.; Molinos, J. EFFECTS OF PH, INITIAL NITRATE CONCENTRATION AND ZEOLITE LOADING ON THE REMOVAL OF NITRATES FROM SYNTHETIC WASTEWATER USING RICE HUSK-DERIVED ZEOLITE, 2016.

(99) Rotz, C. A.; Taube, F.; P. Russelle, M.; Oenema, J.; Sanderson, M.; Wachendorf, M. Whole-Farm Perspectives of Nutrient Flows in Grassland Agriculture. *Crop Sci.* **2005**, *45*.

(100) Kim Loan, D.; Hong Con, T.; Hong, T.; Luong, M. L. Quick Determination of Ammonia Ions in Water Environment Based on Thymol Color Creating Reaction. *Environ. Sci.* **2013**, *1*, 83–92.

(101) Grizzetti, B.; Bouraoui, F.; Billen, G.; Grinsven, H.; Cardoso, A.; Thieu, V.; Garnier, J.; Curtis; Howarth, R.; Johnes, P. *Nitrogen as a Threat to European Water Quality*; 2011.

(102) Hunt, D., t; dee, a. s; oakes, d. b. Updating an Estimate of the Source Apportionment of Nitrogen to Waters in England and Wales http://www.fwr.org/defrawqd/wqd0002.htm (accessed Oct 8, 2018).

(103) Postma, D.; Boesen, C.; Kristiansen, H.; Larsen, F. Nitrate Reduction in an Unconfined Sandy Aquifer: Water Chemistry, Reduction Processes, and Geochemical Modeling. *Water Resour. Res.* **1991**, *27* (8), 2027–2045.

(104) Kirchmann, H.; Johnston, A. E. J.; Bergström, L. F. Possibilities for Reducing Nitrate Leaching from Agricultural Land. *AMBIO J. Hum. Environ.* **2002**, *31* (5), 404–408.

(105) Jordan, C.; Smith, R. V. Methods to Predict the Agricultural Contribution to Catchment Nitrate Loads: Designation of Nitrate Vulnerable Zones in Northern Ireland. *J. Hydrol.* **2005**, *304* (1), 316–329.

(106) Song, X.-Z.; Zhao, C.-X.; Wang, X.-L.; Li, J. Study of Nitrate Leaching and Nitrogen Fate under Intensive Vegetable Production Pattern in Northern China. *C. R. Biol.* **2009**, *332* (4), 385–392.

(107) Fan, A. M.; Steinberg, V. E. Health Implications of Nitrate and Nitrite in Drinking Water: An Update on Methemoglobinemia Occurrence and Reproductive and Developmental Toxicity. *Regul. Toxicol. Pharmacol. RTP* **1996**, *23* (1 Pt 1), 35–43.

(108) Cherian, T.; Narayana, B. A New System for the Spectrophotometric Determination of Trace Amounts of Nitrite in Environmental Samples. *J. Braz. Chem. Soc.* **2006**, *17* (3), 577–581.

(109) Shao, Y.; He, Y. Nitrogen, Phosphorus, and Potassium Prediction in Soils, Using Infrared Spectroscopy. *Soil Res.* **2011**, *49* (2), 166–172.

(110) Blasco, B.; Rios, J. J.; Cervilla, L. M.; Sánchez-Rodríguez, E.; Rubio-Wilhelmi, M. M.; Rosales, M. A.; Romero, L.; Ruiz, J. M. Iodine Application Affects Nitrogen-Use Efficiency of Lettuce Plants (Lactuca Sativa L.). *Acta Agric. Scand. Sect. B — Soil Plant Sci.* **2011**, *61* (4), 378–383.

(111) Edwards, A. C.; Hooda, P. S.; Cook, Y. Determination of Nitrate in Water Containing Dissolved Organic Carbon by Ultraviolet Spectroscopy. *Int. J. Environ. Anal. Chem.* **2001**, *80* (1), 49–59.

(112) Brunet, D.; Barthes, B.; Chotte, J.-L.; Feller, C. Determination of Carbon and Nitrogen Contents in Alfisols, Oxisols and Ultisols from Africa and Brazil Using NIRS Analysis : Effects of Sample Grinding and Set Heterogeneity. *Geoderma* **2007**, *139* (1–2), 106–117.

(113) Payero, J.; Tarkalson, D.; Irmak, S. Use Of Time Domain Reflectometry For Continuous Monitoring Of Nitrate-Nitrogen In Soil And Water. *Biol. Syst. Eng. Pap. Publ.* **2006**.

(114) Schmidhalter, U. Development of a Quick On-Farm Test to Determine Nitrate Levels in Soil. *J. Plant Nutr. Soil Sci.* **2005**, *168* (4), 432–438.

(115) Martínková, E.; Křžek, T.; Coufal, P. Determination of Nitrites and Nitrates in Drinking Water Using Capillary Electrophoresis. *Chem. Pap.* **2014**, *68* (8), 1008–1014.

(116) Padarauskas, A.; Paliulionyte, V.; Pranaityte, B. Single-Run Capillary Electrophoretic Determination of Inorganic Nitrogen Species in Rainwater. *Anal. Chem.* **2001**, *73* (2), 267–271.

(117) Moliner-Martínez, Y.; Herráez-Hernández, R.; Campíns-Falcó, P. Improved Detection Limit for Ammonium/Ammonia Achieved by Berthelot's Reaction by Use of Solid-Phase Extraction Coupled to Diffuse Reflectance Spectroscopy. *Anal. Chim. Acta* **2005**, *534* (2), 327–334.

(118) Rendl, J.; Bier, D.; Groh, T.; Reiners, C. Rapid Urinary Iodide Test. *J. Clin. Endocrinol. Metab.* **1998**, *83* (3), 1007–1012.

(119) Zhang, W.; Mnatsakanov, A.; Hower, R.; Cantor, H.; Wang, Y. *Urinary Iodine Assays and Ionophore Based Potentiometric Iodide Sensors*; 2005; Vol. 10.

(120) Dunn, J. T. Iodine Deficiency--the next Target for Elimination? *N. Engl. J. Med.* **1992**, *326* (4), 267–268.

(121) Shelor, C. P.; Dasgupta, P. K. Review of Analytical Methods for the Quantification of Iodine in Complex Matrices. *Anal. Chim. Acta* **2011**, *702* (1), 16–36.

(122) Pearce, E. N.; Andersson, M.; Zimmermann, M. B. Global Iodine Nutrition: Where Do We Stand in 2013? *Thyroid Off. J. Am. Thyroid Assoc.* **2013**, *23* (5), 523–528.

(123) Gnat, D.; Dunn, A. D.; Chaker, S.; Delange, F.; Vertongen, F.; Dunn, J. T. Fast Colorimetric Method for Measuring Urinary Iodine. *Clin. Chem.* **2003**, *49* (1), 186–188.

(124) Jooste, P. L.; Strydom, E. Methods for Determination of Iodine in Urine and Salt. *Best Pract. Res. Clin. Endocrinol. Metab.* **2010**, *24* (1), 77–88.

(125) Foss, O. P.; Hankes, L.; Van Slyke, D. D. A Study of the Alkaline Ashing Method for Determination of Protein-Bound Iodine in Serum. *Clin. Chim. Acta Int. J. Clin. Chem.* **1960**, *5*, 301–326.

(126) Stuewer, D.; Jakubowski, N. Elemental Analysis by Inductively Coupled Plasma Mass Spectrometry with Sector Field Instruments: A Progress Report. *J. Mass Spectrom.* **1998**, *33* (7), 579–590.

(127) Macours, P.; Aubry, J. C.; Hauquier, B.; Boeynaems, J. M.; Goldman, S.; Moreno-Reyes, R. Determination of Urinary Iodine by Inductively Coupled Plasma Mass Spectrometry. *J. Trace Elem. Med. Biol.* **2008**, *22* (2), 162–165.

Chapter 2 Single strip solid contact ion selective electrodes on simple platform prepared using household items

2.1 Introduction

Over the past decade, significant effort has been placed into developing techniques and methodologies that are fully applicable to real-time sample analysis while significantly lowering per-sample and per-measurement costs. Such advancements are expected to make a great impact in many different fields ranging from environmental analysis to health, security, and manufacturing industries.

Ion selective electrodes (ISEs) are a class of chemical sensors that, in recent years, went through a renaissance and showed excellent potential as tools for routine environmental monitoring and clinical analysis. They are easy to manufacture, show excellent selectivity and sensitivity, are readily miniaturized and can be connected to simple communication devices.

Recently, several studies have focused on the development of paper-based ISEs utilizing carbon nanotubes (CNTs) either as the underlying solid contact (electron conductor) or as ion to electron transducer separating the solid contact from the ion selective membrane.[1–10] This versatile character can be attributed to their excellent electrical conductivity, high tensile strength and ability to function simultaneously as recognition element and transducer (transduction via the formation of electrical double layer).[11–15] Moreover, inherent hydrophobicity of CNTs prevents water layer formation between the membrane and the underlying substrate.[7,16] Interestingly, other reports indicate that the presence of sputtered gold and conductive polymer such as poly(3-octylthiophene) is necessary to produce stable paper based ISEs.[5]

This discrepancy between reported data could perhaps arise from differences in the thickness of CNTs layer deposited onto the paper surface, the concentration of surfactant (unwashed surfactant may reduce contact angle between water droplet and the substrate, thus increasing surface wetting)[17] and purity of used materials.

However, to produce functional sensing devices, CNTs have to be typically dispersed in a liquid[18–20] (often water and surfactant solution) via ultrasonication and are later deposited onto the paper/electrode by drop-casting,[21,22] ink-jet printing,[23–25] dip-coating[26–28] or spin coating.[27,29] Such processes may take several hours and are strongly limited by the low solubility of CNTs in most solvents,[20,30] the need of specialized instrumentation for the preparation of ISEs (ultarsonicator; sputter coater) and relatively high cost of materials required (e.g. CNTs and gold). Recently, mechanical abrasion of compressed single- or multi-walled CNTs directly onto the surface of the paper was suggested as an alternative approach to develop chemiresistive sensors for gas detection.[31–35] These sensing devices exhibited sufficient conductivity (10-30 kΩ) and showed similar/improved sensing characteristics to their counterparts prepared using solvent-dispersion techniques.

More recently, pencil drawn electrodes (PDEs) prepared via mechanical abrasion of graphite on solid substrate have been developed and used as voltammetric sensors for the detection of metal ions.[36–38] They offered very good performance characteristics while maintaining low cost and ease of fabrication.

Previously, weighing paper (compressed cellulose) has been identified as an excellent substrate for the fabrication of sensing devices using both solvent and solvent-free methods.[6,39–44] The widespread use of paper arises from its global accessibility, low manufacturing cost and high compatibility with various printing devices.[40,41,45–49]

Moreover, it is a common substrate for abrasion based drawing and writing using wax or graphite pencils.[31–34,50] The transport of water by capillary action in paper is identified as an important advantage in designing microfluidic devices. However, the same phenomenon may lead to potential instability in ISEs – diffused water is absorbed by the paper and transported towards the connectors. Therefore, special attention should be drawn to cheap, accessible and more hydrophobic surfaces that could be used as alterative materials to commonly employed weighting/filter paper in ISEs.

An important consequence of the above analysis is that despite of the significant simplification and cost reduction, preparation of sensors is still limited to highly skilled personnel and/or access to specialized chemicals. Interestingly, we have witnessed highly exciting advances in fields that were able to open its doors to members of public. Citizen science contributed to a wide variety of fields from astronomy, to zoo science and even to art history. The growth of fields like Big Data heavily relies on the ability to collect large amounts of data, and it has been argued that the next big leap in communication will happen by integrating chemical sensors with mobile communication devices.[35,51,52] Clearly, to enable such advances in chemistry, it would be important to involve members of the public in the collection of chemical data. This could be achieved with sensors that are so simple and cheap that citizens can prepare and use them at home using simple household items.

Herein, an approach to prepare ultra-simple and inexpensive ISE platforms by using commonly accessible household items was demonstrated. The electron conductive layer was prepared by mechanical abrasion of a very cheap graphite pencil directly onto a substrate cut from acetate sheet, while the whole setup was finished using simple adhesive tape (e.g. sellotape). All materials are readily available in ordinary

bookstores. After the application of ion selective membranes, the performance of such sensing devices was assessed for the determination of biologically and environmentally important ions.

2.2 Experimental

2.2.1 Reagents

Nonactin (ammonium ionophore I), sodium ionophore X (4-tert-Butylcalix[4]arene-tetraacetic acid tetraethylester), sodium tetrakis[3,5-bis- (trifluoromethyl)-phenyl]borate (NaTFPB), tetradodecylammonium chloride (TDMACl), poly-(3-octylthiophene) (POT), high molecular weight poly(vinyl chloride) (PVC), bis(2-ethylhexyl)- sebacate (DOS), 2-nitrophenyl octyl ether (σ-NPOE), and tetrahydrofuran (THF) were obtained from Sigma-Aldrich. All aqueous solutions were prepared in ultra-pure water obtained with Purelab Ultra water purification system (resistance 18 MΩ cm).

2.2.2 Preparation of pencil-drawn conductive substrate

Firstly, a 1.5 cm x 3.0 cm strip was cut from a parent office-type acetate sheet and was subsequently etched with aluminium oxide (grit240) for 30 s to provide the surface with enhanced porosity in order to improve adhesion of graphite onto the surface of acetate. With the use of a typical graphite pencil, a line of carbon was applied/drawn by hand onto the acetate sheet. In this work, pencils used were from a set called Artists' Pencils, which contained 10 pencils of different hardness going from 4B to 4H indicating that the ratio of graphite to clay decreases in order to provide increasing hardness. The schematic of the fabrication of each sensor is shown in figure 2.1. The steps are described below as; Step I: acetate paper roughened by sand paper to allow for step II. Step II: sensor made conductive by drawing a line of carbon on acetate paper using household pencils. Step III: insulation provided to the platform through an office-type sellotape leaving a small opening at the distal end of the platform for

electrical contact. (Note, a hole of about 0.3 cm in diameter was previously punched on one end of the sellotape to serve as an aperture to allow for the application of POT/ion selective membrane layers. Step IV: the application of membrane components by drop casting suitable cocktails.

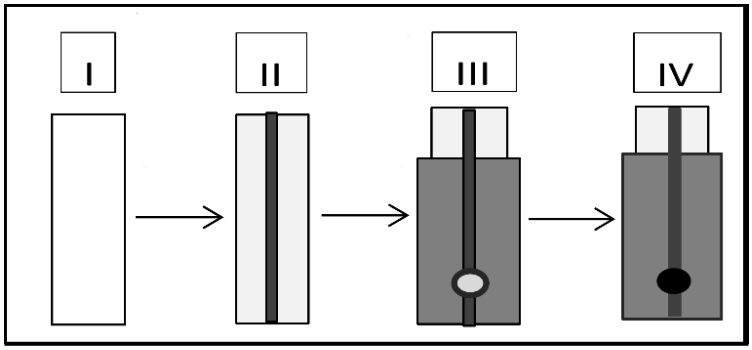

Figure 2.1 Schematic representation of paper electrodes fabricated via mechanical abrasion as discussed in section 2.2.2.

2.2.3 Preparation of sodium-, nitrate- and ammonium-sensing membranes, and solid-contact reference electrode

The NO_3^--selective membrane contained 5.0 mmol/ kg of TDMACl, PVC (33.2 wt %) and σ-NPOE (66.4 wt %). Na^+- and NH_4^+- selective membranes contained 10.0 mmol/ kg of sodium ionophore X and ammonium ionophore I respectively, 5.0 mmol/ kg of NaTFPB, PVC (32.9 wt %) and DOS (65.8 wt %). Solid-contact reference electrode contained 12.5 % tetrabutylammonium tetrabutylborate (TBA-TBB), PVC (29.2 wt %) and σ-NPOE (58.3 wt %). All electrodes were prepared by dissolving the above-mentioned components in 1.5 mL THF and the resulting cocktail was vortexed for 30 mins for complete dissolution of components.

2.2.4 Development of ISEs

For potentiometric measurements, a solution of POT, derived from previously dissolving 10^{-3} M of the monomer in chloroform, was drop cast onto the aperture of the graphite-based electrodes (for measurements involving POT underlay), or otherwise electrodes were used without POT. The electrodes were then left at room temperature to dry. An aliquot (∼20 μL) of each sensing membrane was then drop cast straight onto the top of each electrode and unto the POT layers of those sensors previously lain with POT, and further left at room temperature to dry overnight. The following day, ISEs were conditioned in 1.0 x 10^{-3} M of respective primary ion solution while the reference electrodes were conditioned in 1.0 x 10^{-2} M of KCl for 18 h prior to the potentiometric experiments.

2.2.5 Preparation of all-solid state single strip potentiometric sensing device

A 10.0 × 3.0 cm strip was cut from parent acetate sheet as was prepared as explained above. Nine lines were subsequently drawn by pencil and electrodes prepared to form a strip that contained one solid contact reference electrode, four NO_3^- - and four NH_4^+ - selective electrodes as illustrated in the Figure 2.2.

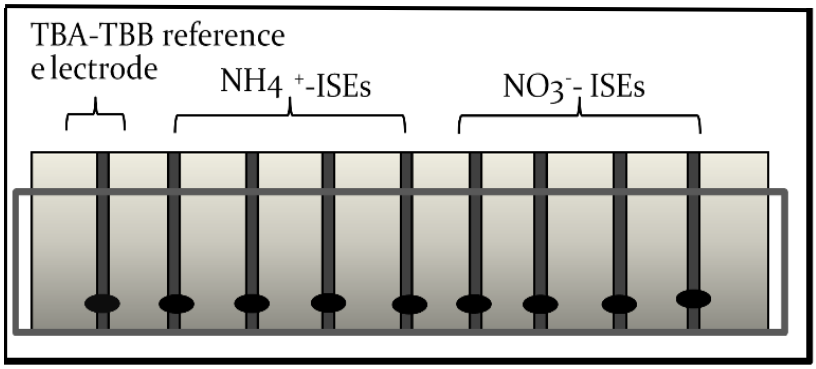

Figure 2.2. A schematic representation of the single strip potentiometric device where one electrode was used for deposition of all-solid-contact reference electrode based on TBA-TBB and the rest used for deposition of the cocktails for required ISEs.

2.2.6 EMF measurements

Potentiometric responses of all electrodes were recorded using Lawson Labs Inc. 16-channel EMF-16 interface (3217 Phoenixville Pike Malvern, PA 19355, USA) in a stirred solution against a double-junction Ag/AgCl reference electrode with a 1 M LiOAc bridge electrolyte (Fluka), except in the case of single strip electrodes when all-solid-contact reference electrode was used. All ISEs were immersed in sample solution (ultra-pure water) followed by addition of aliquots of known concentration of the required salt.

2.2.7 Selectivity measurements

The ammonium-selective electrodes were prepared and conditioned in 0.1 M NaCl, while the nitrate-selective electrodes were conditioned in 0.1 M $MgSO_4$. Responses towards interfering ions were recorded according to separate solution method as described by Bakker.[53]

2.2.8 Electrochemical impedance spectroscopy (EIS)

Electrochemical impedance measurements were performed by using an Ivium Technologies CompactStat Impedance Analyser coupled to a Himux XR 8 channel electrochemical multiplexer (Ivium Technologies). The EIS measurements of the ion selective membranes were performed as described previously.[51] Briefly, EIS spectra were collected using excitation amplitude of 0.01 V within the frequency range spanning from 100 kHz to 0.1 Hz for graphite electrodes only (no membrane). However, amplitude of 0.1 V was used for electrodes coated with ion selective membrane to improve signal to noise ratio. A conventional three electrodes set-up was used in this study using platinum auxiliary electrode and a silver-silver chloride electrode as the reference. Each measurement was carried out at open-circuit potential in 0.1 M solutions of metal salts at room temperature. All impedance spectra were fitted to equivalent circuits using the IviumStat software version 2.0. The impedance measurements were repeated several times to analyze the capacitance and resistance properties of the sensors.

2.3 Results and Discussion

2.3.1 Characterisation of different graphite-substrates by scanning electron microscope (SEM) with energy dispersive X-ray spectroscopy (EDS)

To test for surface pattern of the sensors, a piece of modified acetate papers were manually shaded with different pencils ranging from 4B to 4H, and scanned by scanning electron microscope (SEM). As shown in figures 2.3 (a - c), the SEM images showed almost the same pattern, with no obvious difference in the surface of the measured papers. Also, to test for the impact different contents of pencils used could have on the sensor performance, spectra showing compositions were obtained by energy dispersive X-ray spectroscopy (EDS) attached to the SEM. Interestingly, there were no differences in the concentrations of carbon and silicon obtained using EDS across the set of pencils. Normally, it is generally perceived that different grades of pencils show some variations in their intrinsic hardness, as a result of the ratio of the percentage carbon and silicon within – a reason that sometimes explains the dark black colours of pencils, or their shinny properties, it was surprising the ratios were similar in this case for all the pencils tested.

Nevertheless electrodes prepared using all pencil types from the box as well as 4B pencils from three different boxes showed no significantly different potentiometric results originating from the pencil type or box. Number of abrasions also did not show to be relevant – it was only important that the resistance of the drawn line is $< \sim 50$ kΩ.

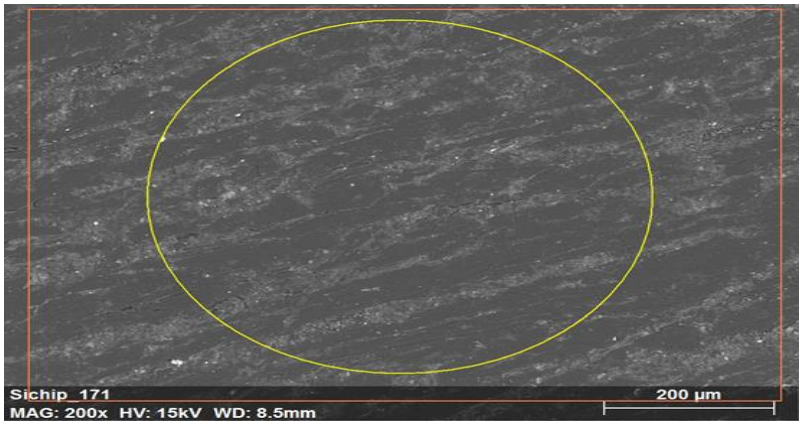

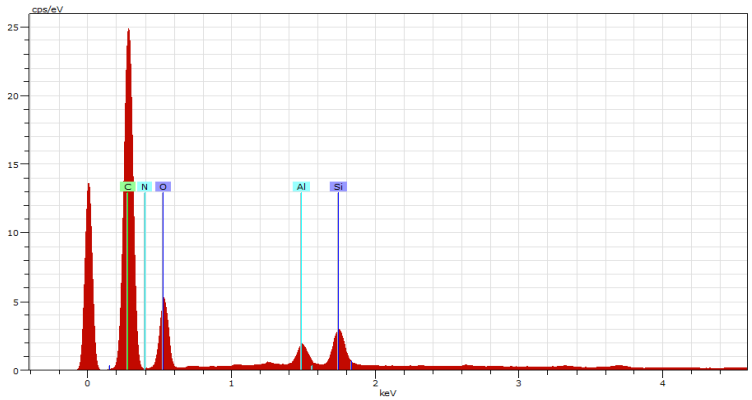

Spectrum: Point

Element	AN	Series	Net unn. C [wt.%]	norm. C [wt.%]	Atom. C [at.%]	Error [%]
Carbon	6	K-series	98918	64.68	64.68	71.37	6.9
Oxygen	8	K-series	20860	27.60	27.60	22.86	3.2
Nitrogen	7	K-series	1189	4.43	4.43	4.19	0.7
Silicon	14	K-series	14460	2.14	2.14	1.01	0.1
Aluminium	13	K-series	7523	1.16	1.16	0.57	0.1
		Total:		100.00	100.00	100.00	

Figure 2.3 a SEM and EDS of 4B pencil

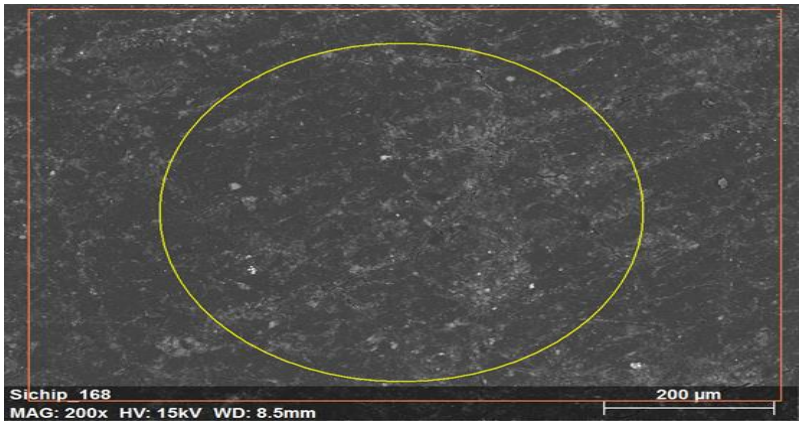

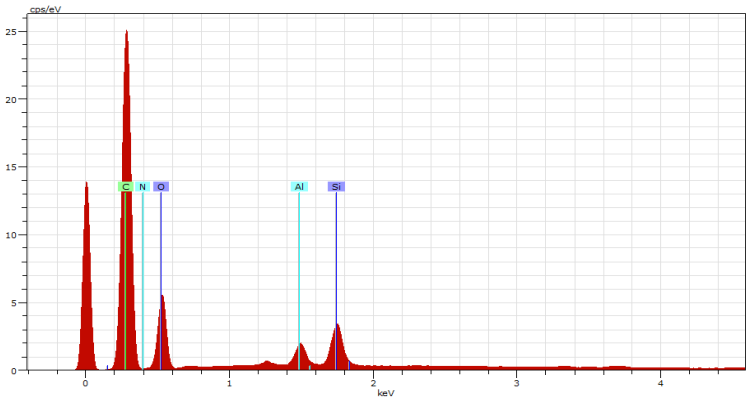

Spectrum: Point

Element	AN	Series	Net unn. C [wt.%]	norm. C [wt.%]	Atom. C [at.%]	Error [%]
Carbon	6	K-series	91788	64.23	64.23	71.00	6.9
Oxygen	8	K-series	20143	27.98	27.98	23.22	3.2
Nitrogen	7	K-series	1113	4.36	4.36	4.13	0.7
Silicon	14	K-series	14839	2.32	2.32	1.10	0.1
Aluminium	13	K-series	6831	1.12	1.12	0.55	0.1
		Total:		100.00	100.00	100.00	

Figure 2.3b SEM and EDS of HB pencil

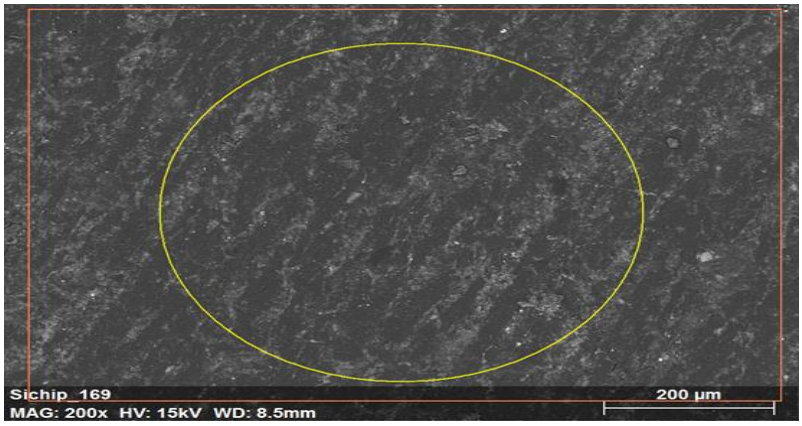

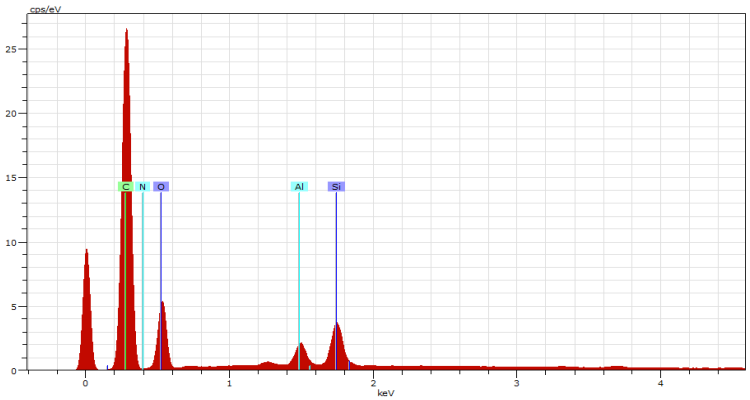

Spectrum: Point

Element	AN	Series	Net unn. C [wt.%]	norm. C [wt.%]	Atom. C [at.%]	Error [%]
Carbon	6	K-series	114695	65.45	65.45	72.18	7.0
Oxygen	8	K-series	23356	26.79	26.79	22.18	3.1
Nitrogen	7	K-series	1278	4.15	4.15	3.92	0.7
Silicon	14	K-series	19329	2.45	2.45	1.16	0.1
Aluminium	13	K-series	8737	1.16	1.16	0.57	0.1
		Total:		100.00	100.00	100.00	

Figure 2.3c SEM and EDS of 4H pencil

2.3.2 Impedance measurement of platforms based on graphite substrate

To evaluate the charge transfer efficiency of the graphite deposited directly onto the acetate platforms, impedance spectrum was recorded for bare graphite-based platforms that contained no membrane. As shown in figure 2.4, it is instantly apparent that the EIS spectrum is dominated by the presence of 90° line that resembles capacitive behavior, thus indicating fast charge transport at the graphite/solution interface as reported previously.[1]

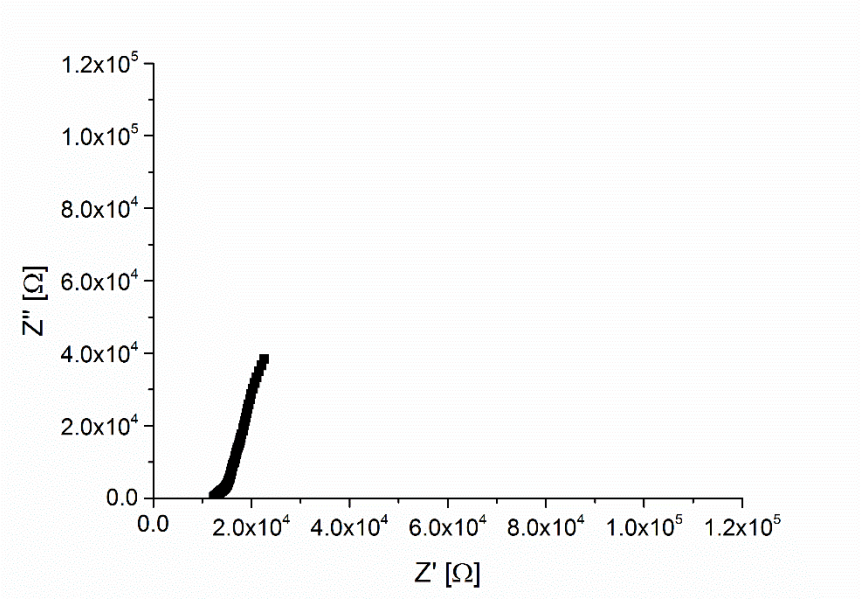

Figure 2.4 Impedance spectrum of a randomly selected electrode made of graphite deposited onto the acetate substrate via mechanical abrasion.

Note that the intercept of the line with the real axis (Z) is determined by the electrolyte resistance rather than by the ohmic resistance of the capacitive (graphite) coating. The small distortion in shape from the ideal 90° response may have arisen from chemical inhomogeneity of the deposited graphite layer, as commercially available pencils can contain significant amounts of clays and other additives that can contribute towards impedance response. Moreover, physical irregularities at the electrode's surface

caused by mechanical abrasion (drawing) of graphite on acetate sheet may produce distortions from the expected theoretical response. Nevertheless, the response for the graphite-coated acetate platform shown above still resembles those obtained for electrodes based on the presence of CNTs, thereby demonstrating that graphite can be used as effective signal transducer.[1,7,8]

However, further studies have to be carried out to understand the above-mentioned transduction mechanism.

2.3.3 Characterization of ISEs based on graphite-substrate using EIS

The presence of a semicircle at high frequency region in figure 2.5 demonstrates that only one relaxation process takes place during impedance measurement. The frequency dispersion in the recorded EIS spectrum resembles a compressed semicircle that is equivalent to membrane resistance in parallel with a geometric capacitance of the membrane. Roughened surface of the electrodes and membrane inhomogeneity have been previously indicated to cause deformations in the impedance spectrum of analyzed polymeric membranes.[52] However, in the context of this work, the frequency distortion can be attributed to the local differences in the thickness of the casted membrane (roughened outer surface due to solvent evaporation).[53] The bulk resistances of membranes deposited directly onto the graphite contact and those prepared with underlying POT layer were found 15.4 ± 0.01 and 16.7 ± 0.01 MΩ, respectively. The discrepancy in measured resistance values may be due to differences in the thickness of ion selective membranes (95 μm for graphite electrodes and 110 μm for POT-on-graphite ISEs). The lack of a second 'kinetic' semicircle in the low frequency part of the spectrum indicates that both the phase-transfer of ions through the solution/membrane interface and transduction from ionic into electronic signal at

the membrane/solid contact interface are fast. This observed behavior for polymeric membrane on graphite ISEs was also observed for ISEs prepared with a conductive polymer like poly-(3-octylthiophene) POT, separating membrane from underlying solid contact (data not shown). Since POT-based electrodes have a well-defined signal transduction mechanism (via electrical double layer) and their impedance characteristics have been extensively studied, one can assume that the lack of a second semicircle in the impedance spectrum of the graphite-based electrodes strengthens the hypothesis that graphite can be used as signal transducer in ISEs.

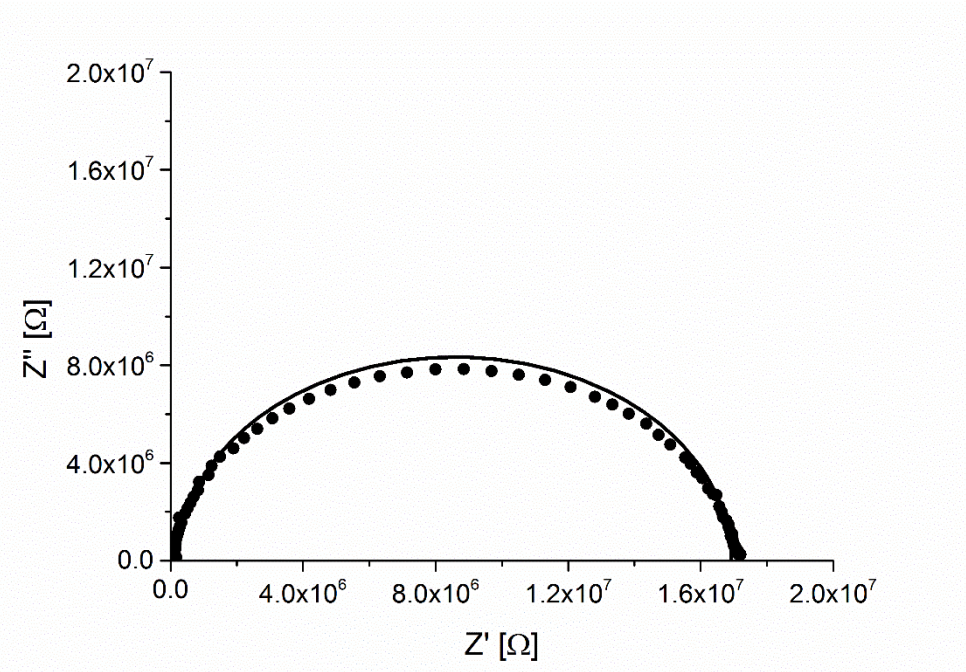

Figure 2.5 Impedance spectrum of the ion selective membrane deposited directly onto graphite-substrate.

2.3.4 Water layer test

It has been previously reported that the presence of a thin aqueous layer between the solid contact and a membrane in ISEs can lead to potential instability and thus limit

long term application of the electrodes.[54] To study if a water layer has been formed, both graphite/ISM and graphite/POT/ISM electrodes were initially conditioned in 0.1 M solution of primary ions for 24 h. Subsequently, all electrodes were placed in the solution of discriminated ions for 4 h and then transferred back into the primary ion solution. No potential drift was observed for graphite and graphite/POT electrodes during the initial exposure to primary ions, as demonstrated in Figure 2.6. The same response characteristics were observed for all electrodes placed in 0.1 M NaCl solution and then exposed to 0.1 M NH_4Cl solution. The lack of potential drift during the measurement indicates that no aqueous layer is formed between the ion selective membrane and underlying solid contact.

These findings could be attributed to the inherent hydrophobicity of both POT and graphite components. Moreover, it indicates that graphite is a suitable alternative to CNTs, which, up to this date, have been extensively used for the preparation of paper-based ISEs. Herein, mechanically deposited graphite demonstrates a stable redox potential and an ability to exhibit ion-to-electron transduction mechanism when used as conductive substrate in ISEs. Therefore, it would be beneficial to use graphite instead of CNTs to manufacture very cheap and simple electrodes without the need of using solvent chemistry, as is often required for the preparation of electrodes based on CNTs.

Furthermore, graphite pencils are very inexpensive and widely accessible which opens more avenues for the application of ISEs worldwide, such as in developing countries. It should be noted that improved signal stability of these proposed electrodes may also be attributed to the use of a water-repelling solid substrate such as acetate sheet rather than ordinary paper (e.g. filter paper). Inherent hydrophobicity of acetate sheet reduces the risk of water diffusion through capillary action (as observed in paper), which

minimizes signal instability that could be caused by water contacting the electrical conductor. Therefore, the possibility for application of graphite onto acetate sheet (via mechanical abrasion) creates endless possibilities to develop a new wave of simplified and accessible ISEs.

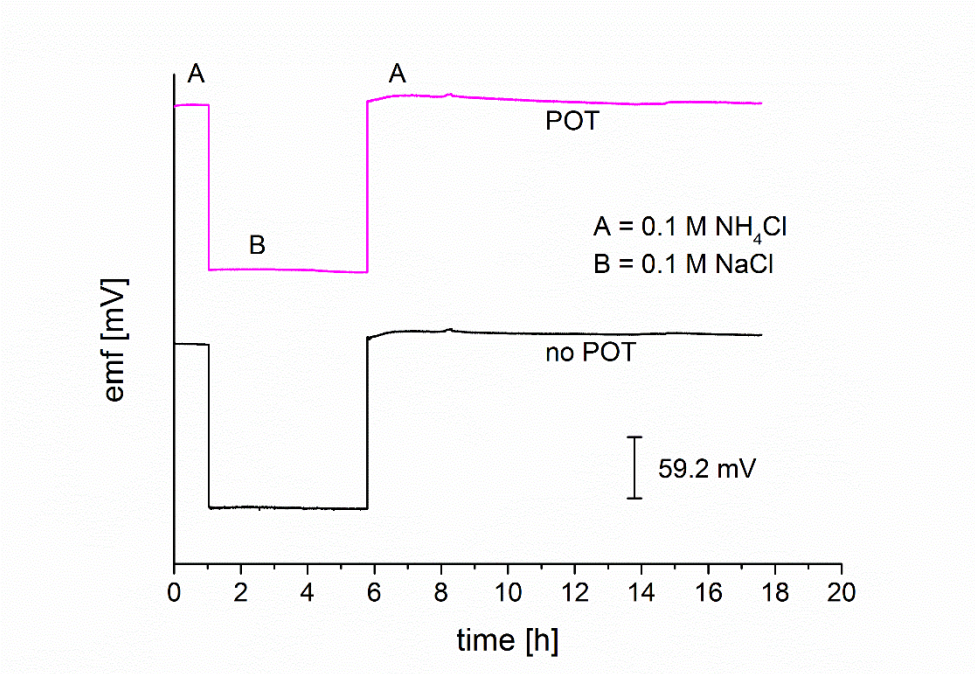

Figure 2.6 Water film tests of solid-contact NH_4^+-ISE based on graphite/NH_4^+ ISM and of the graphite/POT/NH_4^+ ISM. At t = 1 h, the solution of the primary ion (0.1 M NH_4Cl) was exchanged to 0.1 M NaCl, and after 5 h, the sample was replaced by the initial solution, and kept for another 12 h.

2.3.5 Potentiometric response of ISEs based on graphite substrate

To demonstrate the applicability of graphite as a conductive substrate in the development of mechanically drawn ion selective electrodes, ammonium, sodium and

nitrate electrodes were fabricated and their potentiometric behavior was evaluated. ISEs for NH_4^+ and Na^+ ions with or without a layer of conductive polymer were compared. Conductive polymers like poly-(3-octylthiophene) (POT), polypyrrole, play an important role in improving conductivity of solid contact electrodes and are also seen as an effective barrier to reduce water layer formation between interface of ion selective membrane and the substrate.[14] Figure 2.7 (A and B) show potentiometric responses of NH_4^+ and Na^+ electrodes, including response for electrode configuration of both ions without a POT underlay. Similar potentiometric responses observed for both set-ups support the findings obtained from the water layer test. This demonstrates that graphite is a suitable material for the preparation of ISEs due to its high hydrophobicity and also suggests acetate sheet as an optimal contact interface for the ISM.

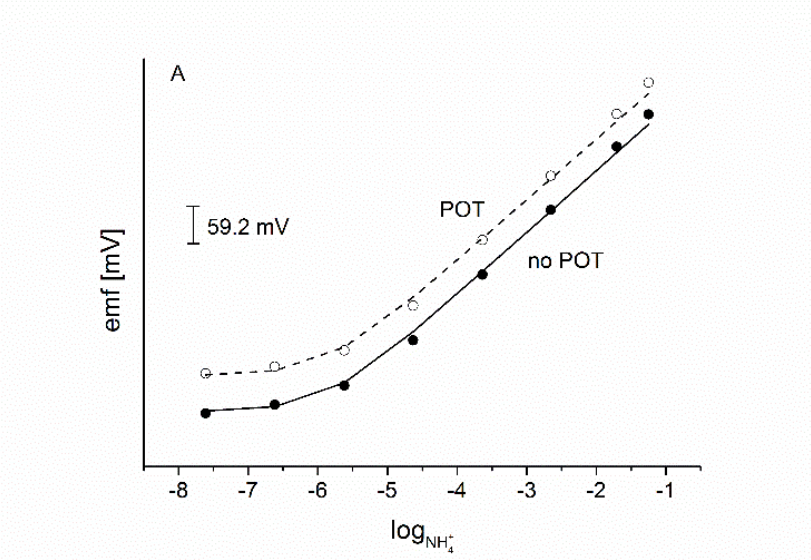

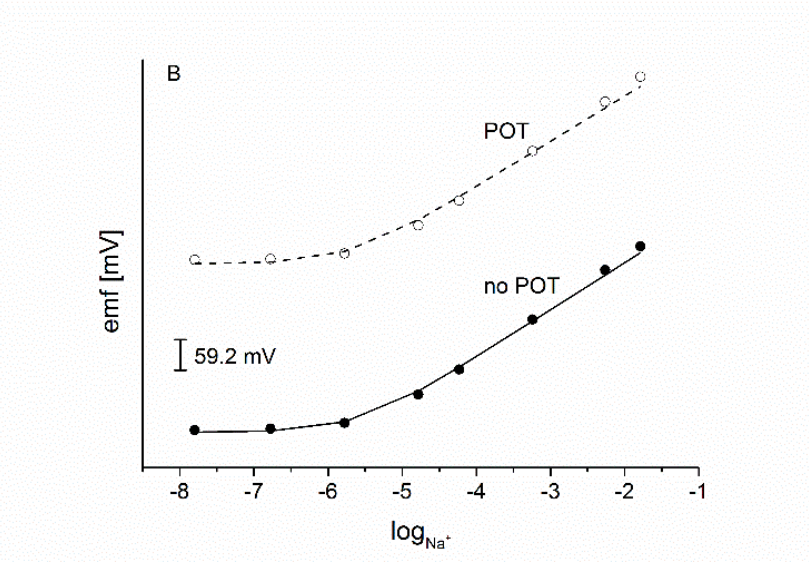

Figure 2.7 Comparison of the effect of conductive polymer POT on the potential stability of A) NH_4^+ and B) Na^+-ISE. Close circles represents acetate sheet/graphite- while open circles denotes acetate sheet/graphite/POT – based electrodes.

The test for the unbiased selectivity coefficients of NH_4^+- and NO_3^- - selective electrodes obtained with the separate solution method. The results in table 2.1 and table 2.2 for ions tested for both ammonium and nitrate electrodes show near-Nernstian slopes, which is a key factor for selectivity coefficient measurement using the separate solution method. The experimentally obtained values in table 2.1 show superior selectivity of the ammonium ISEs over sodium and cesium, and slightly towards potassium. However, while the selectivity results for the nitrate electrodes towards the measured anions were expected, positive values for iodide and perchlorate ions means high preference of the nitrate ISEs towards those ions.

Overall, the measured selectivity values closely match those reported for other electrodes based on solid contact design,[6,58–60] which indicates that graphite can be successfully employed as a conductive substrate for the preparation of ISEs without having any significant influence on their potentiometric response characteristics.

Table 2.1 Selectivity coefficients for selected ions obtained for NH_4^+ - selective electrode using acetate sheet/graphite – based substrate and traditional membrane composition.

Ion	$logK_{I,J}^{pot}$ ± S.D	Slope ± S.D
Na^+	-2.96 ± 0.03	57.53 ± 0.27
Cs^+	-2.56 ± 0.03	54.05 ± 0.06
K^+	-0.98 ± 0.02	55.24 ± 0.15
NH_4^+	0	56.35 ± 0.30

Table 2.2 Selectivity coefficients for selected ions obtained for NO_3^- - selective electrode using acetate sheet/graphite – based substrate and traditional membrane composition.

Ion	$logK_{I,J}^{pot}$ ± S.D	Slope ± S.D
Cl^-	-2.48 ± 0.02	-52.93 ± 0.30
NO_2^-	-1.27 ± 0.03	-53.57 ± 0.54
I^-	1.4 ± 0.03	-55.24 ± 0.15
CLO_4^-	3.25 ± 0.02	-54.35 ± 0.25
NO_3^-	0	-55.78 ± 0.21

2.3.6 Long-term stability of graphite-based ISEs

To this day, only a small number of non-disposable paper-based ISEs have been reported, as they often exhibit poor performance over time. Limited robustness of such sensing devices can be attributed to either mechanical issues related to the

substrate/conductor itself (fragility of paper, washing away CNTs due to the presence of surfactant on the surface) or chemical problems caused by leaching of components from ISM into the sample. Therefore, long-term stability studies was aimed to assess whether the mechanically deposited graphite layer (onto the modified acetate sheet) could be used to fabricate ISEs for prolonged and repeated potentiometric measurements. For that purpose, the potentiometric behavior of seven graphite/NH_4^+ electrodes (i.e. containing no POT as intermediate layer) was studied at different day intervals for a total number of 14 days. Prior to use, electrodes were conditioned overnight in 1.0 x 10^{-3} M NH_4Cl solution after casting. For potentiometric calibrations, the same electrodes were allowed to rehydrate one hour before commencing successive additions of ammonium standards. After each measurement, all electrodes were thoroughly rinsed with the deionized water and then stored dry until the next use. Overall, figure 2.8 (electrode 1-7) demonstrates exceptional reproducibility of ISEs over the given time. Average response slope of electrodes from day 1 through till day 14 was 53.2 ± 0.68 mV/decade with response range being 1.0 x 10^{-5} M to 1.0 x 10^{-1} M.

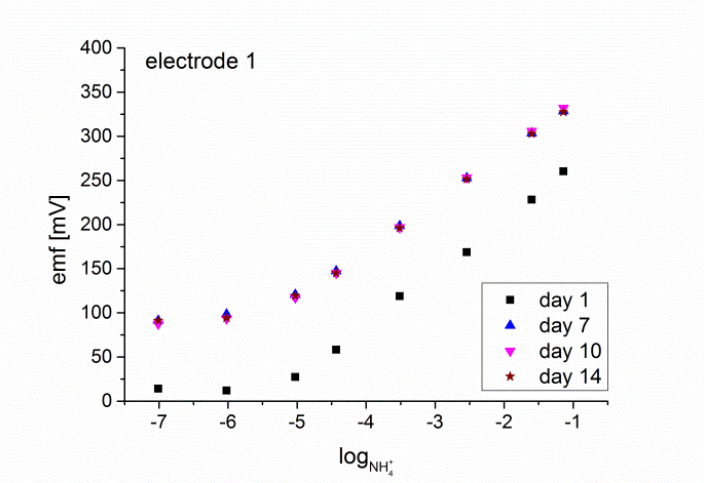

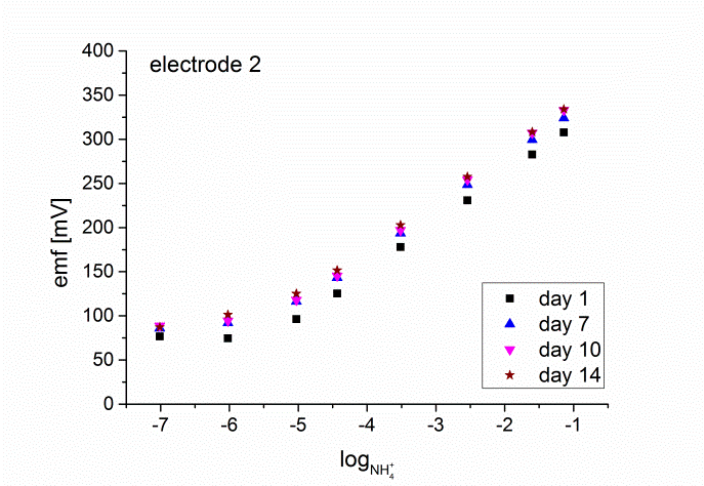
electrode 2
emf [mV]
400
350
300
250
200
150
100
50
0
-7
-6
-5
-4
-3
-2
-1
log$_{NH_4^+}$
day 1
day 7
day 10
day 14

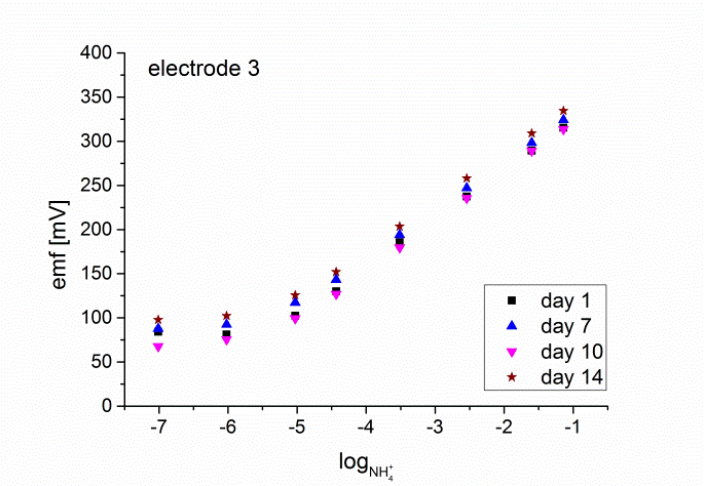
electrode 3
emf [mV]
400
350
300
250
200
150
100
50
0
-7
-6
-5
-4
-3
-2
-1
log$_{NH_4^+}$
day 1
day 7
day 10
day 14

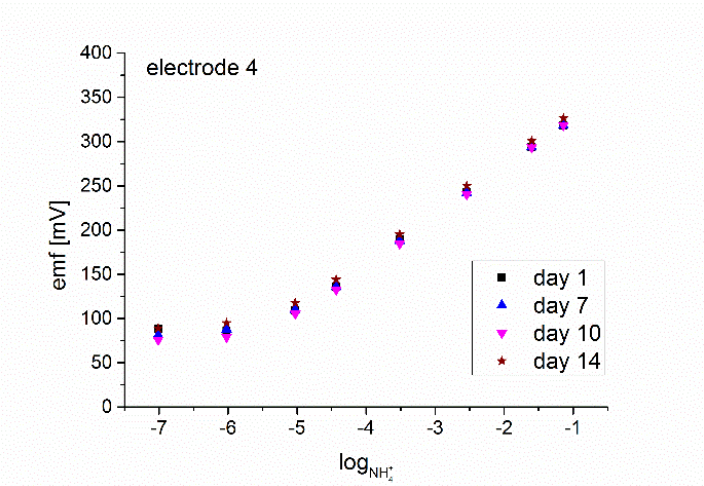
electrode 4
emf [mV]
400
350
300
250
200
150
100
50
0
-7
-6
-5
-4
-3
-2
-1
log$_{NH_4^+}$
day 1
day 7
day 10
day 14

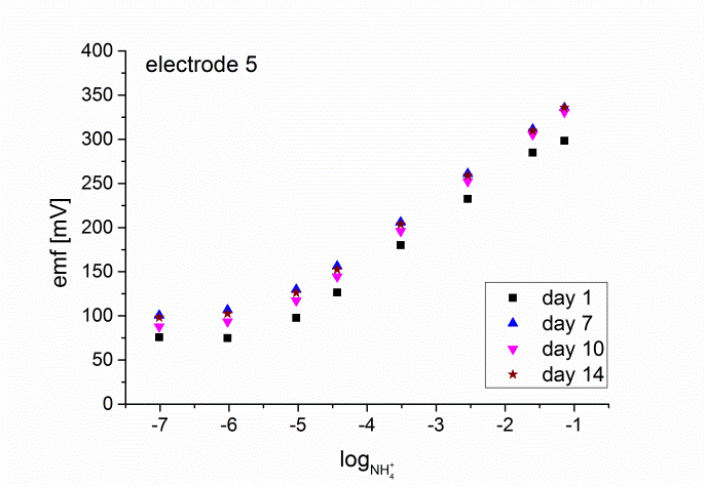

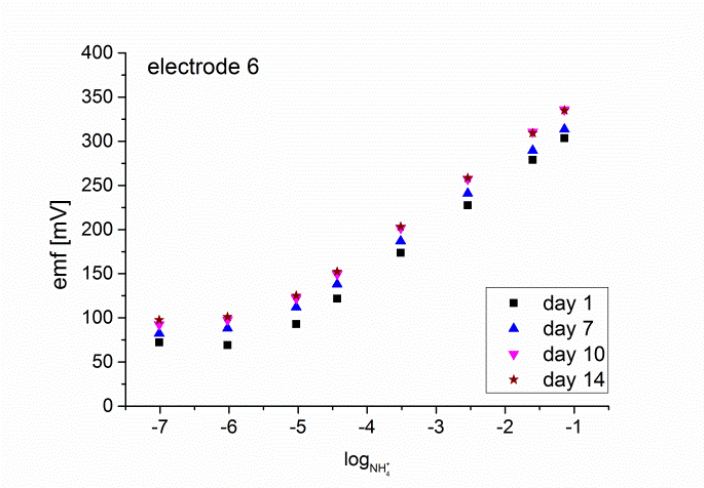

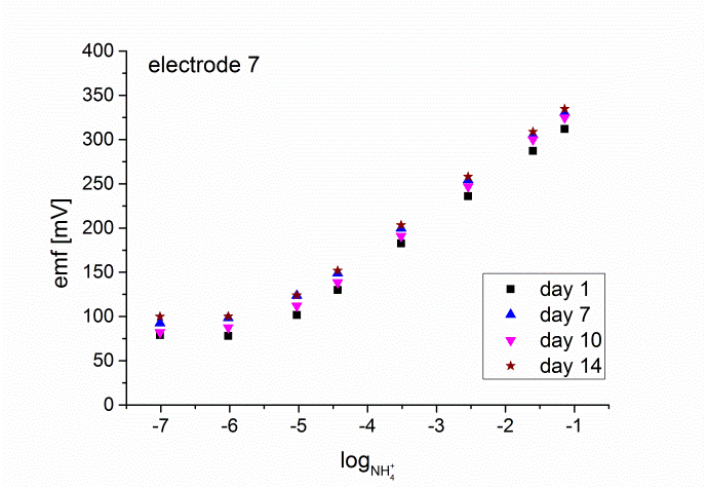

Figure 2.8 Long term stability of NH_4^+ - selective ISEs on acetate sheet/graphite – based substrate. Prior the first use electrodes were conditioned overnight 1.0 x 10^{-3} M NH_4Cl solution and stored in air. Electrodes were rehydrated in the same solution for 1 hour prior to subsequent calibration.

More importantly, the E^0 identified by Lindner et al as critical parameters for evaluation of stability of ISEs was 383.59 ± 4.05 mV while the base line was 83.6 ± 6.26 mV[61]. Such a small deviation of E^0 and base line potential after fairly simple storage and re-conditioning protocol bears a potentially significant consequence on the actual, true cost of sensor. In other words, large variations would necessitate relatively complicated calibration protocol ultimately driving the per sample and per measurement cost.[62]

As observed in table 2.3, E^o and base line is surprisingly stable especially considering the incredibly simple protocol for electrode preparation. No training is necessary and platforms are prepared using typical household materials. Interestingly, major source of instability originates from the response during the first day. In fact, excluding electrode 1 with slightly different E^o on day 1 (see figure 2.8), average E^o across all electrodes and all days is 386±15 mV while base line potential is 86±11 mV.

Table 2.3 E^0 and base line potential averaged over 14 days period.

Electrode	E^0	Base line
1	376.18 ± 34.13	71.0 ± 38.03
2	388.21 ± 13.05	84.6 ± 5.44
3	384.98 ± 9.26	84.3 ± 12.47
4	383.59 ± 4.05	83.6 ± 6.26
5	388.8 ± 18.28	90.5 ± 11.28
6	385.01 ± 17.14	86.1 ± 11.2
7	388.76 ± 10.13	88.4 ± 9.66

It is known that signal instability (i.e. deviations of E^0 and base line potential) of ISEs, as evident on day 1 of electrode 1, is consequence of minor variations in the transducer layer induced by fabrication protocols,[63] changes in sensing layer composition due to chemical,[64] and/or slow and spontaneous charging/discharging processes followed or caused by ion fluxes through the membrane.[65–67] The latter two are addressed by the chemistry of the sensing layer utilizing a variety of strategies including, for example, designing a single component sensing layer.[68,69] Important for this research is that the former factors require careful manufacturing or/and precise design instrumental protocols[70,71] which inevitably drive the cost of the device upward. Moreover, this work shows that a simple preparation of substrate (mechanical abrasion of pencil) can result in very reproducible and stable E^0 and base line potential implying minimal need for complex calibration protocols, and thus ultimately leading to true cost reduction of measurements. Further studies in the origins of the noticed slight instability can result in improved protocols for the preparation of sensors on a truly mass scale at very low cost.

2.3.7 Characterization of all-solid-contact reference electrode

A reference electrode is an essential tool in potentiometry because it functions as a fixed constant that completes an electrochemical cell. The potential of a reference electrode should ideally be insensitive to any changes occurring in the background solution and should maintain constant and stable potential throughout the measurement. Therefore, the proposed substrate (modified acetate sheet with mechanically deposited graphite) was investigated to see if it could be used for the development of functional potentiometric sensing devices. For that purpose, solid-contact reference electrodes based on the highly lipophilic tetrabutylammonium

tetrabutylborate (TBA-TBB) salt were fabricated using the acetate paper substrate and prepared according to an experimental protocol by Mattinen et al.[72]

The subsequent paper electrodes were characterized against a classical glass double-junction reference electrode (Fluka) to investigate potential stability due to changes in electrolyte concentrations in slightly modified protocol developed by Mattinen et al.[72] According to table 2.4, protocol I was performed to test the responses of the sensors (TBA-TBB electrode and classical electrode) in different concentrations of the same solution by immersing in 0.1 M and 0.01 M KCl for 10 min at a time. Electrodes were rinsed with deionized water between solutions. Protocol II tested the responses of both sensors in solutions containing different concentrations of different ions at similar interval as protocol I. While protocol III tested the electrode responses in similar solutions at a much lesser time interval. The first two protocols were performed to primarily test the long term stability of the fabricated electrodes in solutions containing the same and different ions, while protocol III was used to test the response time of the electrodes which can be linked to the stability of the electrode potentials.

Table 2.4 Protocol for investigating potential stability of solid-contact TBA-TBB – based reference electrode on graphite-based substrate.

Protocol	Solution concentration	Time/ min
I	0.1 M KCl	10
	0.01 M KCl	10
	0.1 M KCl	10
	0.01 M KCl	10

II	0.1 M KCl	10
	0.0001 M KCl	10
	0.0001 M NaCl	10
	0.1 M NaCl	10
	0.1 M KCl	10
III	0.01 M KCl	0.5
	0.1 M KCl	0.5
	0.01 M KCl	0.5

When comparing the response of the classical reference electrodes to the responses observed with the TBA-TBB – based electrodes, a slow response/ stabilization time was evident according to figure 2.9. This is in accordance with the response for TBA-TBB – based reference electrodes observed in the original work by Mattinen et al.[72] The slow stabilization or equilibration time is even more evident in protocol III where the classical reference electrodes outperform the TBA-TBB based electrodes in reaching stabilization within 30 seconds when changing between 0.01 and 0.1 M KCl. Nevertheless, as seen in results for protocol I and protocol II, it was evident that the TBA-TBB-based electrodes showed a degree of insensitivity towards concentration changes.

To further explain this phenomenon, Mattinen et al hypothesized an intimate interplay between the phase boundary and the diffusion potential for TBA-TBB – based electrodes resulting in small but leachable salt, which contributes to the buildup of a transmembrane diffusion potential that will only become reproducible and stable when steady-state in the membrane is reached. [72]

Clearly, applications that require fast measurements will be impeded; however, excellent stability of the signal after equilibration is very encouraging for development of ultra-cheap sensing devices for majority of applications.

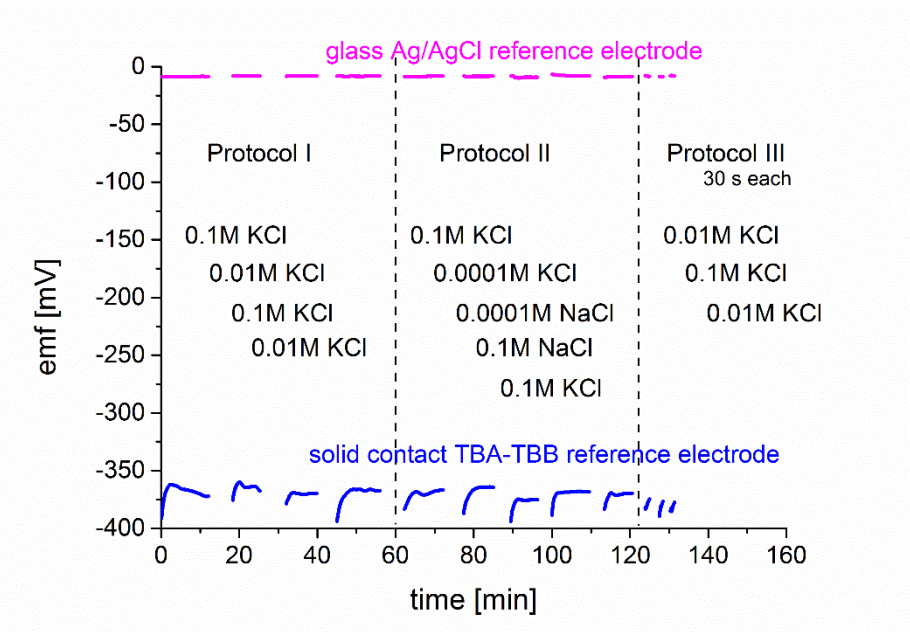

Figure 2.9 Potential behavior of the reference electrode based on TBA-TBB on graphite substrate compared to a conventional glass double-junction reference electrode.

2.3.8 All solid-state single strip potentiometric sensing device

Encouraged by the confirmation of suitable potentiometric response/stability towards several ions as well as upon confirmation of suitability of TBA-TBB-based all-solid-state reference electrode, a single strip electrode consisting of a reference electrode drawn onto the modified acetate sheet together with a series of NH_4^+ and NO_3^- electrodes were fabricated. As demonstrated in Figure 2.10, simultaneous responses for NH_4^+- and NO_3^--selective electrodes relative to an all-solid-contact reference electrode were obtained. The electrodes fabricated, and included in the single-strip

potentiometric sensing device exhibited near-Nernstian response characteristics. The experimental slopes and LODs for NH_4^+ and NO_3^- electrodes were 53.5 mV/decade and 6.0 x 10^{-6} M, and 54.2 mV/decade and 2.5 x 10^{-6} M respectively. This is an important finding as it clearly demonstrates that very simple and cheap sensing devices can be fabricated using only inexpensive and readily available components such as graphite pencils and acetate sheets.

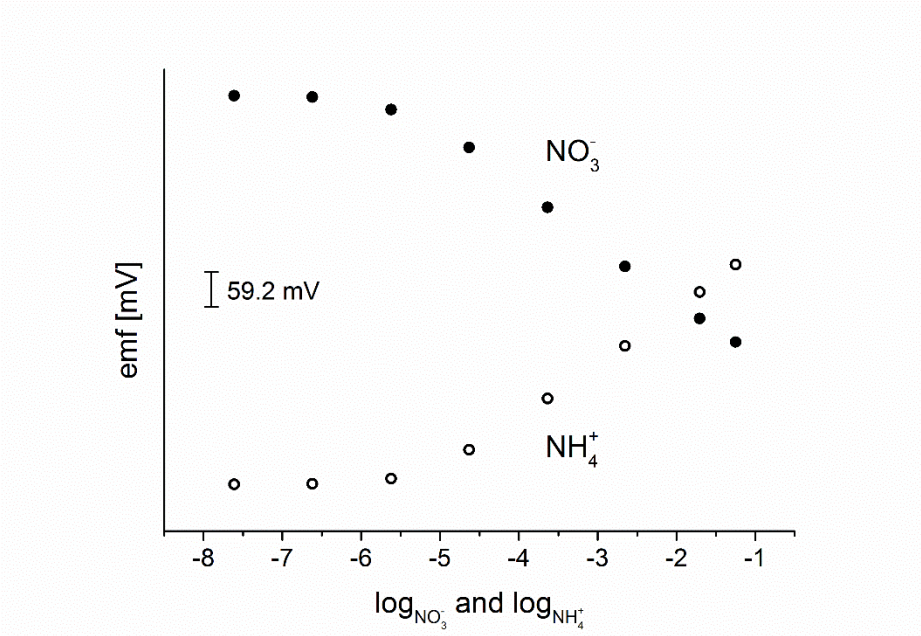

Figure 2.10 Simultaneous responses of NH_4^+ - and NO_3^- - selective electrodes containing an all-solid-state TBA-TBB reference electrode prepared on a single acetate sheet/graphite substrate.

2.4 Conclusions

In this work, a simple and robust approach for the fabrication of solid-contact ISEs via mechanical drawing of graphite material onto acetate substrate has been proposed. Graphite, as compared to other forms of carbon such as CNTs, can be used as both an ion-electron transducer and an electron conductive substrate. Therefore, it can be considered as a significantly cheaper alternative to traditionally employed materials. Due to its strong hydrophobicity, the use of acetate sheet eliminates the "wetting" effect that other forms of paper substrate are deemed to suffer, improving signal stability. In general, the electrodes manufactured using these simple and very cheap components have demonstrated excellent sensing properties towards all ions of interest. The resulting sensing devices demonstrated near-Nernstian response characteristics, good selectivity, and short response time, and thus create numerous opportunities for the development of ultra-simple and inexpensive potentiometric sensors.

References

(1) Crespo, G. A.; Macho, S.; Bobacka, J.; Rius, F. X. Transduction Mechanism of Carbon Nanotubes in Solid-Contact Ion-Selective Electrodes. *Anal. Chem.* **2009**, *81* (2), 676–681.

(2) Athavale, R.; Kokorite, I.; Dinkel, C.; Bakker, E.; Wehrli, B.; Crespo, G. A.; Brand, A. *In Situ* Ammonium Profiling Using Solid-Contact Ion-Selective Electrodes in Eutrophic Lakes. *Anal. Chem.* **2015**, *87* (24), 11990–11997.

(3) Yuan, D.; Anthis, A. H. C.; Ghahraman Afshar, M.; Pankratova, N.; Cuartero, M.; Crespo, G. A.; Bakker, E. All-Solid-State Potentiometric Sensors with a Multiwalled Carbon Nanotube Inner Transducing Layer for Anion Detection in Environmental Samples. *Anal. Chem.* **2015**, *87* (17), 8640–8645.

(4) Cuartero, M.; Crespo, G. A.; Bakker, E. Tandem Electrochemical Desalination–Potentiometric Nitrate Sensing for Seawater Analysis. *Anal. Chem.* **2015**, *87* (16), 8084–8089.

(5) Mensah, S. T.; Gonzalez, Y.; Calvo-Marzal, P.; Chumbimuni-Torres, K. Y. Nanomolar Detection Limits of Cd^{2+}, Ag^{+}, and K^{+} Using Paper-Strip Ion-Selective Electrodes. *Anal. Chem.* **2014**, *86* (15), 7269–7273.

(6) Novell, M.; Parrilla, M.; Crespo, G. A.; Rius, F. X.; Andrade, F. J. Paper-Based Ion-Selective Potentiometric Sensors. *Anal. Chem.* **2012**, *84* (11), 4695–4702.

(7) Parra, E. J.; Crespo, G. A.; Riu, J.; Ruiz, A.; Rius, F. X. Ion-Selective Electrodes Using Multi-Walled Carbon Nanotubes as Ion-to-Electron Transducers for the Detection of Perchlorate. *The Analyst* **2009**, *134* (9), 1905.

(8) Rius-Ruiz, F. X.; Crespo, G. A.; Bejarano-Nosas, D.; Blondeau, P.; Riu, J.; Rius, F. X. Potentiometric Strip Cell Based on Carbon Nanotubes as Transducer Layer: Toward Low-Cost Decentralized Measurements. *Anal. Chem.* **2011**, *83* (22), 8810–8815.

(9) Rius-Ruiz, F. X.; Bejarano-Nosas, D.; Blondeau, P.; Riu, J.; Rius, F. X. Disposable Planar Reference Electrode Based on Carbon Nanotubes and Polyacrylate Membrane. *Anal. Chem.* **2011**, *83* (14), 5783–5788.

(10) Hu, J.; Ho, K. T.; Zou, X. U.; Smyrl, W. H.; Stein, A.; Bühlmann, P. All-Solid-State Reference Electrodes Based on Colloid-Imprinted Mesoporous Carbon and Their Application in Disposable Paper-Based Potentiometric Sensing Devices. *Anal. Chem.* **2015**, *87* (5), 2981–2987.

(11) Yáñez-Sedeño, P.; Pingarrón, J. M.; Riu, J.; Rius, F. X. Electrochemical Sensing Based on Carbon Nanotubes. *TrAC Trends Anal. Chem.* **2010**, *29* (9), 939–953.

(12) De Volder, M. F. L.; Tawfick, S. H.; Baughman, R. H.; Hart, A. J. Carbon Nanotubes: Present and Future Commercial Applications. *Science* **2013**, *339* (6119), 535–539.

(13) Thostenson, E. T.; Ren, Z.; Chou, T.-W. Advances in the Science and Technology of Carbon Nanotubes and Their Composites: A Review. *Compos. Sci. Technol.* **2001**, *61* (13), 1899–1912.

(14) Hu, J.; Stein, A.; Bühlmann, P. Rational Design of All-Solid-State Ion-Selective Electrodes and Reference Electrodes. *TrAC Trends Anal. Chem.* **2016**, *76*, 102–114.

(15) Schnorr, J. M.; Swager, T. M. Emerging Applications of Carbon Nanotubes †. *Chem. Mater.* **2011**, *23* (3), 646–657.

(16) Crespo, G. A.; Macho, S.; Rius, F. X. Ion-Selective Electrodes Using Carbon Nanotubes as Ion-to-Electron Transducers. *Anal. Chem.* **2008**, *80* (4), 1316–1322.

(17) Bruil, H. G.; van Aartsen, J. J. The Determination of Contact Angles of Aqueous Surfactant Solutions on Powders. *Colloid Polym. Sci.* **1974**, *252* (1), 32–38.

(18) Huang, Y. Y.; Terentjev, E. M. Dispersion of Carbon Nanotubes: Mixing, Sonication, Stabilization, and Composite Properties. *Polymers* **2012**, *4* (4), 275–295.

(19) Ma, P.-C.; Siddiqui, N. A.; Marom, G.; Kim, J.-K. Dispersion and Functionalization of Carbon Nanotubes for Polymer-Based Nanocomposites: A Review. *Compos. Part Appl. Sci. Manuf.* **2010**, *41* (10), 1345–1367.

(20) Vaisman, L.; Wagner, H. D.; Marom, G. The Role of Surfactants in Dispersion of Carbon Nanotubes. *Adv. Colloid Interface Sci.* **2006**, *128–130*, 37–46.

(21) Li, J.; Lu, Y.; Ye, Q.; Cinke, M.; Han, J.; Meyyappan, M. Carbon Nanotube Sensors for Gas and Organic Vapor Detection. *Nano Lett.* **2003**, *3* (7), 929–933.

(22) Bardecker, J. A.; Afzali, A.; Tulevski, G. S.; Graham, T.; Hannon, J. B.; Jen, A. K.-Y. Directed Assembly of Single-Walled Carbon Nanotubes via Drop-Casting onto a UV-Patterned Photosensitive Monolayer. *J. Am. Chem. Soc.* **2008**, *130* (23), 7226–7227.

(23) Beecher, P.; Servati, P.; Rozhin, A.; Colli, A.; Scardaci, V.; Pisana, S.; Hasan, T.; Flewitt, A. J.; Robertson, J.; Hsieh, G. W.; et al. Ink-Jet Printing of Carbon Nanotube Thin Film Transistors. *J. Appl. Phys.* **2007**, *102* (4), 043710.

(24) da Costa, T. H.; Song, E.; Tortorich, R. P.; Choi, J.-W. A Paper-Based Electrochemical Sensor Using Inkjet-Printed Carbon Nanotube Electrodes. *ECS J. Solid State Sci. Technol.* **2015**, *4* (10), S3044–S3047.

(25) Kwon, O.-S.; Kim, H.; Ko, H.; Lee, J.; Lee, B.; Jung, C.-H.; Choi, J.-H.; Shin, K. Fabrication and Characterization of Inkjet-Printed Carbon Nanotube Electrode Patterns on Paper. *Carbon* **2013**, *58*, 116–127.

(26) Mirri, F.; Ma, A. W. K.; Hsu, T. T.; Behabtu, N.; Eichmann, S. L.; Young, C. C.; Tsentalovich, D. E.; Pasquali, M. High-Performance Carbon Nanotube Transparent Conductive Films by Scalable Dip Coating. *ACS Nano* **2012**, *6* (11), 9737–9744.

(27) LeMieux, M. C.; Sok, S.; Roberts, M. E.; Opatkiewicz, J. P.; Liu, D.; Barman, S. N.; Patil, N.; Mitra, S.; Bao, Z. Solution Assembly of Organized Carbon Nanotube Networks for Thin-Film Transistors. *ACS Nano* **2009**, *3* (12), 4089–4097.

(28) Spotnitz, M. E.; Ryan, D.; Stone, H. A. Dip Coating for the Alignment of Carbon Nanotubes on Curved Surfaces. *J. Mater. Chem.* **2004**, *14* (8), 1299.

(29) Wang, F.; Swager, T. M. Diverse Chemiresistors Based upon Covalently Modified Multiwalled Carbon Nanotubes. *J. Am. Chem. Soc.* **2011**, *133* (29), 11181–11193.

(30) Chen, J. Solution Properties of Single-Walled Carbon Nanotubes. *Science* **1998**, *282* (5386), 95–98.

(31) Mirica, K. A.; Weis, J. G.; Schnorr, J. M.; Esser, B.; Swager, T. M. Mechanical Drawing of Gas Sensors on Paper. *Angew. Chem. Int. Ed.* **2012**, *51* (43), 10740–10745.

(32) Weis, J. G.; Ravnsbæk, J. B.; Mirica, K. A.; Swager, T. M. Employing Halogen Bonding Interactions in Chemiresistive Gas Sensors. *ACS Sens.* **2016**, *1* (2), 115–119.

(33) Frazier, K. M.; Mirica, K. A.; Walish, J. J.; Swager, T. M. Fully-Drawn Carbon-Based Chemical Sensors on Organic and Inorganic Surfaces. *Lab Chip* **2014**, *14* (20), 4059–4066.

(34) Mirica, K. A.; Azzarelli, J. M.; Weis, J. G.; Schnorr, J. M.; Swager, T. M. Rapid Prototyping of Carbon-Based Chemiresistive Gas Sensors on Paper. *Proc. Natl. Acad. Sci.* **2013**, *110* (35), E3265–E3270.

(35) Azzarelli, J. M.; Mirica, K. A.; Ravnsbæk, J. B.; Swager, T. M. Wireless Gas Detection with a Smartphone via Rf Communication. *Proc. Natl. Acad. Sci.* **2014**, *111* (51), 18162–18166.

(36) Bernalte, E.; Foster, C. W.; Brownson, D. A. C.; Mosna, M.; Smith, G. C.; Banks, C. E. Pencil It in: Exploring the Feasibility of Hand-Drawn Pencil Electrochemical Sensors and Their Direct Comparison to Screen-Printed Electrodes. *Biosensors* **2016**, *6* (3).

(37) W. Foster, C.; C. Brownson, D. A.; Souza, A. P. R. de; Bernalte, E.; Iniesta, J.; Bertotti, M.; E. Banks, C. Pencil It in: Pencil Drawn Electrochemical Sensing Platforms. *Analyst* **2016**, *141* (13), 4055–4064.

(38) Honeychurch, K. C. The Voltammetric Behaviour of Lead at a Hand Drawn Pencil Electrode and Its Trace Determination in Water by Stripping Voltammetry. *Anal. Methods* **2015**, *7* (6), 2437–2443.

(39) Ammu, S.; Dua, V.; Agnihotra, S. R.; Surwade, S. P.; Phulgirkar, A.; Patel, S.; Manohar, S. K. Flexible, All-Organic Chemiresistor for Detecting Chemically Aggressive Vapors. *J. Am. Chem. Soc.* **2012**, *134* (10), 4553–4556.

(40) Martinez, A. W.; Phillips, S. T.; Whitesides, G. M.; Carrilho, E. Diagnostics for the Developing World: Microfluidic Paper-Based Analytical Devices. *Anal. Chem.* **2010**, *82* (1), 3–10.

(41) Siegel, A. C.; Phillips, S. T.; Dickey, M. D.; Lu, N.; Suo, Z.; Whitesides, G. M. Foldable Printed Circuit Boards on Paper Substrates. *Adv. Funct. Mater.* **2010**, *20* (1), 28–35.

(42) López-Marzo, A. M.; Merkoçi, A. Paper-Based Sensors and Assays: A Success of the Engineering Design and the Convergence of Knowledge Areas. *Lab Chip* **2016**.

(43) Ahmed, S.; Bui, M.-P. N.; Abbas, A. Paper-Based Chemical and Biological Sensors: Engineering Aspects. *Biosens. Bioelectron.* **2016**, *77*, 249–263.

(44) Liana, D. D.; Raguse, B.; Gooding, J. J.; Chow, E. Recent Advances in Paper-Based Sensors. *Sensors* **2012**, *12* (12), 11505–11526.

(45) Tobjörk, D.; Österbacka, R. Paper Electronics. *Adv. Mater.* **2011**, *23* (17), 1935–1961.

(46) Barr, M. C.; Rowehl, J. A.; Lunt, R. R.; Xu, J.; Wang, A.; Boyce, C. M.; Im, S. G.; Bulović, V.; Gleason, K. K. Direct Monolithic Integration of Organic Photovoltaic Circuits on Unmodified Paper. *Adv. Mater.* **2011**, *23* (31), 3500–3505.

(47) Martinez, A. W.; Phillips, S. T.; Butte, M. J.; Whitesides, G. M. Patterned Paper as a Platform for Inexpensive, Low-Volume, Portable Bioassays. *Angew. Chem. Int. Ed.* **2007**, *46* (8), 1318–1320.

(48) Thom, N. K.; Yeung, K.; Pillion, M. B.; Phillips, S. T. "Fluidic Batteries" as Low-Cost Sources of Power in Paper-Based Microfluidic Devices. *Lab. Chip* **2012**, *12* (10), 1768.

(49) Wang, P.; Ge, L.; Yan, M.; Song, X.; Ge, S.; Yu, J. Paper-Based Three-Dimensional Electrochemical Immunodevice Based on Multi-Walled Carbon Nanotubes Functionalized Paper for Sensitive Point-of-Care Testing. *Biosens. Bioelectron.* **2012**, *32* (1), 238–243.

(50) Petroski, H. *The Pencil: A History of Design and Circumstance*, 11. printing.; Knopf: New York, 2003.

(51) Lopez-Ruiz, N.; Curto, V. F.; Erenas, M. M.; Benito-Lopez, F.; Diamond, D.; Palma, A. J.; Capitan-Vallvey, L. F. Smartphone-Based Simultaneous PH and Nitrite Colorimetric Determination for Paper Microfluidic Devices. *Anal. Chem.* **2014**, *86* (19), 9554–9562.

(52) Matzeu, G.; O'Quigley, C.; McNamara, E.; Zuliani, C.; Fay, C.; Glennon, T.; Diamond, D. An Integrated Sensing and Wireless Communications Platform for Sensing Sodium in Sweat. *Anal Methods* **2016**, *8* (1), 64–71.

(53) Bakker, E. Determination of Unbiased Selectivity Coefficients of Neutral Carrier-Based Cation-Selective Electrodes. *Anal. Chem.* **1997**, *69* (6), 1061–1069.

(54) Radu, A.; Anastasova-Ivanova, S.; Paczosa-Bator, B.; Danielewski, M.; Bobacka, J.; Lewenstam, A.; Diamond, D. Diagnostic of Functionality of Polymer Membrane – Based Ion Selective Electrodes by Impedance Spectroscopy. *Anal. Methods* **2010**, *2* (10), 1490.

(55) Rammelt, U.; Reinhard, G. The Influence of Surface Roughness on the Impedance Data for Iron Electrodes in Acid Solutions. *Corros. Sci.* **1987**, *27* (4), 373–382.

(56) Wang, L. The Extraction of Cadmium(II) and Copper(II) from Hydrochloric Acid Solutions Using an Aliquat 336/PVC Membrane. *J. Membr. Sci.* **2000**, *176* (1), 105–111.

(57) Fibbioli, M.; Morf, W. E.; Badertscher, M.; de Rooij, N. F.; Pretsch, E. Potential Drifts of Solid-Contacted Ion-Selective Electrodes Due to Zero-Current Ion Fluxes Through the Sensor Membrane. *Electroanalysis* **2000**, *12* (16), 1286–1292.

(58) Sasaki, S.; Amano, T.; Monma, G.; Otsuka, T.; Iwasawa, N.; Citterio, D.; Hisamoto, H.; Suzuki, K. Comparison of Two Molecular Design Strategies for the Development of an Ammonium Ionophore More Highly Selective than Nonactin. *Anal. Chem.* **2002**, *74* (18), 4845–4848.

(59) Paczosa-Bator, B.; Cabaj, L.; Piech, R.; Skupień, K. Potentiometric Sensors with Carbon Black Supporting Platinum Nanoparticles. *Anal. Chem.* **2013**, *85* (21), 10255–10261.

(60) Paczosa-Bator, B. Effects of Type of Nanosized Carbon Black on the Performance of an All-Solid-State Potentiometric Electrode for Nitrate. *Microchim. Acta* **2014**, *181* (9–10), 1093–1099.

(61) Lindner, E.; Umezawa, Y. Performance Evaluation Criteria for Preparation and Measurement of Macro- and Microfabricated Ion-Selective Electrodes (IUPAC Technical Report). *Pure Appl. Chem.* **2008**, *80* (1).

(62) Byrne, R.; Diamond, D. Chemo/Bio-Sensor Networks. *Nat. Mater.* **2006**, *5* (6), 421–424.

(63) Anastasova, S.; Radu, A.; Matzeu, G.; Zuliani, C.; Mattinen, U.; Bobacka, J.; Diamond, D. Disposable Solid-Contact Ion-Selective Electrodes for Environmental

Monitoring of Lead with Ppb Limit-of-Detection. *Electrochimica Acta* **2012**, *73*, 93–97.

(64) Lindner, E.; Gyurcsányi, R. E. Quality Control Criteria for Solid-Contact, Solvent Polymeric Membrane Ion-Selective Electrodes. *J. Solid State Electrochem.* **2009**, *13* (1), 51–68.

(65) Michalska, A.; Maksymiuk, K. The Influence of Spontaneous Charging/Discharging of Conducting Polymer Ion-to-Electron Transducer on Potentiometric Responses of All-Solid-State Calcium-Selective Electrodes. *J. Electroanal. Chem.* **2005**, *576* (2), 339–352.

(66) Michalska, A.; Dumańska, J.; Maksymiuk, K. Lowering the Detection Limit of Ion-Selective Plastic Membrane Electrodes with Conducting Polymer Solid Contact and Conducting Polymer Potentiometric Sensors. *Anal. Chem.* **2003**, *75* (19), 4964–4974.

(67) Dumańska, J.; Maksymiuk, K. Studies on Spontaneous Charging/Discharging Processes of Polypyrrole in Aqueous Electrolyte Solutions. *Electroanalysis* **2001**, *13* (7), 567–573.

(68) Mendecki, L.; Chen, X.; Callan, N.; Thompson, D. F.; Schazmann, B.; Granados-Focil, S.; Radu, A. Simple, Robust, and Plasticizer-Free Iodide-Selective Sensor Based on Copolymerized Triazole-Based Ionic Liquid. *Anal. Chem.* **2016**.

(69) Qin, Y.; Peper, S.; Radu, A.; Ceresa, A.; Bakker, E. Plasticizer-Free Polymer Containing a Covalently Immobilized Ca2+-Selective Ionophore for Potentiometric and Optical Sensors. *Anal. Chem.* **2003**, *75* (13), 3038–3045.

(70) Vanamo, U.; Bobacka, J. Instrument-Free Control of the Standard Potential of Potentiometric Solid-Contact Ion-Selective Electrodes by Short-Circuiting with a Conventional Reference Electrode. *Anal. Chem.* **2014**, *86* (21), 10540–10545.

(71) Vanamo, U.; Bobacka, J. Electrochemical Control of the Standard Potential of Solid-Contact Ion-Selective Electrodes Having a Conducting Polymer as Ion-to-Electron Transducer. *Electrochimica Acta* **2014**, *122*, 316–321.

(72) Mattinen, U.; Bobacka, J.; Lewenstam, A. Solid-Contact Reference Electrodes Based on Lipophilic Salts. *Electroanalysis* **2009**, *21* (17–18), 1955–1960.

Chapter 3 Simple and robust potentiometric technique for concurrent measurement of nitrate and ammonium in water samples, and soil from various land use types

3.1 Introduction

Of great concern in recent studies towards the fate and balance of nitrogen in our environment is the increase in anthropogenic inputs arising greatly from the use of fertilizers and organic manures, industrial wastes, and sewages, as evident by the increasingly elevated levels of reactive nitrogen (Nr) emitted to the biosphere over the past century.[1–3] Important to the improvement of the world's food circulation is the application of nitrogen-containing fertilizers to boost crop production. However, if applied in excess of plant nutrient requirements, it can have serious negative impact on water quality, health of aquatic ecosystems and human life.[4–6] This is because of the release of substantial amount of reactive nitrogen (all nitrogen species apart from inert nitrogen) into soils, surface, coastal and groundwater resources, which form part of a series of nitrogen losses involving nitrate leaching, volatization of ammonia, and emergence of nitrous oxide – a greenhouse gas from denitrification.[7–9]

Crucially, it is well reported that consuming drinking water with concentrations in excess of the nitrate limit can result in adverse health effects, for example the occurrence of the widely-known methemoglobinemia - also known as blue-baby syndrome - more common in infants.[10] Excessive nitrate in foods has also been linked to gastric cancer due to the formation of carcinogenic nitrosamines in the acidic conditions of the stomach,[11] therefore, nitrate pollution as a result of excessive pressure on water sources, especially from agricultural origin cannot be overlooked.

In the UK, nitrate losses to surface water because of intense fertilization through the use of inorganic fertilizers and organic manures has called for control of the Nitrate Vulnerable Zones (NVZs), which is part of control measures in soil/ agriculture management system within the European union (EU). As a guideline within its member states, the EU has set an alert limit, and maximum allowable concentration of 50 mg/ L NO_3^- for groundwater and drinking waters respectively (The Nitrates Directive, 91/676/EEC).[12]

In soil solution, nitrate (NO_3^-) and nitrite (NO_2^-) are the more soluble forms of Nr, hence, more vulnerable to losses through leaching. However, the short life span of nitrite due to its conversion, and its insignificant proportion in the terrestrial ecosystem makes it a less significant entity when assessing the overall reactive nitrogen implication. Ammonium (NH_4^+) on the other hand, can be highly adsorbed and immobilized onto the negatively charged soil's colloidal surface owing to its positive charge.[13] This degree of attraction between NH_4^+ & NO_3^- ions, and soil materials play a huge role in the loss of available nitrogen from the soil.

3.2 Measurement of reactive nitrogen

While several researches have focused on the impacts of different land management systems to optimize nutrients availability to plants, hence suggesting possible ways of reducing nutrients loss, [14–17] other researchers have focused more on improving scientific methodologies for qualitative- and quantitative analysis.

Traditional analytical techniques such as colorimetry, spectroscopy, and chromatography have been used for measuring Nr in various environmental samples.[18–21] Colourimetry methods widely used for the measurements of reactive nitrogen in soil and water samples involve the cadmium-reduction method for nitrate/nitrite and the Berthelot method for ammonium. This set up which generally utilizes a highly specialized flow-injection analyzer, involves the production of coloured species that can be measured at specific wavelengths. Spectroscopic methods reported include; near-infrared spectroscopy for measurement of nitrate in vegetables and plants,[22,23] ultraviolet resonance Raman (UVRR) spectroscopy for nitrate in wastewaters,[24] and laser-induced breakdown spectroscopy (LIBS) for soil nitrate.[25] Ion chromatography is an example of standard analytical techniques used for the measurement of Nr, mostly nitrate and nitrite in water and soil samples.

Even though the analysis of Nr in soil samples using the aforementioned conventional techniques has become a standard practice in soil science, it is worth noting that the existence of some set-backs such as sample pre-treatment, analysis time, deterioration of the sample, cost per analysis, limit their suitability towards routine practical applications for precision agriculture, and overshadow the important advantage like sensitivity.[26,27] This can often cause major barriers towards the implementation of sustainable agricultural system especially in developing and underdeveloped countries with less readily available technology resources.

While a simple pre-treatment stage is only required for successful analysis of NH_4^+ & NO_3^- in water, measurement of nitrate and ammonium in soils still necessarily requires an additional extraction/clarification process using a suitable electrolyte (extractant). In most soil analysis of nitrate, simple extraction using water is deemed acceptable due to its solubility, [20,26] however, it is generally perceived that a stronger salt solution is needed to extract the more immobilized ammonium. Although 1 – 2 M KCl is seen as the widely used extraction solution for Nr, other studies have also compared and reported extraction process for analyzing NH_4^+ in soil by standard analytical techniques using 0.01 M $CaSO_4$, 0.5 M K_2SO_4 and 0.01 M $CaCl_2$. [28–33]

However, in a different approach and one inspired by the recently renewed interest in developing improved portable sensing techniques to monitor bioavailable analytes deemed potentially harmful to public health, [34,35] measurement of Nr within several environmental samples have been achieved using potentiometric analysis with ion-selective electrodes (ISEs) which allows for the simple and low-cost determination of amount of bioavailable ions within a solution. [20,21,36,37] These sensors are easily miniaturized and connected to a simple communication device to read out measured bioavailable composition of the analytes. The simplicity of design and use, the portability of sensors and the ability to perform analysis of raw complex samples confirm the suitability of ion-selective electrodes for cheap and fast routine analysis of Nr when compared to the other standard analytical methods.

While several studies have focused on the designing of more robust solid-contact ISEs as a better alternative to replacing the conventional liquid-contact electrodes, [38–40] majority of research in this field has focused on improving the sensing components of ISEs through the development of new/ improved ionophores, polymers, ion transducers, or additives. [41–49] This combined approach has paved the way for the

development of newly improved polymeric ISEs with more stable electrode signals, better detection limits and selectivities, which are crucial for routine analysis of important contaminants.

Despite all these attributes, common commercial ISEs used for environmental purposes still exhibit limits of detection (LODs) close to critical levels (e.g. regulatory limits of ions being investigated). [50] In practical applications involving the use of ISEs in real samples, this restricted trademark LODs do not seem enough as a significant presence of interfering ions can result in an overestimation of the actual sample concentration of main ion – a phenomenon greatly observed near the non-linear region of the ISE graphs (see figure 1.5 in chapter 1). In addition, bias caused by electrode noise can further render precisions for low-activity measurements untenable thereby introducing some forms of errors.

The concentration of Nr species in soil and water samples ranges from a few to decades of µmol/ L depending on the ambient environment, which means for most commercially available NH_4^+ and NO_3^- sensors and those developed for research purposes - whose low detection limit is around ~ 1 µmol/ L range (in other words 0.018 ppm for NH_4^+ and 0.062 ppm for NO_3^-), more alternative efforts to further extend the usable range of the ISE calibration plot is important. [51]

Using the Bayesian modelling – a method which provides estimates of measurement precision by incorporating uncertainty in calibration parameters and inherent random noise in EMF response, Dillingham et al reported an improvement in the response of ISE for analysis of lead in soil samples. [52] Therefore, by introducing Bayesian modelling into our analysis, this project was aimed to improve accuracy and precision

of measured nitrate and ammonium activities in soil and water samples from different areas in the UK using a multi-electrode system based on paper electrodes.

In summary, the purpose of this work was;

Firstly, to evaluate the extraction efficiency of 0.1 M $MgSO_4$ against a standard (2 M KCl) extractant for concurrent measurement of NH_4^+ and NO_3^- ions using an automated colourimetry (FIA) method.

Secondly, to validate with standard instrumental method, the result from simultaneous analysis of Nr extracted by 0.1 M $MgSO_4$ solution using ion-selective electrodes (ISEs).

And thirdly, to test the Bayesian modelling for improvement in accuracy and precision of measured Nr in various samples using standard addition method.

3.3 Experimental

3.3.1 Reagents

Nonactin (ammonium ionophore I), sodium tetrakis[3,5-bis- (trifluoromethyl)-phenyl]borate (NaTFPB), tetradodecylammonium chloride (TDACl), high molecular weight heir poly(vinyl chloride) (PVC), bis(2-ethylhexyl)- sebacate (DOS), 2-nitrophenyl octyl ether (σ-NPOE), sodium phenolate, sodium hypochlorite, sodium hydroxide, disodium ethylenediaminetetraacetic acid (Na_2EDTA), sodium nitroprusside, sulfanilimide, phosphoric acid (H_3PO_4), concentrated nitric acid (HNO_3), N-1-napthylethylenediamine dihydrochloride (NED), magnesium chloride ($MgSO_4$), potassium nitrate (KNO_3), ammonium chloride (NH_4Cl), ammonium sulphate ($(NH_4)_2SO_4$), sodium chloride (NaCl), potassium chloride (KCl), and tetrahydrofuran (THF) were obtained from Sigma-Aldrich. Additionally, 100 mg/L N as nitrate in water, prepared with high purity sodium chloride ($NaNO_3$) and water, and 1000 mg/ L N as ammonium in water, prepared with high purity ammonium chloride (NH_4Cl) and water, were also bought as stock solutions from Sigma-Aldrich. Multi-element stock standards for ICP-OES and ion chromatography were obtained from Fisher Scientific UK. All aqueous solutions and dilutions were prepared in ultra-pure water obtained with Purelab Ultra water purification system (resistance 18 MΩ cm).

3.3.2 Study sites and sampling

To investigate the performance of the sensor for practical application in soils, four sampling plots were selected randomly in four major land use types from around the North Wales & Staffordshire regions of the UK as shown in figure 3.1. The soil type from grassland is denoted as GL; improved grassland is denoted as IGL; arable land is

denoted as AR; and the three forest soils which contained vegetation from ash, oak and Scottish pine (SP) trees, were from the Free-Air Carbon dioxide Enrichment (FACE) facility in Staffordshire, UK set up by The Birmingham Institute of Forest Research (BIFoR).

The grassland land type was a non-mowed, non-limed or unfertilised grassland where grazing activity is restricted to small sheep numbers, while the improved grassland type was more characterised by seasonally waterlogged soils grazed perennially by both sheep and cattle, where fertiliser (range 100 – 200 kg N ha^{-1}) and manure are applied twice per year during spring and summer months. The arable land type receives significantly more amount of fertiliser and manures and predominantly grows barley and wheat. The forest land types were from a poorly drained, never fertilised land type containing more acidic soil with gently sloping topography.

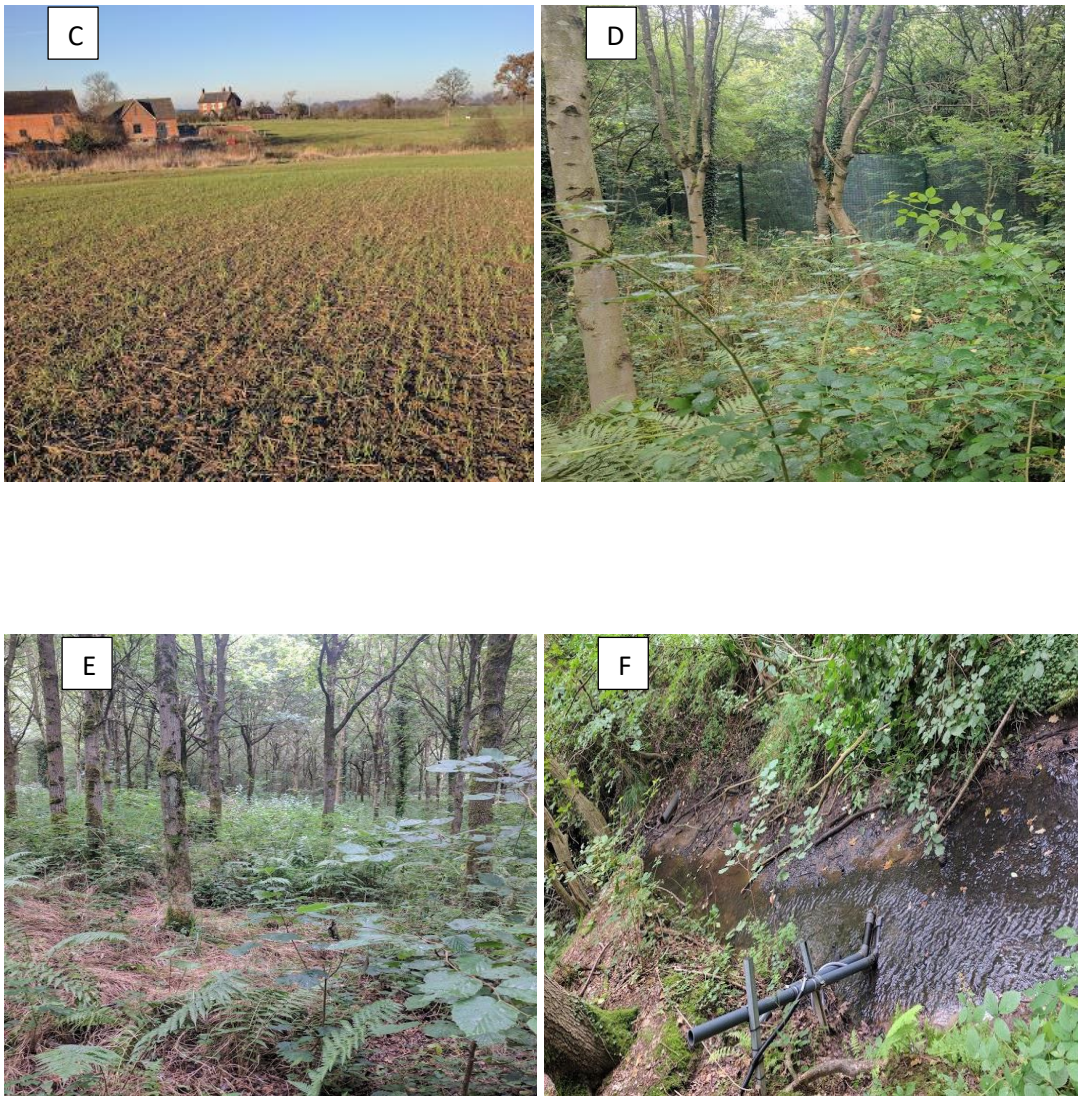

Figure 3.1 Photographs showing various vegetation on the different land use types: A - grasslands; B - improved grassland; C - arable; D, E and F - forest (F also shows a picture of the stream where water sample was collected).

For all the soil types, overlying vegetation covering sample plots were removed for proper sample collection. One soil core (2 – 15 cm depth; 5 cm diameter) was collected for each sample plot using a hand auger. Each soil core was then homogenized by manual mixing and divided into four sub-samples, representing the number of replicate (i.e. n = 4). All the soils were stored in gas permeable polyethylene bags and transported on ice to the laboratory. Immediately prior to analysis, the soil was sieved

to 4 mm to remove plant materials, large stones, and earthworms and then thoroughly mixed.

Additionally, for more extensive comparison of the potentiometric procedure to standard methods, water samples (n = 4) from upstream and downstream of the BIFoR woodlands were sampled according to standard water sampling procedure.[53,54] All samples, including one travel blank and two filtered blanks, for quality control purpose, were transferred on ice to the laboratory within 2 h of collection, where they were refrigerated at < 5 °C until needed for experimental procedures. Water analysed for Nr included filtered and unfiltered samples. Since most sophisticated standard methods like ion chromatography or FIA require a filtration step for samples to be free of suspension, filtered samples were necessary for easy comparison of results measured using potentiometric and standard analytical methods. Lastly, the purpose of an unfiltered sample collection was to evaluate the efficiency of the ISEs in direct measurement of Nr without the need for further clarification steps.

3.3.3 Baseline soil analysis

The main physico-chemical soil analysis shown in table 3.1 were performed on air-dried soils, and according to established methods.[19,26]. Soil moisture content was measured gravimetrically as moisture lost from a subsample of air-dried soils by continuous heating (105 ^{o} C) for up to 24 h until constant weight was achieved. Soil pH was measured at (soil: water mix = 1: 2.5) by a standard pH probe. For all analysis, the precision was calculated as standard deviations. For analysis involving standard analytical methods, samples were blank corrected to check for the effect of signals other than from the analyte. This was done by preparing some reagent blanks (usually water or appropriate extractant) as additional samples, in the same procedure as the

other samples examined. The results of the blanks were then averaged, and subtracted from individual sample value to give the reported concentration of the analyte in each sample.

Table 3.1 Baseline soil analysis for three types of soil sampled around North Wales and Staffordshire. Four replicates sampled for each soil type.

Soil sample (n = 4)	pH	Moisture content (g/ g)
Grassland (GL)	6.66 ± 0.03	0.14 ± 0.05
Improved grassland (IGL)	6.26 ± 0.03	0.08 ± 0.02
Arable soil (AR)	6.38 ± 0.02	0.15 ± 0.03
Ash	6.14 ± 0.04	0.35 ± 0.04
Oak	5.86 ± 0.02	0.29 ± 0.05
Scottish pine	6.03 ± 0.02	0.14 ± 0.03

3.3.4 Standard extraction procedure for NH_4^+ and NO_3^- in soil using 2 M KCl

For measurement of reactive N (NH_4^+ and NO_3^-) in soil, 20 g of air-dried sieved (<2 mm) soil were weighed into 250-mL HDPE Nalgene bottles. This was followed by a routine extraction process of the soils with 100 mL of 2 M KCl as shown in figure 3.2. Briefly, the soil slurries - a combination of measured soil sample and extractant - were continuously shaken on a reciprocating shaker at 200 rpm for 1 h before being centrifuged at 4000 rpm for 30 minutes followed by a two-step filtration into 20 mL scintillation vials through a no. 42 Whatman filter paper, and then 0.45 micron syringe filters (Whatman). All analysis were carried out immediately unless otherwise stated where samples were frozen until analysis.

Figure 3.2 A flowchart showing the extraction process to sample analysis (Please note: shaking and centrifugation not shown).

3.3.5 Determination of reactive nitrogen in soil and water samples by standard analytical method (flow injection analyzer)

3.3.5.1 Overview of method

The analysis of NH_4^+ and NO_3^- in soil type and water samples was performed on an automated Lachat flow injection analyzer (Hach, Colorado, USA) according to standard colorimetric techniques. [19,32] Nitrate was measured by the cadmium reduction procedure. The sample is passed through a copperized cadmium column which reduces nitrate quantitatively to nitrite. The total nitrite (reduced nitrate plus original nitrite) is then determined by diazotizing with sulfanilamide followed by coupling with N-(1-naphthyl) ethylenediamine dihydrochloride. The resulting water soluble magenta coloured dye is measured colourimetrically at 520 nm. Nitrite alone can also be determined by removing the cadmium column.

Ammonium was measured according to the Berthelot reaction. An alkaline phenol and sodium hypochlorite react with ammonia to form a blue indophenol compound which is proportional to the ammonia concentration. The presence of EDTA in the buffer prevents precipitation of calcium and magnesium. The colour is intensified by adding sodium nitroprusside. The resulting water soluble coloured dye is measured colourimetrically at 630 nm.

The applicable range of the ammonia channel is 0.02-1.0 mg N/ L. while that of the nitrate channel is 0.02-20.0 mg N/ LThe ranges may be extended with the digital diluter. The limit of detection for nitrate was 0.03 mg N/ L and for ammonium 0.01 mg N/ L. High extract samples were further diluted to obtain concentration within the calibration range of the instrument. The samples were blank corrected. Please note as guide, since the atomic weight of nitrogen is 14.0067, and the molar mass of nitrate

(NO_3^-) and ammonium (NH_4^+) are 62.0049 g/ mol and 18.01 g/ mol respectively, nitrate-nitrogen (NO_3^--N) is converted to NO_3^- by a multiplication factor of 4.427. Similar is also for the conversion of ammonium-nitrogen (NH_4^+-N) to NH_4^+ which requires a multiplication factor of 1.286.

3.3.5.2 Reagents for the ammonia-nitrogen (Berthelot reaction) method

1) Sodium Phenolate: In a 200 mL volumetric flask, 17.6 mL of 88% liquefied phenol was dissolved in approximately 120 mL of deionised water. While stirring, 6.4 g NaOH was slowly added. The solution was cooled, filled up to the required mark on the flask and mixed by inverting few times.

2) Sodium Hypochlorite: In a 100 mL flask, 50 mL of a 5.25% sodium hypochlorite was added to 50 mL deionised water and inverted to mix.

3) Disodium EthylenediamineTetraacetate (NA_2EDTA): In a 200 mL volumetric flask, 10g EDTA was dissolved with 2.8 g NAOH in about 150mL deionised water. The resulting solution was filled up to the required point with more deionised water and inverted several times to mix.

4) Sodium Nitroprusside: In a 200 mL flask, 0.7 g of sodium nitroprusside was dissolved in deionized water and filled up to the required point on the flask. The solution was mixed with a magnetic stirrer until dissolved and stored solution in a dark bottle.

3.3.5.3 Reagents for the nitrate-nitrogen cadmium reduction method

1) 3 M Sodium hydroxide: To a 50 mL of deionised water in a 100 mL beaker, 60 g of sodium hydroxide was added slowly and swirled until dissolved. This was then stored in plastic bottle.

2) Ammonium chloride: In a 200 mL, 16 g of ammonium chloride was dissolved in about 160 mL deionised water. 0.2 g of EDTA was added with the pH adjusted to 8.5 with sodium hydroxide. The solution was diluted to the mark with more deionised water.

3) Sulfanilamide: In a 200 mL volumetric flask, 20 mL of phosphoric acid was added to 120 mL deionized water. 8 g of sulfanilamide and 0.2 g NED were added, shaken to wet and stirred for 20mins to dissolve. The solution was diluted to the mark with deionised water and stored in a dark bottle.

3.3.5.4 Standards preparation

100mL stock solution of NH_4^+-N standard of 100 ppm was made from 1000 ppm by adding 10 mL of 1000 ppm and 90 mL of 1 M extractant to make a final volume of 100 mL. Six working standards ranging from (0 ppm, 0.05 ppm, 0.01 ppm, 0.1 ppm, 0.5 ppm, 1 ppm) in 50mL volumetric flasks were made from the 100 ppm stock.

Note: 0 ppm only contained 50mL of extractant

For nitrate-nitrogen NO_3^--N standards, a 100 mL stock solution of 20 ppm was made from 100 ppm NO_3^--N stock solution. Other working standards done by serial dilution stock standard.

3.3.5.5 Sample Analysis

This set-up was to be able to measure concurrently both ammonium and nitrate by using a QuickChem 8500 series 2 continuous flow injection analysis (FIA) system (Lachat Instruments). A schematic of this is represented below in figure 3.3 showing an autosampler for samples, an injection valve, a peristaltic pump linked to all lines entering the system, a detector containing a flow cell, and a waste line. The nitrate manifold included a cd-reduction column for reduction to nitrite when required. The ammonium line was set up such that its phenolate waste was channelled to a separate corked bottle because of toxicity. At the start of operation, deionized water was passed through all the reagent lines of both manifolds to check for leaks and smooth flow. The heater was set to the 60 degrees Celsius set point for (only for ammonium channel) for necessary reaction temperature to be attained and reagents were passed through to enable the system to equilibrate and achieve a stable base line. The required sequence data was then loaded, and compared to match the positions of the samples, starting with some blanks, appropriate standards and the samples to be analysed. The reaction was then started and calibration curve checked to ensure a good linearity (> 0.9995) with blanks and check standards run after 4 to 5 samples for data validation and QC.

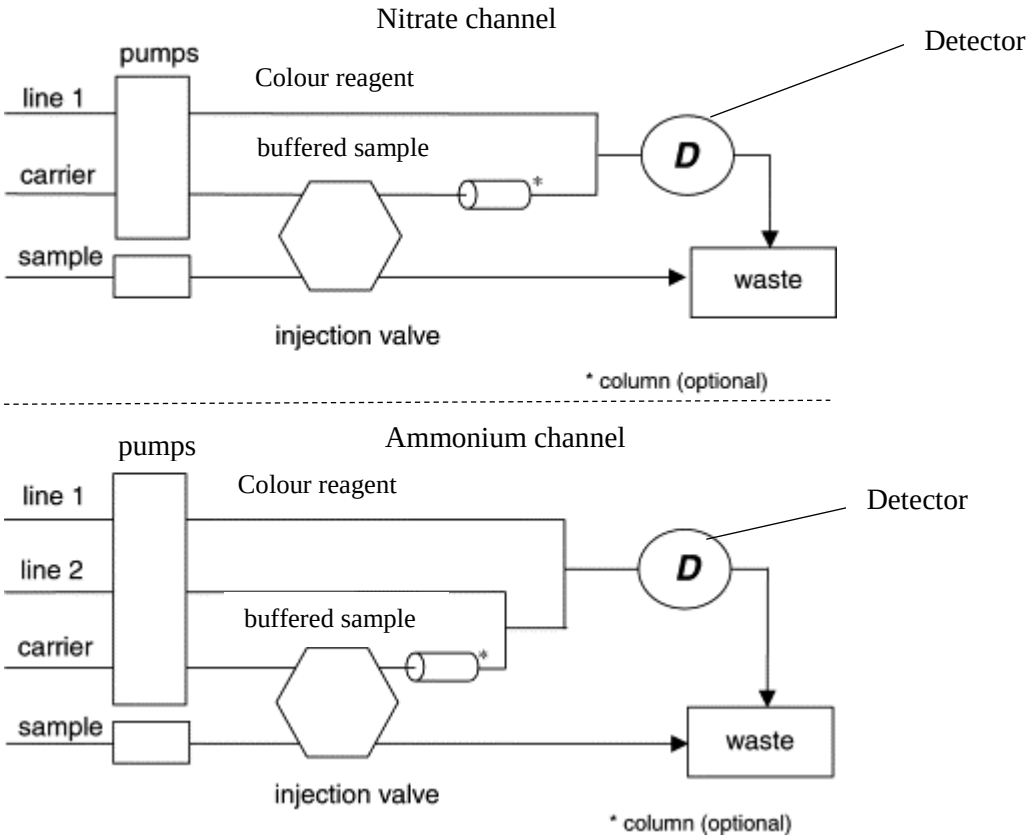

Figure 3.3 A flow diagram of a two-channel continuous FIA method for simultaneous measurements of ammonium and nitrate using the QuickChem 8500 series 2 (FIA) system (Lachat Instruments). For both channels, line 1 represents the colour reagent (sulfanilimide for nitrate line and sodium nitroprusside for ammonium line), while line 2 in ammonium line channel is the phenolate line. Carrier for both lines are typically deionised water or appropriate extractant. The reaction is buffered by NH4Cl for nitrate measurement and EDTA for ammonium measurement.

3.3.5.6 Data validation and QA/QC

Sample concentrations were calculated from the regression equation having values close to 0.9995. Only data that fell within the lowest and highest calibration standards were used. If some data exceed this highest point, dilute and reanalyzed.

3.3.6 Evaluation of extraction potential of 0.1 M $MgSO_4$ for analysis of NH_4^+ and NO_3^- ions in soil samples

To validate the potentiometric measurement using ISE, 0.1 mol/ L $MgSO_4$ was investigated as a single extracting medium for simple simultaneous measurement of NH_4^+ and NO_3^-. This was a procedural adoption of previously reported protocols where different extractants had been used for inorganic N analysis as highlighted above. This extraction utilized the same extraction procedure as in section 3.3.4 above.

3.3.7 Elemental determination of cations in soil samples by inductively coupled-plasma – optical emission spectrophotometer (ICP-OES)

3.3.7.1 Overview of method

The elemental analysis of soil and water samples were performed using a Varian MPX Vista ICP-OES. The method uses a high energy argon plasma to convert elements in samples and standards into a gaseous, excited state form that emits electromagnetic radiation at characteristic wavelengths. The colours of the emitted light and the light intensity can be used to identify the element and determine how much of the element is present in a sample. The ICP-OES uses an array of detectors which simultaneously measure elements by optical spectroscopy.

3.3.7.2 Digestion of soil samples

All samples analyzed were acidified using concentrated nitric acid. However, a digestion process was needed to extract the elements under examination from the soil samples. This was achieved by weighing accurately 0.50 g (±0.01 g) of dried soil sample into a PTFE microwave vessel, followed by the addition of 10 mL of concentrated nitric acid. Please note, if a vigorous reaction occurs, sometimes maybe

due to nature of samples, the vessels are left open for about 15 mins before capping. The vessels were capped, and placed evenly in the microwave for digestion process. To begin the digestion, a ramp 15 mins, and digestion at 200 ^{o}C for 10 mins was selected in the program setting. Samples were then left in the microwave oven for 20 mins to cool down. Vessels were allowed to cool further, and then transferred to a fume hood for further analysis. The samples transferred into centrifuge tubes and were centrifuged for 10 mins. For samples that required dilutions, 1 mL of clear digestate were pipetted into clean PTFE vial or into ICP/OES sampled tubes (appr. 10 mL) and 9 mL of 1% nitric acid was added. This dilutions were accounted for during calculations of actual concentration, otherwise, concentrations were reported as actual concentration for samples that required no dilutions.

The concentrations determined in the digestate were reported on the basis of the dry weight of the sample, in units of milligrams per kilogram (mg/kg) as:

Soil Sample Concentration

Concentration (dry wt.) (mg/kg) = $\frac{C\ X\ V}{W\ X\ S}$ X DF

Where, C = concentration (mg/ L)

V = final sample volume (L)

W = wet sample weight (kg)

S = % solids/ 100

DF = dilution factor

3.3.7.3 Analysis

To start the operations, the required sequence data was loaded, and compared to match the positions of the samples, starting with some blanks, appropriate multi-element standards and the samples to be analysed. After a constant flow was achieved in all the lines going in, the plasma was lit, and left to attain thermal stabilisation by running deionised water or carrier solution for few minutes. The analysis was initiated after all the samples (soil digestate) had been placed in the autosampler, and an acceptable calibration plot achieved, usually with correlation coefficient (r-value) equal or greater than 0.995. Blanks and check standards were run after 4 to 5 samples for data validation and QC/QA, and to minimise carry-overs that can result in contamination of samples.

3.3.8 Determination of anions in soil samples by ion chromatography

3.3.8.1 Overview of method

The composition of anions in the soil and water samples were determined using an ion chromatography (Dionex ICS 5000). This is a liquid chromatographic technique based on an ion exchange mechanism and suppressed conductivity detection for the separation and determination of anions. Like other chromatographic techniques, ion chromatography involves separation of ions whereby each ion's affinity for the exchange site, known as its selectivity quotient, is largely determined by its radius and its valence. As samples are loaded through the autosampler, the eluent and the sample ions migrate along the packed column based upon their migration velocities. Then the eluent and sample ions enter a suppressor that selectively enhances ion detection and suppresses the conductivity of the eluent. Each ion is identified by its retention time

within the ion exchange column and quantifiable by comparison of the peak heights and peak areas of the calibration to the measured peaks of the samples.

3.3.8.2 Analysis

After an initial preparation of the eluent (sodium carbonate/ sodium bi-carbonate), appropriate flow rate was selected for the analysis, and the system was initially left to run for about 1 hour to allow for a stable base line. Using a computer-aided software in form of Chromeleon 7.2, a sequence was loaded from a list of previously saved analysis of anions. A 0.5 mL of each of the calibration standards was placed into the vials and passed through the autosampler for the calibration process. After acceptable calibration plot, 0.5 mL of each sample was also loaded into the vials already placed in the cassettes and passed through the autosampler. The samples vials were then aligned in the sampling tray according the sequence. The order of the sequence usually started with the calibration standard solutions, deionized water, and the sample to be measured. In addition, check standards and blanks were added after every four samples for data validation and QC/QA purposes. The analysis was then started after an error check was done to ensure smooth running.

3.3.9 NH_4^+ and NO_3^- determination using ion-selective electrode (ISE)

3.3.9.1 Preparation of conductive substrate

Preparation of the sensing platforms was based on our previous work on paper ISEs. [21] Briefly, a 9.0 × 3.0 cm strip was cut from parent acetate sheet and prepared similarly to section 2.2.2 (chapter 2) of this thesis. Eight lines of carbon were subsequently drawn onto the roughened surface of acetate by pencil and the electrodes set up to form a strip that contained four NO_3^- - and four NH_4^+ - selective electrodes .

3.3.9.2 Preparation of nitrate- and ammonium-sensing membranes

The NO_3^--selective membrane contained 5.0 mmol kg^{-1} of TDACl, PVC (33.2 wt %) and σ-NPOE (66.4 wt %). NH_4^+-selective membrane contained 10.0 mmol kg^{-1} of ammonium ionophore I and 5.0 mmol kg-1 of NaTFPB, PVC (32.9 wt %) and DOS (65.8 wt %). These represented the optimal membrane components reported in previous study [21] and in chapter 2 of this thesis. All electrodes were prepared by dissolving the above-mentioned components in 1.5 mL THF and the resulting cocktail was vortexed for 30 min for complete dissolution of components.

3.3.9.3 Development of ISEs

For potentiometric measurements, an aliquot (~20 μL) of relevant sensing membrane cocktail was drop cast onto the top of each electrode, and left at room temperature to dry overnight. The following day, the ISEs were conditioned in 1.0 x 10^{-3} M of respective primary ion solution while reference electrodes were conditioned in 1.0 x 10^{-2} M of KCl for 18 h prior to the potentiometric experiments.

3.3.9.4 EMF measurements

Potentiometric responses of all electrodes were recorded using Lawson Labs Inc. 16-channel EMF-16 interface (3217 Phoenixville Pike Malvern, PA 19355, USA) in a stirred solution against a double-junction Ag/AgCl reference electrode with a 1 M LiOAc bridge electrolyte (Fluka). Before measurement of analytes, a calibration step was initially carried out by immersing all electrodes into a beaker of appropriate background sample solution followed by stepwise addition of required standard solutions of NH_4^+ and NO_3^- using standard addition methods. Electrodes were properly rinsed with ultra-pure water before immersing into the next sample to avoid

carryovers. Potential responses (EMF) were then measured, and activities calculated from the calibration curve using the Nikolskii-Eisenman equation. Figure 3.4 shows the work flow of the potentiometric measurement from electrode fabrication to analysis:

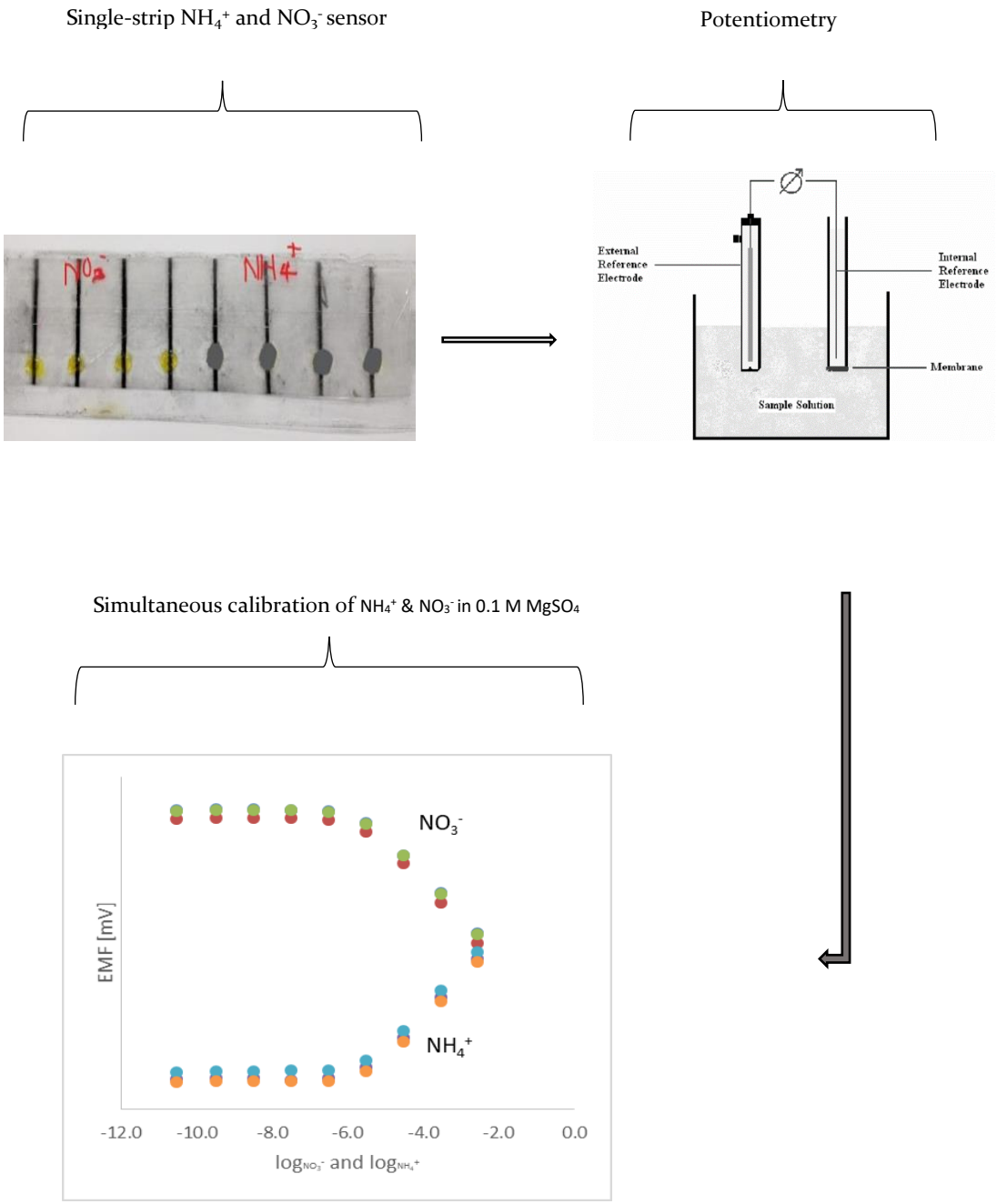

Figure 3.4 A flow diagram showing concurrent measurement of NH_4^+ & NO_3^- using single strip paper-based potentiometric platform. The sensor comprises an array of 8 electrodes, 4 for each ion.

3.3.9.5 Selectivity measurements

For selectivity coefficient measurement, ammonium-selective electrodes were prepared and conditioned overnight in 0.01 M NaCl, while nitrate-selective electrodes were conditioned in 0.01 M $(NH_4)_2SO_4$ overnight. Responses towards interfering ions were recorded according to separate the solution method as described by Bakker at al. [55]

3.4 Calculations and statistical analysis

3.4.1 Equations for conversion and Bayesian analysis

Concentrations given in this chapter are reported in mg/ L or mol/ L of each analyte.

Therefore, for a concentration X of nitrate, conversion from (X mg/ L) to (mol/ L) can be rewritten as;

Concentration (mol/ L) = X / 62,000 (3.1)

For a concentration Y of ammonium, conversion from Y (mg/ L) to (mol/ L) can be rewritten as;

Concentration (mol/ L) = Y / 18,000. (3.2)

Simulations and all nonlinear analyses were done using the OpenBUGS variant (version 3.0.3) of BUGS, linked to R-studios using the R2WinBUGS library.[52]

3.4.2 Statistical analysis

Statistical analyses were performed separately for each electrode to obtain average result of the amount of Nr in the samples. For repeated samples, the corresponding standard deviations show the precision of the reading range. The t-test ($p < 0.05$) was computed to test for statistical significance between the amount of respective analyte in different extraction media, and the statistical difference between soil's Nr obtained using different techniques. The Pearson's correlation (r) values with respective p-values were calculated from a scatter plot to test for the correlation of the concentration of Nr in soil and water using FIA and ion-selective electrodes,

3.4.3 Standard addition method

The measurement of species in samples by ISEs mainly involve using the direct potentiometry method or standard/ sample addition method. While the former, known for its simplicity has been used for a very long time, it tends to suffer where there is significant matrix effect that can affect complete analyte measurement within samples examined. This is why the standard/ samples addition, which minimises such problem is seen as a better option for potentiometric measurements involving more complex samples. Another advantage of the standard addition method also lie in the fact that measurements are done under similar experimental conditions like temperature, stirring rate, ionic strength. This gives measurements similar electrode properties (i.e. slope and standard potential). In addition, unlike the direct potentiometric method where electrodes need to be taken out, and dipped into different solutions, the standard addition method requires the electrodes to be completely immersed in the same solution it started with, therefore minimising junction potentials which could introduce further errors into the analysis.[56] The standard addition method given by the formula in equation 3.3 was done by taking a first electrode reading of a predetermined volume of the sample after a stable baseline. A second electrode reading was then taken after an aliquot of standard of ion of interest was added to the sample. This was used to calculate the unknown activity of the ion of interest (nitrate or ammonium).[50]

$$C_x = \frac{C_S * \left[\frac{V_S}{V_x + V_S}\right]}{\left[10^{\frac{E_2 - E_1}{m}} - \frac{V_x}{V_x + V_S}\right]} \qquad (3.3)$$

From the equation, C_x and C_S are concentration of the unknown sample and the standard respectively, V_x and V_S are volumes of sample and standard solutions, E_1 and E_2 are electrode potentials (mV) of the sample and after the addition of the standard and m is the slope.

3.5 Results and discussion

3.5.1 Efficiency of 0.1 M $MgSO_4$ as a single extractant for analysis of Nr

Soils are made of various levels of ions – a factor that could render the accurate potentiometric measurement of primary ions (NH_4^+ & NO_3^-) by ISEs biased, therefore an approach based on the differences in selectivity coefficients of the sensing components towards major interfering ions (expected to be present in the samples) was developed (see experimental section 3.3.9.5 and result table 3.5 for more information about selectivity coefficient). The selectivity coefficient values of NH_4^+-ISE and NO_3^--ISE towards magnesium and sulphate are very small. For this reason, 0.1 M $MgSO_4$ was chosen as extracting medium to extract NH_4^+ & NO_3^- from soil samples, with the approach aimed at providing a short-cut procedure for concurrent measurement of ammonium and nitrate, therefore reducing the already lengthy stages of sample preparation.

To investigate the efficiency of 0.1 M $MgSO_4$ in extracting Nr, the concentrations of extractable ions (NH_4^+ & NO_3^-) by 0.1 M $MgSO_4$ were compared to a standard extractant (2 M KCl). As seen in table 3.2, a very good correlation between concentrations of soil nitrate and ammonium extracted with KCl and $MgSO_4$, measured using standard colorimetry (FIA) method suggests adequate extraction efficiency of the salt, thereby confirming the possibility of using 0.1 M $MgSO_4$ as a possible alternative for commonly used extractant. In addition, the t-test performed on the ammonium and nitrate concentrations in table 3.2 resulted to *p*-values of 0.51 and 0.99 respectively. Since these are higher than 0.05, it indicates that there is no statistically significant difference between each analyte concentration obtained from

both extracting media. This supports the claim that 0.1 M $MgSO_4$ is a suitable extractant for analysis of both ions.

Table 3.2 Analysis of soil ammonium and nitrate (n = 4) extracted by 2 M KCl & 0.1 M $MgSO_4$ using the colourimetric (FIA) method.

	NO_3^- ± SD (mg/ L)		NH_4^+ ± SD (mg/ L)	
Soil sample	2 M KCl	0.1 M $MgSO_4$	2 M KCl	0.1 M $MgSO_4$
GL	17.89± 3.58	17.00 ± 1.94	0.76 ± 0.35	0.70 ± 0.25
IGL	17.31 ± 3.70	17.80 ± 1.60	1.00 ± 0.19	0.90 ± 0.19
AR	9.40 ± 1.72	9.24 ± 0.38	0.81 ± 0.08	0.53 ± 0.08
Ash	0.98 ± 2.08	0.91 ± 1.28	0.63 ± 0.45	0.42 ± 0.45
Oak	1.92 ± 0.94	1.72 ± 0.94	0.63 ± 0.62	0.57 ± 0.62
SP	2.45 ± 1.15	2.91 ± 1.15	1.62 ± 0.39	1.44 ± 0.39

Further analysis of common interfering ions present in soil was performed by ion chromatography and ICP-OES for anions and cations respectively. For the soils tested, ICP-OES was used to evaluate the cationic species after a digestion process in a microwave as described in experimental section (3.3.7). As shown in table 3.3, it is seen that calcium and magnesium both have the largest proportion of cations tested in all the soil samples. However, because the selectivity of ammonium sensors towards them are lower, it implies that their influence is less significant. Although, high level of potassium can still cause interference to ammonium sensors. In addition, the Pearson's correlation (*r*) values of the tested cations towards ammonium in the order

- K, Na, Ca, Mg corresponds to 0.033, 0.049, 0.023, and 0.353. This shows that magnesium is the most positively correlated to ammonium.

Table 3.3 Elemental analysis of cations in soil samples (n = 4) using ICP-OES.

Sample Concentration in (mg/ L ± SD)				
Sample Labels	K	Na	Ca	Mg
GL	1.85 ± 0.36	3.20 ± 0.69	21.30 ± 1.96	3.06 ± 0.78
IGL	2.82 ± 0.82	3.51 ± 1.11	46.79 ± 3.00	6.09 ± 0.72
AR	0.98 ± 0.11	1.49 ± 0.45	16.67 ± 2.47	2.60 ± 0.53
Ash	0.45 ± 0.31	1.14 ± 0.38	5.62 ± 0.56	14.68 ± 2.66
Oak	0.29 ± 0.36	0.86 ± 0.10	6.36 ± 0.41	12.29 ± 1.71
SP	0.36 ± 0.14	1.35 ± 0.28	6.35 ± 0.11	16.37 ± 2.34

Measurement of anions using ion chromatography was done firstly, to determine the concentrations of anions deemed commonly present in soils and major environmental samples which might interfere with potentiometric analysis. Then secondly, to compare the concentrations of the extractable nitrate determined by FIA (Cd reduction) in table 3.2 above with concentration obtained alongside with other anions using ion chromatography. Table 3.4 shows the concentrations of anions in the soil samples using ion chromatography.

Table 3.4 Analysis of major anions present in soil samples (n = 4) using ion chromatography (Dionex).

Sample Concentration in (mg/ L ± SD)							
Sample Labels	Fluoride	Chloride	Nitrite	Bromide	Nitrate	Phosphate	Sulfate
GL	0.42 ± 0.19	0.89 ± 0.33	NA	NA	15.94 ± 1.98	2.16 ± 0.68	3.03 ± 1.15
IGL	0.12 ± 0.02	0.86 ± 0.61	NA	NA	16.24 ± 3.66	6.96 ± 1.07	2.08 ± 0.77
AR	0.63 ± 0.07	1.98 ± 0.30	NA	NA	8.4 ± 2.09	0.73 ± 0.26	2.02 ± 0.37
Ash	0.13 ± 0.05	0.86 ± 0.43	NA	NA	0.77 ± 0.04	NA	0.69 ± 0.24
Oak	0.03 ± 0.04	0.78 ± 0.29	NA	NA	1.72 ± 0.59	NA	1.04 ± 0.31
SP	0.19 ± 0.06	4.51 ± 1.84	NA	NA	2.83 ± 0.76	NA	3.16 ± 0.68

Comparisons between table 3.2 and table 3.4 show similar nitrate results for the soils tested by both methods. This is also evident from the scatter plot in figure 3.7 below where it can be seen that the concentrations of nitrate in soils, extracted by 0.1 M $MgSO_4$ and detected by both methods are comparable. This gives a level of confidence that either methods can be used to validate the values measured by ISE as show later.

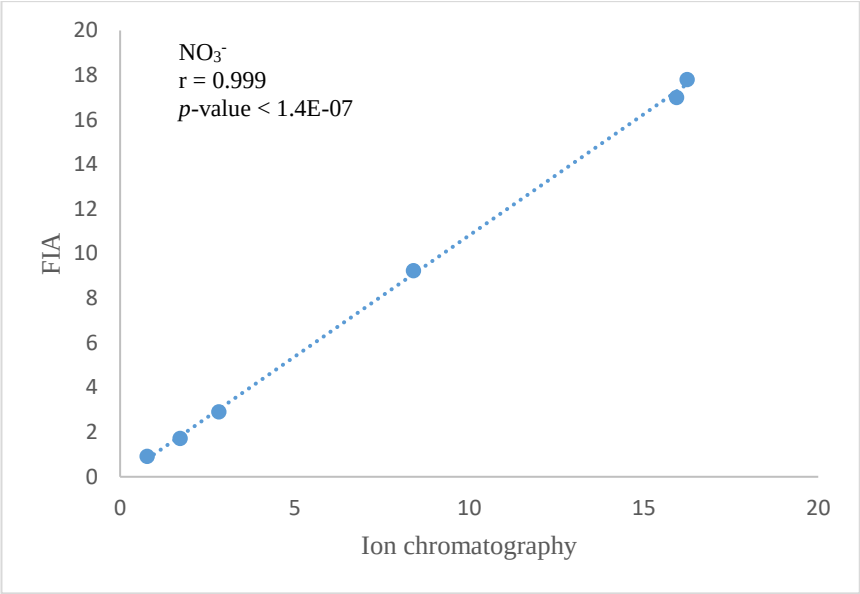

Figure 3.7 Scatter plot for comparison of the average concentration of 0.1 M $MgSO_4$-extractable NO_3^- in 4 soil types (n = 4), using FIA and ion chromatography. Inset shows *r* and *p*-value from the regression analysis for both methods.

3.5.2 Potentiometric behaviour of NH_4^+- & NO_3^- - ISEs in different solutions

The relationship amongst the potentiometric characteristics of ISEs including slope, limit of detection (LOD), working range and selectivity coefficient, as illustrated by the calibration plot of an ISE measurement is fundamentally guided by the Nernst equation. [57] Crucially, the overall selectivity coefficient of an ISE towards primary ions and other interfering ions, especially those with similar charges, greatly dictates its lower limit of detection. [37,58–60] As a result, nitrate ISE would normally suffer greatly, if the amount of chloride to nitrate is higher than 300th times. Similar for ammonium ISE, is the influence of a ten times more concentration of potassium relative to ammonium ion. The result in table 3.5 shows the selectivity coefficient values of both ISEs towards relevant interfering ions. This means even after extraction with 0.1 M $MgSO_4$, the resulting total concentration of each primary ion in the soil/

extractant mixture will still allow for accurate measurement of NH_4^+ & NO_3^- by electrodes containing nonactin (ionophore) or TDMACl (ion exchanger) respectively. Ultimately, the significance of replacing KCl by 0.1 M $MgSO_4$ as extractant is to avoid unnecessary loading of the more-selective potassium and chloride ions into the potentiometric analysis. Moreover, considering the selectivity coefficient values obtained for the ISEs, the ratio of the amount of interfering ions present in all the soils compared to the primary ion does not seem to pose any major effect on the potentiometric analysis.

Table 3.5 Selectivity coefficients and experimental slopes for selected ions obtained for fabricated NO_3^- - & NH_4^+ - selective electrodes using separate solution method.

Ion	$log\ K_{i,J}^{pot}$ ± S.D	Slope ± S.D	Ion	$log\ K_{i,J}^{pot}$ ± S.D	Slope ± S.D
Na^+	-2.96 ± 0.03	57.53 ± 0.27	Cl^-	-2.48 ± 0.02	-52.93 ± 0.30
Cs^+	-2.56 ± 0.03	54.05 ± 0.06	NO_2^-	-1.27 ± 0.03	-53.57 ± 0.54
K^+	-0.98 ± 0.02	55.24 ± 0.15	I^-	1.4 ± 0.03	-55.24 ± 0.15
Ca^{2+}	-4.54 ±0.01	25.11 ± 0.20	ClO_4^-	3.25 ± 0.02	-54.35± 0.25
Mg^{2+}	-4.33 ± 0.02	26.89 ± 0.11	SO_4^{2-}	-4.72± 0.09	-25.18 ± 0.39
NH_4^+	0	56.35 ± 0.30	NO_3^-	0	-55.78 ± 0.21

The success of good analysis in analytical science greatly depends on its calibration. Therefore based on the promising results attained by using 0.1 M $MgSO_4$ as extracting solution for the measurement of NH_4^+ and NO_3^- in soil by standard method, the potentiometric behaviour of ammonium and nitrate ISEs in a background solution of 0.1 M $MgSO_4$ was explored and compared to the usual calibration in a solution of water. This was to evaluate the realistic performance of the electrodes in such situation like soil Nr analysis where extraction is required. Briefly, electrodes were tested for concurrent calibration of NH_4^+ and NO_3^- in water, and then in 0.1 M $MgSO_4$ to show the effect of magnesium and sulphate on both ISEs.

Calibration curves of both ions from figure 3.8A & 3.8B show similarities in electrode responses measured in background samples of water and in 0.1 M $MgSO_4$. Near - Nernstian slopes (54.25 mV/ dec and -53.91 mV/ dec for NH_4^+ and NO_3^- electrodes respectively) were observed in both cases with similar lower limit of detection in μmolar range. More precisely, a similar linear range of 7.0×10^{-6} M to 2.0×10^{-2} M was attained for both ISEs, with an LOD of 5.0×10^{-6} M observed for NH_4^+ -ISEs and 4.0×10^{-6} M for NO_3^- -ISEs. This is in agreement with previously studied ammonium and nitrate ISEs. [20,46,51,61,62] The effect of interference from foreign ions on electrode response is also shown in figures 3.8A & 3.8B where a third plot involving the Nikolskii-Eisenman modelled response of both ISEs in a 2 M KCl environment, shows its unlikeliness as extracting background for measurement of both ions.

This relationship - based on selectivity coefficient - implies magnesium and sulphate, which are relatively present in larger quantity in most soils pose insignificant interference towards the fabricated NH_4^+ and NO_3^- sensors respectively. In general, it also explores the possibility of limiting the complexity, and possibly contamination

arising from the time-consuming handling of dynamic samples like soils, as a result of different extractions of ions.

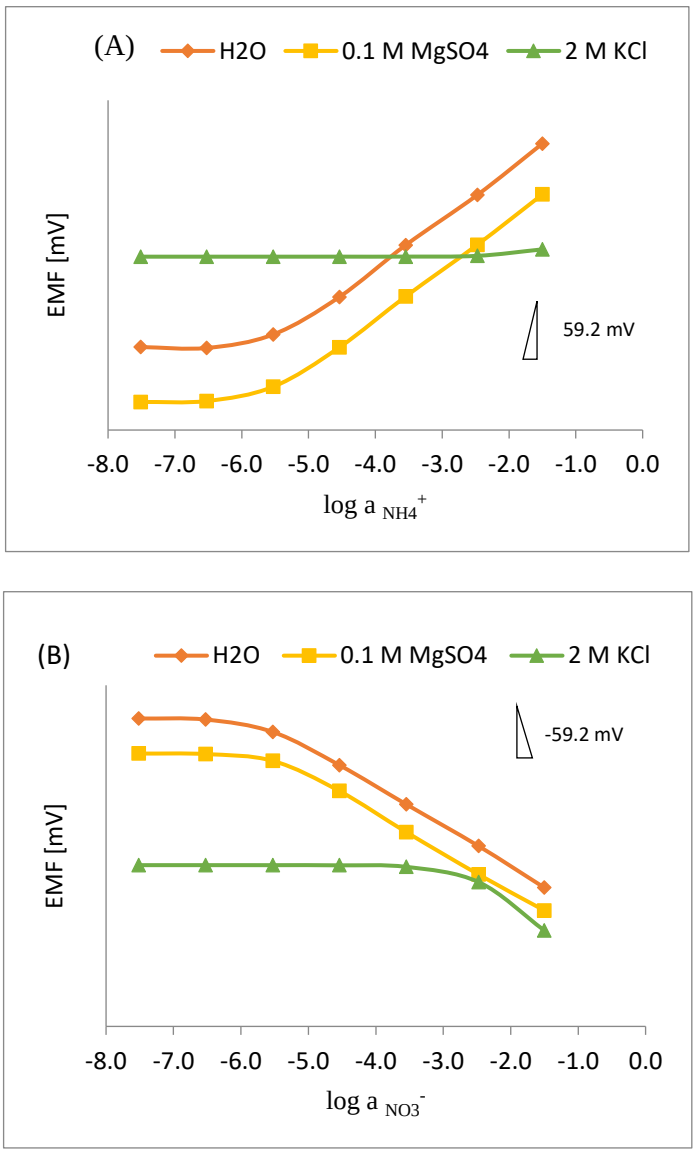

Figure 3.8 Response curves of NH_4^+ electrode (A) and NO_3^- electrode (B) in different background samples: diamond represents solution sample of ultra-pure water, block represents an initial background solution of 0.1 M $MgSO_4$, and triangle represents calibration plot in 2 M KCl modelled by the Nikolskii-Eisenman equation.

3.5.3 Comparison of the amount of Nr in environmental samples measured by FIA and ISE

In order to evaluate the suitability of the fabricated paper ISEs for a simple potentiometric measurement of both target ions (NH_4^+ and NO_3^-), soil samples extracted by 0.1 M $MgSO_4$ were analyzed using paper electrodes. The activities of the analytes were calculated from the standard addition method and compared to values from a reference technique (FIA). The measured concentration range of nitrate measured by ISE (~ 1.5 mg/ L to ~ 17 mg/ L or ~ 2.4 x 10^{-5} M to ~ 2.7 x 10^{-4} M) for all the soil types fell totally within the linear calibration range of the ISE response. However, the slight discrepancies observed in the concentration measured by both methods could be as a result of the dynamic transformation of NO_3^- to other forms of nitrogen as observed by Miegroet,[31] especially since the two analyses were done separately. In general, closeness of concentrations obtained for nitrate by both methods can be explained by the absolutely insignificant contribution from interfering anions present in the samples (see table 3.4). Slightly higher differences were observed in ammonium measurement which could majorly be as a result of high proportion of potassium, amongst other interfering cations as shown in table 3.3.

To further verify the similarities between concentrations of Nr measured by ISE and the reference method, the suitability of the sensors in measuring the ammonium and nitrate contents of samples from an upstream and downstream water running across the BIFoR site was tested. Overall, the relationship between the Nr measured by potentiometry and the standard analytical method for the environmental samples (water & soil) tested, are presented in table 3.6.

Table 3.6 Comparison of the concentration of extractable NH_4^+ & NO_3^- in 4 soil types (n = 4), and concentration of NH_4^+ & NO_3^- in two water samples (n = 4) measured by ISE and standard method (FIA).

		NO_3^- ± SD (mg/ L)		NH_4^+ ± SD (mg/ L)	
	Sample (n = 4)	FIA	ISE	FIA	ISE
Soil	GL	17.00 ± 1.94	16.89 ± 3.68	0.70 ± 0.25	0.84 ± 0.47
	IGL	17.80 ± 1.60	16.90 ± 3.46	0.90 ± 0.19	1.19 ± 0.35
	AR	9.24 ± 0.38	8.06 ± 2.10	0.53 ± 0.08	0.65 ± 0.11
	ASH	0.91 ± 1.28	1.46 ± 2.74	0.42 ± 0.45	0.74 ± 0.61
	OAK	1.72 ± 0.94	2.55 ± 3.01	0.57 ± 0.62	0.80 ± 0.34
Water	SP	2.91 ± 1.15	3.95 ± 2.57	1.44 ± 0.39	2.10 ± 0.29
	DS	15.3 ± 6.42	13.55 ± 6.16	0.28 ± 0.07	0.15 ± 0.03
	US	20.25 ± 1.90	18.44 ± 0.72	0.33 ± 0.07	0.25 ± 0.10

The values of Nr for all the samples shown in table 3.6 were correlated using regression analysis. The respective Pearson's correlation (*r*) values of 0.995 & 0.980 for NO_3^- and NH_4^+ in figure 3.9 below represent good comparison of the two techniques used, thereby indicating excellent robustness of sensors for measuring the concentration of bioavailable Nr within samples with varying levels of primary and interfering ions. Similar results of filtered and unfiltered Nr in water samples tested (results not shown), indicate the insignificance of suspensions and turbidity towards the potentiometric measurement.

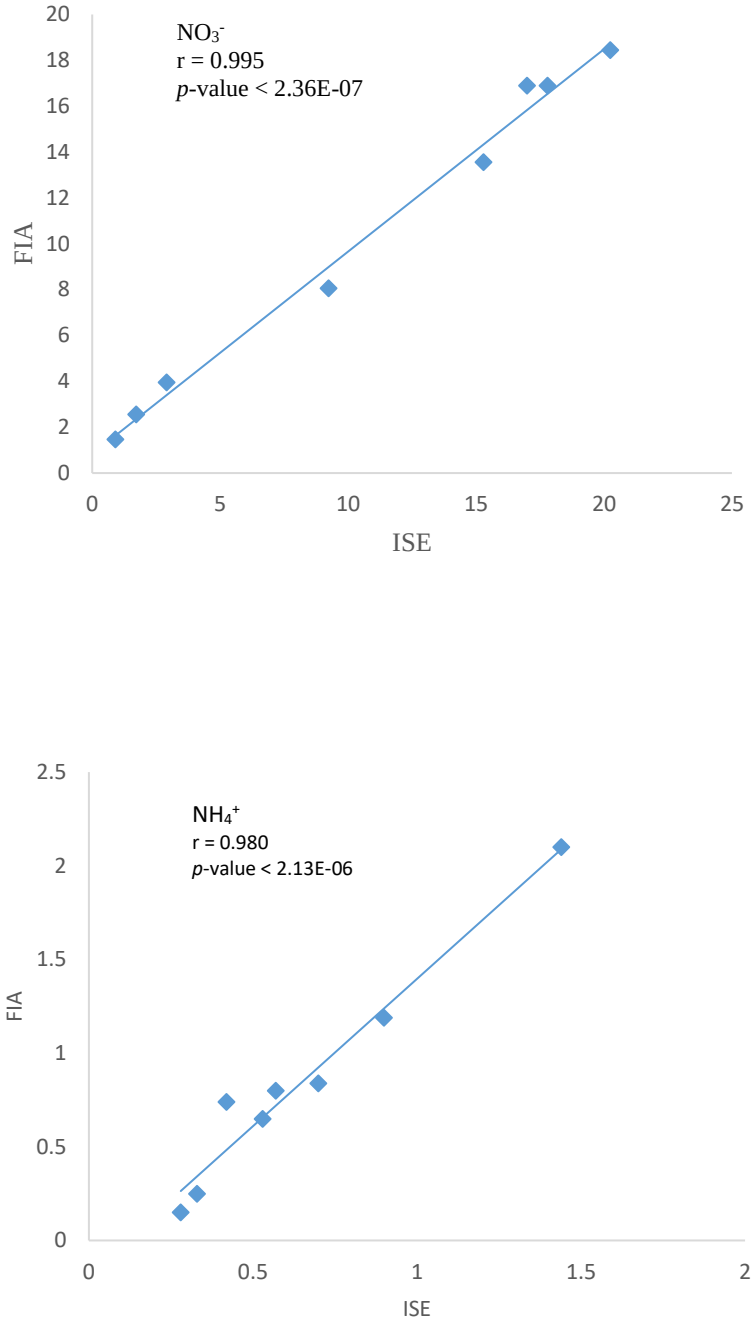

Figure 3.9 Scatter plot for comparison of the average concentration of extractable NH_4^+ & NO_3^- in 4 soil types (n = 4), and average concentration of NH_4^+ & NO_3^- in two water samples (n = 4) measured by ISE and standard method (FIA). Inset shows *r* and *p*-value from the regression analysis for each ion.

3.5.4 Bayesian model for estimating concentrations of NH_4^+ and NO_3^- in environmental samples

The majority of on-going research in the field of chemical sensors have been carried out in the laboratory under controlled conditions. But with increasing interest in rapid and on-site monitoring of environmentally-relevant nutrients and/or contaminants, [34,35] there is a need for precise measurement of reported values for a complete analysis. In order to improve accuracy and precision of the amount of NH_4^+ and NO_3^- measured by potentiometric measurement, the Bayesian modelling was tested on three forest soils from BIFoR as discussed above namely: ash, oak, and Scottish pine, and upstream and downstream water - also running across the BIFoR site. The measurement was carried out using standard addition.

It can be seen from figure 3.10 that, in general, the point estimates obtained by the Bayesian modelling (represented by the midpoint of the intervals) are closer to the true or reference values (denoted by red circles) than to the typical potentiometric standard addition measurement (x marks). The significance of the Bayesian modelling is further indicated by the closeness (overlapping) of the point estimates of the activities of both NH_4^+ and NO_3^- to the true values of the reference method obtained by FIA. This observed trend supports report by Dillingham et al, that accuracy can be improved by introducing the standard addition method to into the Bayesian modelling to minimize bias usually introduced by drifts,[52] thereby opening a door for more research into optimising potentiometric analysis for monitoring important nutrients by statistically modelling data acquired through the use of simple and rapid remote sensors.

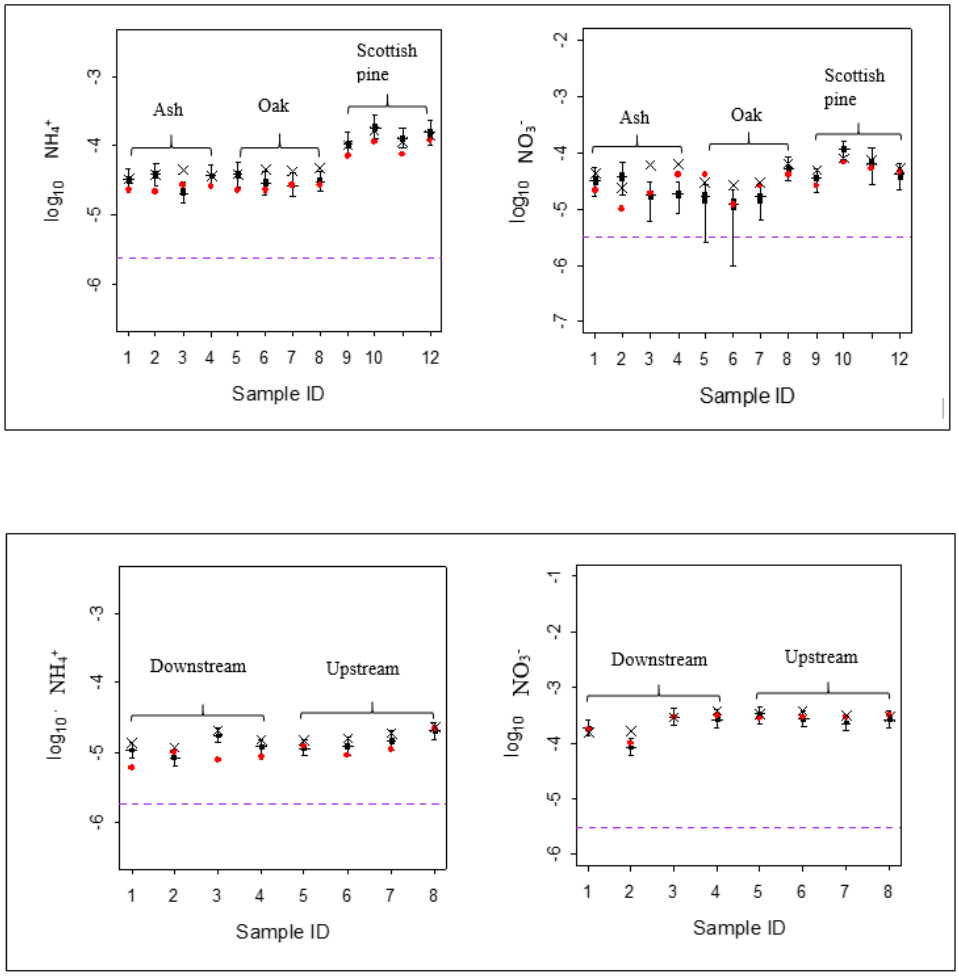

Figure 3.10 Estimations of NH_4^+ and NO_3^- in; top) three types of soil samples (n = 4), and bottom) two water samples (n = 4) from single-ISEs using the standard addition Bayesian model. Error bars indicate 95 % confidence intervals; lower and upper limits are indicated by thick bars; midpoints of intervals represent Bayesian estimates; true values measured by FIA are indicated by red circles; standard addition potentiometric values are indicated by x mark and improved LODs as a result of the Bayesian modelling are shown by dash lines (…..).

Dillingham et al reported precision of estimated activities of lead in soil samples modelled by Bayesian method was improved using multiple ISEs as compared to a single-ISE system.[52] To illustrate this, estimates of activities of NO_3^- modelled by four single ISEs was compared with that obtained from a multiple-ISE system. Figure 3.11e resulting from modelling of four separate single nitrate ISEs (figures 3.11a to 3.11d) showed improved precision as evident from the reduction in the long, extremely variable width of the intervals of the single ISEs, which is essential for reporting correctly, values of important contaminants. In addition, similar patterns shown amongst the estimates of nitrate in the water samples by all the single ISEs as shown in figures 3.11 (a - d), and with the reference (FIA) method, show accuracy of the potentiometric analysis.

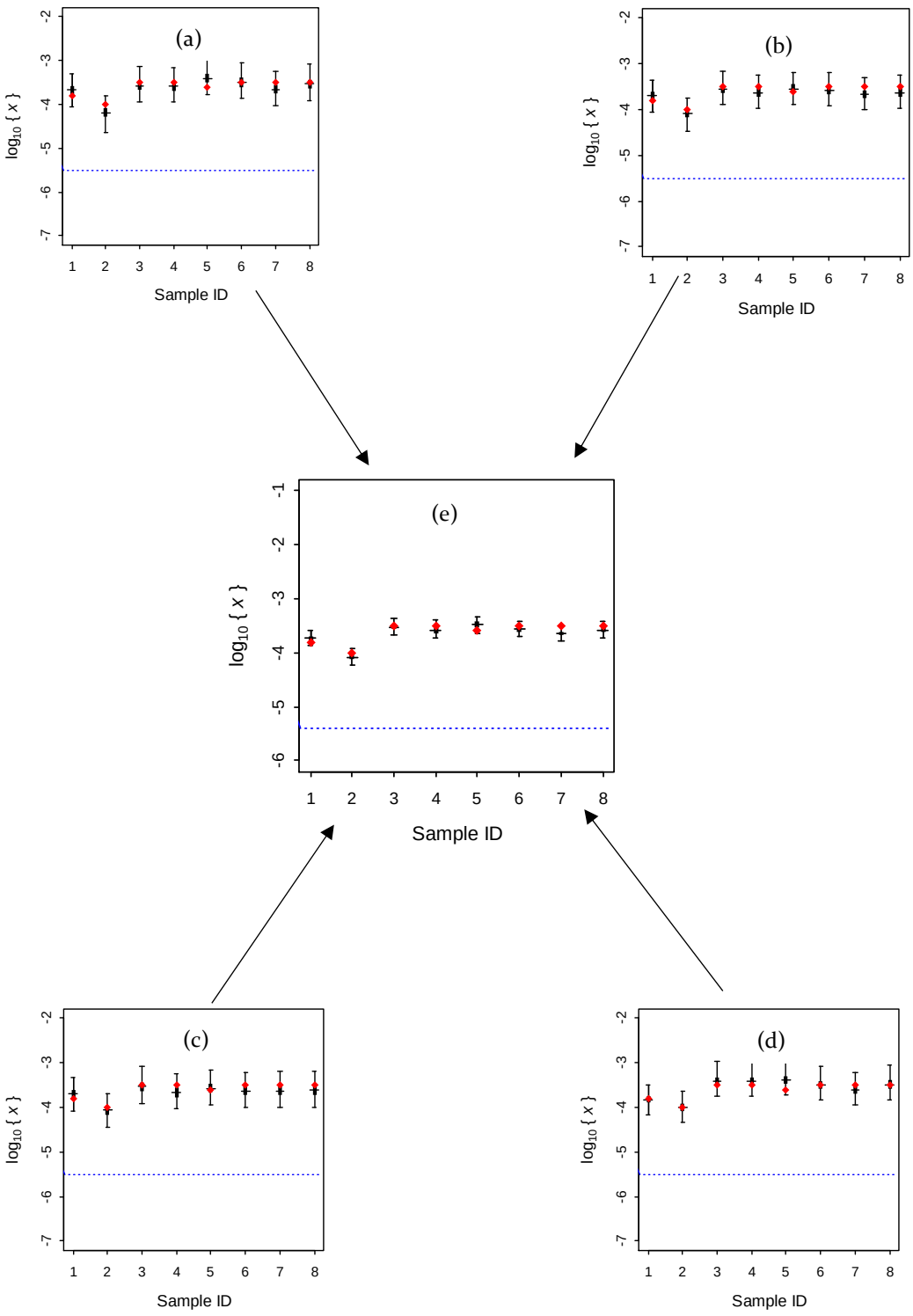

Figure 3.11 Improvement in precision of nitrate estimates is observed by using the multiple-ISE model in (e), resulting in reduction of the long tails, asymmetry, and extreme variability in the width of calibration intervals from individual single-ISEs in (a, b, c and d).

3.6 Implications and conclusions

This work describes a simple and robust methodology for simplifying the pretreatment and clarification step for potentiometric measurement of multiple ions in a sample by combining extraction step for nitrate and ammonium using a single extracting solution, therefore allowing for concurrent measurement of ammonium and nitrate without any major loss of sensitivity. Furthermore, concurrent measurement of Nr was also done in water samples draining a forest site modelled to understand how forests react to threat from climate change as a result of future increases in atmospheric carbon dioxide (CO_2) (see BIFoR webpage for more information). This is important to our study because of the link between the influence of carbon's existence on nitrogen speciation in different habitats and vice-versa, for example, the dependence of plants' Nr availability on the carbon: nitrogen ratio.[63,64] Statistical approach using Bayesian modeling was tested to improve accuracy and precision of measurement values. To further state an importance of this method, it is noteworthy to mention the ease of fabrication of these sensors which was based on very cheap and readily available materials, i.e. sello-tape, pencils, acetate papers. In general, the overall activities measured from this simple and very low-cost potentiometric set up correlated with results from standard analytical methods used for validation thereby suggesting the suitability of this approach for more detailed routine analysis.

References

(1) Turner, R.; Rabalais, N. *Coastal Eutrophication near the Mississippi River Delta*; 1994; Vol. 368.

(2) M. Vitousek, P.; D. Aber, J.; Howarth, R.; E. Likens, G.; A. Matson, P.; W. Schindler, D.; Schlesinger, W.; G. Tilman, D. Human Alteration Of The Global Nitrogen Cycle: Sources And Consequences. *Ecol. Appl.* **1997**, *7*, 737–750.

(3) Galloway, J. N.; Dentener, F. J.; Capone, D. G.; Boyer, E. W.; Howarth, R. W.; Seitzinger, S. P.; Asner, G. P.; Cleveland, C. C.; Green, P. A.; Holland, E. A.; et al. Nitrogen Cycles: Past, Present, and Future. *Biogeochemistry* **2004**, *70* (2), 153–226.

(4) Kugler, S.; Horváth, L.; Machon, A. Estimation of Nitrogen Balance between the Atmosphere and Lake Balaton and a Semi Natural Grassland in Hungary. *Environ. Pollut.* **2008**, *154* (3), 498–503.

(5) Erisman, J. W.; Galloway, J. N.; Seitzinger, S.; Bleeker, A.; Dise, N. B.; Petrescu, A. M. R.; Leach, A. M.; de Vries, W. Consequences of Human Modification of the Global Nitrogen Cycle. *Philos. Trans. R. Soc. B Biol. Sci.* **2013**, *368* (1621).

(6) Grizzetti, B.; Pistocchi, A.; Liquete, C.; Udias, A.; Bouraoui, F.; van de Bund, W. Human Pressures and Ecological Status of European Rivers. *Sci. Rep.* **2017**, *7* (1), 205.

(7) Fowler, D.; Coyle, M.; Skiba, U.; Sutton, M. A.; Cape, J. N.; Reis, S.; Sheppard, L. J.; Jenkins, A.; Grizzetti, B.; Galloway, J. N.; et al. The Global Nitrogen Cycle in the Twenty-First Century. *Philos. Trans. R. Soc. B Biol. Sci.* **2013**, *368* (1621).

(8) Grizzetti, B.; Passy, P.; Billen, G.; Bouraoui, F.; Garnier, J.; Lassaletta, L. The Role of Water Nitrogen Retention in Integrated Nutrient Management: Assessment in a Large Basin Using Different Modelling Approaches. *Environ. Res. Lett.* **2015**, *10* (6), 065008.

(9) Liu, S.; Wang, J. J.; Tian, Z.; Wang, X.; Harrison, S. Ammonia and Greenhouse Gas Emissions from a Subtropical Wheat Field under Different Nitrogen Fertilization Strategies. *J. Environ. Sci.* **2017**, *57* (Supplement C), 196–210.

(10) Ward, M. H.; deKok, T. M.; Levallois, P.; Brender, J.; Gulis, G.; Nolan, B. T.; VanDerslice, J. Workgroup Report: Drinking-Water Nitrate and Health—Recent Findings and Research Needs. *Environ. Health Perspect.* **2005**, *113* (11), 1607–1614.

(11) Butler, A. Nitrites and Nitrates in the Human Diet: Carcinogens or Beneficial Hypotensive Agents? *J. Ethnopharmacol.* **2015**, *167*, 105–107.

(12) Grizzetti, B.; Bouraoui, F.; Billen, G.; Grinsven, H.; Cardoso, A.; Thieu, V.; Garnier, J.; Curtis; Howarth, R.; Johnes, P. *Nitrogen as a Threat to European Water Quality*; 2011.

(13) Cresser, M.; Killham, K.; Edwards, T. *Soil Chemistry and Its Applications*; Cambridge University Press, 1993.

(14) Davidson, E. A.; Ackerman, I. L. Changes in Soil Carbon Inventories Following Cultivation of Previously Untilled Soils. *Biogeochemistry* **1993**, *20* (3), 161–193.

(15) Guo, L. B.; Gifford, R. Soil Carbon Stocks and Land Use Change: A Meta-Analysis. *Glob. Change Biol.* **2002**, *8*, 345–360.

(16) Guillaume, T.; Damris, M.; Kuzyakov, Y. Losses of Soil Carbon by Converting Tropical Forest to Plantations: Erosion and Decomposition Estimated by Δ13C. *Glob. Change Biol.* **2015**, *21* (9), 3548–3560.

(17) Wei, X.; Shao, M.; Gale, W.; Li, L. Global Pattern of Soil Carbon Losses Due to the Conversion of Forests to Agricultural Land. *Sci. Rep.* **2014**, *4*, srep04062.

(18) Shao, Y.; He, Y. Nitrogen, Phosphorus, and Potassium Prediction in Soils, Using Infrared Spectroscopy. *Soil Res.* **2011**, *49* (2), 166–172.

(19) Sgouridis, F.; Ullah, S. Denitrification Potential of Organic, Forest and Grassland Soils in the Ribble-Wyre and Conwy River Catchments, UK. *Environ. Sci. Process. Impacts* **2014**, *16* (7), 1551–1562.

(20) Pan, P. Preparation and Evaluation of a Stable Solid State Ion Selective Electrode of Polypyrrole/Electrochemically Reduced Graphene/Glassy Carbon Substrate for Soil Nitrate Sensing. *Int. J. Electrochem. Sci.* **2016**, *11*, 4779–4793.

(21) Fayose, T.; Mendecki, L.; Ullah, S.; Radu, A. Single Strip Solid Contact Ion Selective Electrodes on a Pencil-Drawn Electrode Substrate. *Anal. Methods* **2017**, *9* (7), 1213–1220.

(22) Itoh, H.; Tomita, H.; Uno, Y.; Shiraishi, N. Development of Method for Non-Destructive Measurement of Nitrate Concentration in Vegetable Leaves by Near-Infrared Spectroscopy. *IFAC Proc. Vol.* **2011**, *44* (1), 1773–1778.

(23) Itoh, H.; Nomura, K.; Shiraishi, N.; Uno, Y.; Kuroki, S.; Ayata, K. Continuous Measurement of Nitrate Concentration in Whole Lettuce Plant by Visible-near-Infrared Spectroscopy. *Environ. Control Biol.* **2015**, *53* (4), 205–215.

(24) Ianoul, A.; Coleman, T.; Asher, S. A. UV Resonance Raman Spectroscopic Detection of Nitrate and Nitrite in Wastewater Treatment Processes. *Anal. Chem.* **2002**, *74* (6), 1458–1461.

(25) Angkat, A. R.; Seminar, K. B.; Rahmat, M.; Sutandi, A. Estimation of Soil Nitrate (NO 3) Level Using Laser-Induced Breakdown Spectroscopy (LIBS). *IOP Conf. Ser. Earth Environ. Sci.* **2018**, *147* (1), 012045.

(26) Shaw, R.; Williams, A. P.; Miller, A.; Jones, D. L. Assessing the Potential for Ion Selective Electrodes and Dual Wavelength UV Spectroscopy as a Rapid On-Farm Measurement of Soil Nitrate Concentration. *Agriculture* **2013**, *3* (3), 327–341.

(27) Wardak, C.; Grabarczyk, M. Analytical Application of Solid Contact Ion-Selective Electrodes for Determination of Copper and Nitrate in Various Food Products and Drinking Water. *J. Environ. Sci. Health Part B* **2016**, *51* (8), 519–524.

(28) Dorich, R. A.; Nelson, D. W. Evaluation of Manual Cadmium Reduction Methods for Determination of Nitrate in Potassium Chloride Extracts of Soils. *Soil Sci. Soc. Am. J.* **1984**, *48* (1), 72–75.

(29) Kim, H.-J.; Hummel, J.; Birrell, S. Evaluation of Ion-Selective Membranes for Real-Time Soil Nutrient Sensing. *Agric. Biosyst. Eng. Conf. Proc. Present.* **2003**.

(30) Kim, H.-J.; Hummel, J. W.; Sudduth, K. A.; Motavalli, P. P. Simultaneous Analysis of Soil Macronutrients Using Ion-Selective Electrodes. *Soil Sci. Soc. Am. J.* **2007**, *71* (6), 1867–1877.

(31) Miegroet, H. Inorganic Nitrogen Determined by Laboratory and Field Extractions of Two Forest Soils. *Watershed Sci. Fac. Publ.* **1995**, *59*.

(32) Hood-Nowotny, R.; Hinko-Najera, N.; Inselsbacher, E.; Lachouani, P.; Wanek, W. Alternative Methods for Measuring Inorganic, Organic, and Total Dissolved Nitrogen in Soil. *Soil Sci. Soc. Am. J.* **2010**, *74*, 1018–1027.

(33) Li, K.; Zhao, Y.; Yuan, X.; Zhao, H.; Wang, Z.; Li, S.; Malhi, S. S. Comparison of Factors Affecting Soil Nitrate Nitrogen and Ammonium Nitrogen Extraction. *Commun. Soil Sci. Plant Anal.* **2012**, *43* (3), 571–588.

(34) Davenport, J. R.; Jabro, J. D. Assessment of Hand Held Ion Selective Electrode Technology for Direct Measurement of Soil Chemical Properties. *Commun. Soil Sci. Plant Anal.* **2001**, *32* (19–20), 3077–3085.

(35) Adamchuk, V. I.; Lund, E. D.; Sethuramasamyraja, B.; Morgan, M. T.; Dobermann, A.; Marx, D. B. Direct Measurement of Soil Chemical Properties On-the-Go Using Ion-Selective Electrodes. *Comput. Electron. Agric.* **2005**, *48* (3), 272–294.

(36) Wardak, C. Solid Contact Cadmium Ion-Selective Electrode Based on Ionic Liquid and Carbon Nanotubes. *Sens. Actuators B Chem.* **2015**, *209*, 131–137.

(37) McGraw, C. M.; Radu, T.; Radu, A.; Diamond, D. Evaluation of Liquid- and Solid-Contact, Pb2+-Selective Polymer-Membrane Electrodes for Soil Analysis. *Electroanalysis* **2008**, *20* (3), 340–346.

(38) Mattinen, U.; Bobacka, J.; Lewenstam, A. Solid-Contact Reference Electrodes Based on Lipophilic Salts. *Electroanalysis* **2009**, *21* (17–18), 1955–1960.

(39) Chumbimuni-Torres, K. Y.; Rubinova, N.; Radu, A.; Kubota, L. T.; Bakker, E. Solid Contact Potentiometric Sensors for Trace Level Measurements. *Anal. Chem.* **2006**, *78* (4), 1318–1322.

(40) Guziński, M.; Lisak, G.; Sokalski, T.; Bobacka, J.; Ivaska, A.; Bocheńska, M.; Lewenstam, A. Solid-Contact Ion-Selective Electrodes with Highly Selective Thioamide Derivatives of p-Tert-Butylcalix[4]Arene for the Determination of Lead(II) in Environmental Samples. *Anal. Chem.* **2013**, *85* (3), 1555–1561.

(41) Suzuki, K.; Siswanta, D.; Otsuka, T.; Amano, T.; Ikeda, T.; Hisamoto, H.; Yoshihara, R.; Ohba, S. Design and Synthesis of a More Highly Selective Ammonium Ionophore Than Nonactin and Its Application as an Ion-Sensing Component for an Ion-Selective Electrode. *Anal. Chem.* **2000**, *72* (10), 2200–2205.

(42) Álvarez-Romero, G. A.; Palomar-Pardavé, M. E.; Ramírez-Silva, M. T. Development of a Novel Nitrate-Selective Composite Sensor Based on Doped Polypyrrole. *Anal. Bioanal. Chem.* **2007**, *387* (4), 1533–1541.

(43) Sathyapalan, A.; Zhou, A.; Kar, T.; Zhou, F.; Su, H. A Novel Approach for the Design of a Highly Selective Sulfate-Ion-Selective Electrode. *Chem. Commun.* **2009**, *0* (3), 325–327.

(44) Rius-Ruiz, F. X.; Kisiel, A.; Michalska, A.; Maksymiuk, K.; Riu, J.; Rius, F. X. Solid-State Reference Electrodes Based on Carbon Nanotubes and Polyacrylate Membranes. *Anal. Bioanal. Chem.* **2011**, *399* (10), 3613–3622.

(45) Hu, J.; Zou, X. U.; Stein, A.; Bühlmann, P. Ion-Selective Electrodes with Colloid-Imprinted Mesoporous Carbon as Solid Contact. *Anal. Chem.* **2014**, *86* (14), 7111–7118.

(46) Wardak, C. Solid Contact Nitrate Ion-Selective Electrode Based on Ionic Liquid with Stable and Reproducible Potential. *Electroanalysis* **2014**, *26* (4), 864–872.

(47) He, M.; Li, Y.; Yu, X.; Yang, H. A Nitrate Ion-Selective Electrode Based on Tetradodecylammonium Bromide. *Sens. Lett.* **2015**, *13* (11), 986–991.

(48) Mendecki, L.; Chen, X.; Callan, N.; Thompson, D. F.; Schazmann, B.; Granados-Focil, S.; Radu, A. Simple, Robust, and Plasticizer-Free Iodide-Selective Sensor Based on Copolymerized Triazole-Based Ionic Liquid. *Anal. Chem.* **2016**, *88* (8), 4311–4317.

(49) Bomar, E. M.; Owens, G. S.; Murray, G. M. Nitrate Ion Selective Electrode Based on Ion Imprinted Poly(N-Methylpyrrole). *Chemosensors* **2017**, *5* (1), 2.

(50) Radu, A.; Radu, T.; McGraw, C.; Dillingham, P.; Anastasova, S.; Diamond, D. Ion Selective Electrodes in Environmental Analysis. *J. Serbian Chem. Soc.* **2013**, *78*, 1729–1761.

(51) Mueller, A. V.; Hemond, H. F. Statistical Generation of Training Sets for Measuring NO3−, NH4+ and Major Ions in Natural Waters Using an Ion Selective Electrode Array. *Environ. Sci. Process. Impacts* **2016**, *18* (5), 590–599.

(52) Dillingham, P. W.; Radu, T.; Diamond, D.; Radu, A.; McGraw, C. M. Bayesian Methods for Ion Selective Electrodes. *Electroanalysis 24*, 316–324.

(53) Korfmacher, J. L.; Musselman, R. C. Evaluation of Storage and Filtration Protocols for Alpine/Subalpine Lake Water Quality Samples. *Environ. Monit. Assess.* **2007**, *131* (1–3), 107–116.

(54) Wilson, B.; Gandhi, J.; Zhang, C. C. Analysis of Inorganic Nitrogen and Related Anions in High Salinity Water Using Ion Chromatography with Tandem UV and Conductivity Detectors. *J. Chromatogr. Sci.* **2011**, *49* (8), 596–602.

(55) Bakker, E. Determination of Unbiased Selectivity Coefficients of Neutral Carrier-Based Cation-Selective Electrodes. *Anal. Chem.* **1997**, *69* (6), 1061–1069.

(56) Standard & Sample Addition Methods for Ion Selective Electrodes http://www.nico2000.net/datasheets/staddl.html (accessed Oct 9, 2017).

(57) Zhang, L.; Zhang, M.; Ren, H.; Pu, P.; Kong, P.; Zhao, H. Comparative Investigation on Soil Nitrate-Nitrogen and Available Potassium Measurement Capability by Using Solid-State and PVC ISE. *Comput. Electron. Agric.* **2015**, *112* (Supplement C), 83–91.

(58) Nägele, M.; Bakker, E.; Pretsch, E. General Description of the Simultaneous Response of Potentiometric Ionophore-Based Sensors to Ions of Different Charge. *Anal. Chem.* **1999**, *71* (5), 1041–1048.

(59) Radu, A.; Peper, S.; Bakker, E.; Diamond, D. Guidelines for Improving the Lower Detection Limit of Ion-Selective Electrodes: A Systematic Approach. *Electroanalysis* **2007**, *19* (2–3), 144–154.

(60) Crespo, G. A. Recent Advances in Ion-Selective Membrane Electrodes for in Situ Environmental Water Analysis. *Electrochimica Acta* **2017**, *245* (Supplement C), 1023–1034.

(61) Athavale, R.; Dinkel, C.; Wehrli, B.; Bakker, E.; Crespo, G. A.; Brand, A. Robust Solid-Contact Ion Selective Electrodes for High-Resolution In Situ Measurements in Fresh Water Systems. *Environ. Sci. Technol. Lett.* **2017**, *4* (7), 286–291.

(62) Paczosa-Bator, B. Effects of Type of Nanosized Carbon Black on the Performance of an All-Solid-State Potentiometric Electrode for Nitrate. *Microchim. Acta* **2014**, *181* (9–10), 1093–1099.

(63) Burton, J.; Chen, C.; Xu, Z.; Ghadiri, H. Gross Nitrogen Transformations in Adjacent Native and Plantation Forests of Subtropical Australia. *Soil Biol. Biochem.* **2007**, *39*.

(64) Berthrong, S. T.; Jobbágy, E. G.; Jackson, R. B. A Global Meta-Analysis of Soil Exchangeable Cations, PH, Carbon, and Nitrogen with Afforestation. *Ecol. Appl.* **2009**, *19* (8), 2228–2241.

Chapter 4 Utilization of Bayesian calibration for improvement of detection limit of polymer membrane-based iodide-selective electrode

4.1 Introduction

Breakthrough in understanding of response mechanism of ion-selective electrodes (ISEs) resulted in great improvement of their low detection limit (LOD).[1,2] With routinely achieved LODs in part-per-billion (ppb) levels and often excellent selectivity coefficients, the utility of ISEs expanded from a technique almost exclusively used for clinical analysis of blood electrolytes to potentially useful tool in the fields previously considered unreachable such as protein/DNA analysis,[3,4] and/or environmental analysis.[5,6] The simplicity of the technique coupled with the ability to produce sensors on mass scale,[7–9] and almost no need for sample preparation opens up unprecedented opportunities to integrate sensors with electronic communication devices and develop large-scale sensing networks as early warning systems and for routine monitoring.[10–12]

Routine monitoring of urinary iodine (UI) is an example where modern ISEs can make a significant impact. Iodine is an essential trace element for life needed for adequate synthesis of thyroid hormones. Iodine insufficiency significantly impairs psycho-physiological growth and metabolism and can result in iodine deficiency disorders (IDD) such as hypothyroidism, goitre, cretinism, mental retardation etc. Approximately 1.6 billion people (mostly in developing countries) are currently at risk of IDD.[13,14] In most circumstances, the determination of UI provides little useful information of the long-term iodine status of an individual, since the results obtained merely reflect recent dietary iodine intake. However, measuring UI in a representative cohort of individuals from a specific population provides a useful index of the iodine

level endemic to that region,[15] and as a recommendation, the UI levels within a population are categorized into; < 20 μg/ L (severely deficient), 20 – 49 μg/ L (moderately deficient), 50 -100 μg/ L (mildly deficient), 100 200 μg/ L (adequate) and > 300 (excessive intake).

Currently, UI is measured by Sandell and Kolthoff (S-K) colourimetric method which is based on the catalytic effect of iodide in the redox reaction between yellow cerium (IV) and arsenic (III), to yield the colourless cerium (III) and arsenic (V).[16] The S-K method requires some sample pre-treatment to remove compounds in urine that interfere with the above reaction. Typically, the pre-treatment requires wet digestion techniques using chloric acid or perchloric acid.[17,18] Since the wet digestion is lengthy (hours) and used acids are potentially explosive, many modifications of the S-K method were proposed and an interested reader can learn more from reviews by Dunn et al[17] or Zhang et al.[19]

Clearly simple, sensitive, and low cost sensors that do not require sample preparation such as ISEs can serve as suitable alternative to the classical technique. However as discussed in section 1.5 of this thesis, ISEs carry an inherent problem – current definition of the LOD prevents utilization of the full response curve and creates a bias in the determination of unknown concentrations near the LOD. As illustrated in figure 4.1, the IUPAC defines LOD of ISEs as the cross-section of two linear segments where one represents the response of ISEs in Nernstian fashion, while the other is the response of the electrode in the absence of the ion of interest (baseline). It should be noted that such definition has theoretical basis and it represents the case in which well-defined part (50% for $z_I = z_J$) of primary ions in the membrane is exchanged with interfering ions.[20] However, the response of ISEs deviates from Nernstian line near the

LOD (as indicated with shaded region) resulting in diminished precision.

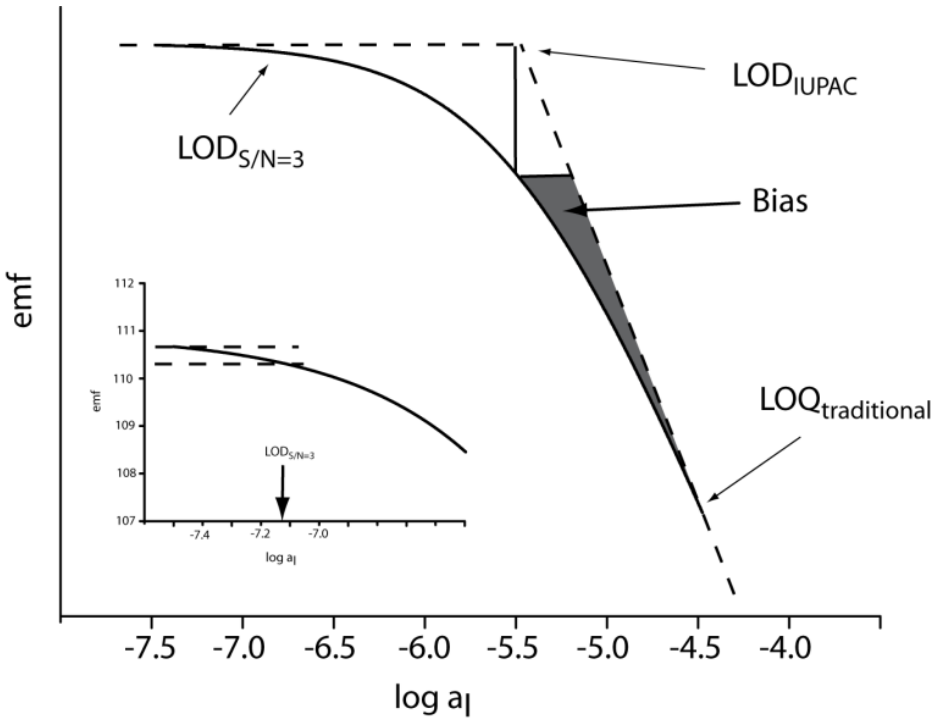

Figure 4.1 Full line – response of MC3/NPOE-based iodide-selective electrode in artificial urine. Traditional (IUPAC) detection limit is at the cross-section of the two dashed lines indicating responses to primary ions (line showing Nernstian slope) and to interfering ions (slope = 0). Shaded region indicates bias in the determination of unknown concentration near LOD. Limit of Quantification ($LOQ_{traditional}$) is the point where the response starts deviating from Nernstian line. Inset: Response at the base line indicating $LOD_{S/N=3}$ (0.1 mV is assumed as potentiometric noise).

Historically, ISEs were used for the analysis of analytes whose concentration was significantly above LOD and the bias was addressed by establishing a 'limit of

quantification' ($LOQ_{traditional}$); experimentators were advised to use ISEs in cases where the expected levels of analytes were at least an order of magnitude higher than LOD_{IUPAC}.

Another practical problem with IUPAC definition is that it completely neglects significant response above the baseline of $17.8/z_I$ mV.[1] Potentiometric measurements have a typical noise of ~0.1mV and analytical devices cannot afford the luxury of neglecting response that is significantly above the baseline. Based on the ability to model the entire range of the potentiometric response curve either using experimentally available parameters,[21,22] or regression analysis,[23–25] Bakker and Pretsch suggested using signal-to-noise ratio ($LOD_{S/N=3}$) to define LOD of ISEs in accordance to almost every other analytical technique.[2]

Bayesian model offers a very interesting approach to statistical calibration of ISEs.[6] Its self-learning ability offers the opportunity to improve measurement precision, to identify and discard data from failing electrodes, and consequently to extend the useful range of the ISEs and utilize $LOD_{S/N=3}$ in place of the Nernstian approximation and LOD_{IUPAC}. This is done by down-weighting poor-performing ISEs and incorporating asymmetry in calibration intervals into the final calibration interval. The method was developed by Dillingham et al[26] using the OpenBUGS variant (version 3.0.3) of BUGS, linked to R using R2WinBUGS library and the code is freely available in the public domain.[27]

This chapter was aimed to demonstrate new iodide-selective electrodes based on MC3/MC4 that utilize the entire response curve. The electrodes were carefully characterized and evaluated for utilization in UI analysis of artificial and real-life

samples. The measurements were done in conjunction with Bayesian method with the aim of effectively reducing their practical LOD below the IUPAC-defined level.

4.2 Experimental

4.2.1 Materials

For membrane preparation, high molecular weight poly(vinylchloride) (PVC), bis(2-ethylhexyl)sebacate (DOS, ≥97%), 2-nitrophenyl octyl ether (o-NPOE, >99%), tetradodecylammonium chloride (TDACl), tetrahydrofuran (THF, ≥99.5%), chloroform and all salts were Selectophore grade from Fluka. [9] Mercuracarborand-3 (MC3) and [12] Mercuracarborand-4 (MC4) were synthesized in-house. Deionized water obtained with Milli-Q reagent-grade water system was used for all sample solutions. All the solutions with a concentration lower than 0.01 mol/ L were prepared immediately prior to use.

4.2.2 Membrane composition and electrode preparation

The cocktail for the I^--selective membrane was prepared by dissolving 7.5 mmol/kg TDMACl, 10 mmol/kg of ionophore (MC3 or MC4), 33 wt% PVC, and 66 wt% of plasticizer (NPOE or DOS) in 1mL THF. Four sets of membrane cocktails were made; MC3/NPOE, MC3/DOS, MC4/NPOE, & MC4/DOS. These were stored in an amber glass bottle and labelled accordingly.

Paper platforms were made in-house as described in chapter 2 of this thesis. Briefly, a 1.5 cm × 3.0 cm strip was cut from a parent acetate sheet and was subsequently etched with aluminum oxide (grit 240) for 30 sec to provide the surface with enhanced porosity in order to improve adhesion of graphite onto the surface of acetate. With the use of a typical graphite pencil, a line of carbon is applied/drawn by hand onto the acetate sheet. Each sensor was partially overlain with mask of non-permeable polyester tape, after which a hole of 0.3 cm in diameter was punched on one top end of the sello-

tape as an aperture to allow for the application of ion selective membrane layers while an area of 0.75 cm^2 of its other end was exposed to provide electrical contact. Once the sensors were fabricated, the ion-selective membrane was drop-cast on it to form a layer of ~ 200 µm thick and dried overnight. After this, the membranes were conditioned overnight in the solution of 10^{-3} M of NaF for the determination of selectivity coefficients. For determination of I^- in artificial and real urine, electrodes were first conditioned overnight in 10^{-5} M NaI followed by a second conditioning process overnight in 10^{-8} M NaI.

4.2.3 Potentiometric measurements

Potentiometric measurements were performed at room temperature (around 21 ◦C) using a Lawson Labs Inc. (3217 Phoenixville Pike Malvern, PA 19355, USA) EMF 16 electrode monitor. EMF measurements were conducted in stirred solutions using a stirring plate. For comparative measurements, a conventional Ag/AgCl reference electrode (IFS, 3 M KCl, Metrohm, 6.0729.100) with 1 M LiOAc as bridge electrolyte was used. All values were corrected for liquid junction potentials using the Henderson formalism and ion activities were calculated according to the Debye-Hückel approximation.

4.2.4 Artificial urine

The composition of human urine is highly variable due to the diet, the level of activity and the overall state of health of an individual. This inevitably leads to wide variation in composition of artificial urine (AU). In this work, we have decided to focus on the urine's chemical composition. The AU used in this work contained the following: 14.1g NaCl, 2.8g KCl, 17.3g Urea, 1.9ml 25% w/v NH_3, 0.6g $CaCl_2$, and 0.43g

$MgSO_4$.[28] All the excipients were dissolved in one litre of distilled water and the pH was adjusted to 3.

4.2.5 Human urine testing

In order to test urine samples, information and consent letters were sent out to twenty individuals. From the samples received, five had to be discarded due to poor storage conditions. 50 mL of each of the remaining samples were tested for their iodine concentrations. Full anonymity was adhered to throughout the sample collection and testing phases. This analysis was done in sequence with another similar project in the group, in which ethical approval was obtained from The Research Ethics committee at Keele University (Approval reference: ERP369).

4.2.6 Measurement of iodide in human urine samples using standard reference method (ICP-MS)

For comparison and validation, inductively coupled plasma-mass spectrometry (ICP-MS) method was used to measure iodine in urine real samples, as this was seen as the gold standard. The general procedure has been covered in literatures. Briefly, human urine samples were centrifuged at 5000 rpm for 10 min and then about 7 mL of each sample was transferred into 10 mL autosampler tubes (PerkinElmer). The resulting urine solutions were either analysed directly, or with extra dilutions for samples with higher concentration. A waters Alliance 2695 coupled to NexION 300D (PerkinElmer) was used for analysis because of its sensitivity. Table 4.1 shows instrumental condition used for the analysis. Calibration standards and serial dilutions were prepared from potassium iodide dissolved in 5% (v/v) HNO_3 and used to produce a calibration curve (Figure 4.2). In between each measurement (including iodide standards and urine

samples), a sample blank was analysed to reduce/eliminate the memory effect. Known checked standards were run randomly between samples to check for the accuracy of the method.

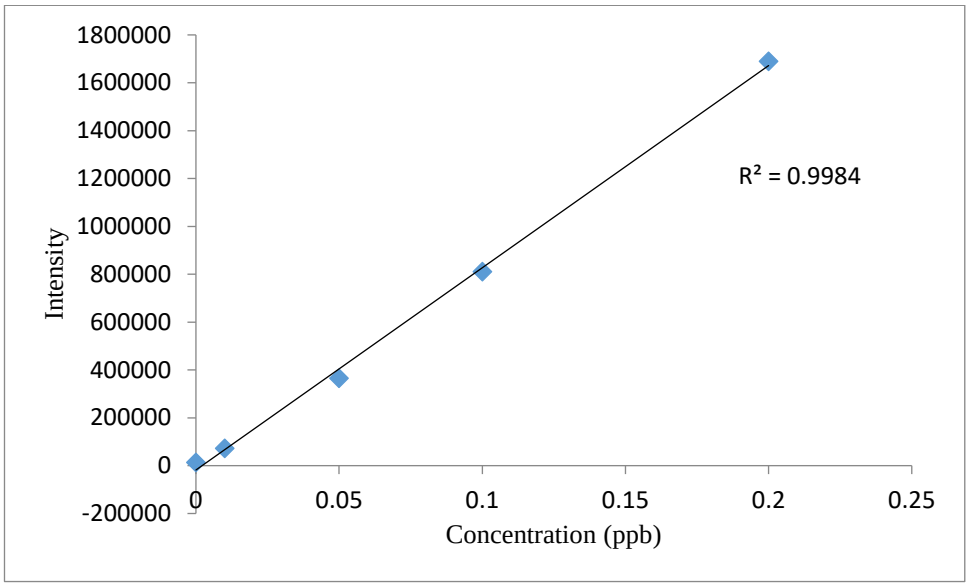

Figure 4.2 Five-point calibration lines obtained for iodide standards by ICP-MS measurements (R^2 = 99.84%).

Table 4.1 ICP-MS instrumental conditions.

Sample uptake rate	0.5 ml/ min
RF power	1600 W
Plasma gas flow	18 L/ min
Auxiliary gas flow	1.2 L/ min
Nebulizer gas flow	1.14 L/ min
Sample run time	120 sec

4.3 Results and discussion

4.3.1 Selectivity

The determination of selectivity coefficients gives important insight in the utility of ISEs in the process of the evaluating of their application potential.[29] While MC3 and MC4 were previously utilized in sensors in the groups of Bachas[30] and Hawthorne,[31] prior to this work, their selectivity coefficients have not been determined in the range of plasticizers. As a result, DOS and NPOE were chosen as the traditionally used plasticizers for fabrication of ISEs.

The group of Bakker has thoroughly studied MC3 as ionophore in ionophore-based sensors and a conclusion relevant for this work is that the optimal ratio of ion exchanger to ionophore is 75 mol %.[32] It was realized that although MC3 can form both 1:1 and 1:2 complexes with halide ions, the latter stoichiometry is obtained when ion exchanger is present in <25 mol %. Consequentially, the resulting 1:2 ion-ionophore complex is significantly stronger which results in significant cation interference. This is illustrated by reversal from anion to cation response resulting in drastically shortened anion measuring range. On the other hand, addition of ion exchanger in the amounts between 50 and 100 mol % favours 1:1 equilibrium. Consequentially, cation interference is reduced and the measuring range is extended. With further optimisation, Malon et al demonstrated iodide-selective electrode with nanomolar detection limit.[33]

In this work, the selectivity had been tested using separate solution method as described by Bakker.[34] Briefly, ISEs were conditioned overnight in an interfering ion solution. This allows recording of slopes for all ions and enables calculation of unbiased selectivity coefficients. Response curves for all ions are separately recorded

beginning with the least interfering ion and finishing with the primary ion. Results presented in table 4.2 show values for selectivity coefficients and slopes calculated as an average of at least three electrodes.

Table 4.2 Selectivity coefficients and slopes of ion-selective membranes based on combinations of MC3 and MC4 as ionophores and DOS and NPOE as plasticizers.

	MC3 (DOS)		MC3 (NPOE)		MC4 (DOS)		MC4 (NPOE)	
	$logK^{pot}$	slope	$logK^{pot}$	slope	$logK^{pot}$	slope	$logK^{pot}$	slope
F^-	-5.35±0.06	-1.46±1.37	-5.55±0.06	-0.20±0.20	N/A	37.55±2.82	-3.79±0.11	-6.44±2.05
SO_4^{2-}	-6.71±0.01	-1.87±0.96	-6.90±0.06	-0.98±0.50	N/A	4.99±0.26	-5.01±0.41	0.87±0.59
PO_4^{3-}	-6.20±0.06	-18.25±1.05	-7.27±0.06	-9.55±0.56	0.01±0.06	-31.51±0.23	-2.62±0.46	N/A
NO_3^-	-4.86±0.16	-27.40±0.56	-3.45±0.05	-61.96±0.39	-0.11±0.05	-17.61±0.12	-3.62±0.32	-22.81±2.88
OH^-	-5.00±0.19	-14.47±2.34	-5.91±0.04	-7.71±0.53	1.82±0.04	-28.48±0.45	-1.68±0.41	N/A
Cl^-	-3.43±0.23	-51.03±0.90	-4.86±0.03	-39.83±0.63	-0.41±0.05	-8.75±0.06	-3.66±0.32	-11.79±1.00
Br^-	-2.10±0.14	-62.69±2.66	-3.12±0.03	-59.09±1.04	-0.35±0.06	-23.27±0.05	3.11±0.03	-32.69±0.66
ClO_4^-	-4.01±0.27	-49.26±0.75	-0.05±0.04	-66.66±0.06	0.23±0.04	-27.77±0.05	-3.28±0.33	-17.95±2.02
I^-	0	-65.99±5.52	0	-63.90±0.53	0	-34.05±0.06	0	-53.65±1.05

Figure 4.3 depicts the response of electrode to ions in the following order F^-, SO_4^{2-}, PO_4^{3-}, NO_3^-, OH^-, Cl^-, Br^-, ClO_4^- & I^-. Selectivity coefficients were then calculated according to Equation 4.1.

$$logK_{I,J}^{pot} = \frac{(E_J - E_I)z_I F}{2.303RT} + log\left(\frac{a_I}{a_J^{\frac{z_I}{z_J}}}\right) \quad (4.1)$$

Where a, E and z are activities, potentials, and charges of primary and interfering ions (I and J respectively). R, T, and F have their usual meaning (universal gas constant, temperature and Faraday constant).

From figure 4.3 it is observed that not all ions demonstrate Nernstian response. This in general applies to ions that are measured before Cl^- for almost all ionophore-plasticizer combinations. The most likely reason for sub-Nernstian response slopes for these ions is the fact ion exchanger used in the membrane formulation is Cl-based. The response for ions for which the membrane is less selective than for Cl^- is consequently mixed between the Cl^- and the ion in question. As a result, sub-Nernstian response slopes are observed.

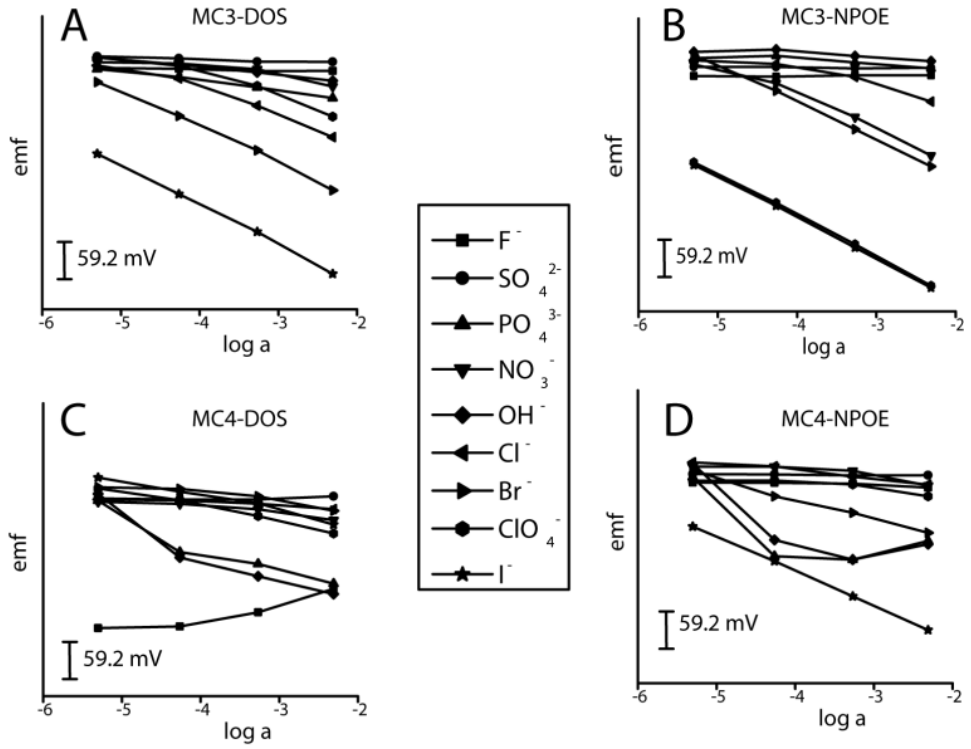

Figure 4.3 Responses of ISEs based on 75 mol% of ion-exchanger to ionophore and ionophore-plasticizer combination of: A) MC3-DOS, B) MC3-NPOE, C) MC4-DOS, and D) MC4-NPOE. The electrodes were conditioned overnight in 10^{-3} M NaF and calibration curves for various ions were recorded in the following order: F^- (square), SO_4^{2-} (circle), PO_4^{3-} (triangle), NO_3^- (upside down triangle), OH^- (diamond), Cl^- (left triangle), Br^- (right triangle), ClO_4^- (hexagon), I^- (star)

In light of this discussion, positive response slope to F^- in MC4-DOS-based membranes is somewhat surprising. It indicates significant cation interference and implies strong MC4 - F^- complexation. MC4 has indeed been shown to be a good complexing agent for fluoride ions;[35] however, for this work it is more important that MC4/DOS – based membranes show poor selectivity for I^- vs other relevant ions which effectively eliminates this membrane from further consideration. Interestingly, in MC4-NPOE membranes responses to Cl^- and I^- are Nernstian, but significant cation interference is observed to OH^- and PO_4^{3-} ions. Both of these ions are present in human

urine in significant concentrations (levels of ~160 mg PO_4-P/l and pH~6.6-8.8 are measured by Gethke et al[36]) so their responses by MC4-NPOE membranes indicate the possibility of significant interference in the determination of iodide.

Another important ion that can pose significant interference in the determination of iodide in human urine is chloride. The concentration of chloride in urine can vary significantly depending on the diet and time of the day[37,38] with some reports stating that chloride in healthy individuals ranges 10-25 mmol/ L.[19] It is therefore essential that an electrode can successfully discriminate against chloride (have sufficient selectivity coefficient). Assuming the presence of iodide in urine in the lower end of scale indicating severe IDD (20 µg/ L = 0.16µmol/ L) in conjunction with 10 mmol/ L of chloride maximum selectivity coefficient should be $\log K_{I,Cl}^{pot}$ = -4.85 as calculated using Equation 4.2.[21]

$$logc_{I,LOD} = \frac{1}{2}\log\left(\frac{qR_T}{zI}\sum K_{I,J}^{pot}c_J\right) \qquad (4.2)$$

Where $K_{I,J}^{pot}c_J$ is a product of thermodynamic selectivity coefficient for primary ion I vs. interfering ion J and the concentration of J, R_T is the concentration of ion exchanger in the membrane, z_I is the charge of ion I and q is the parameter that relates diffusion coefficients of primary ion and ion-ionophore complex in water and membrane respectively, and thicknesses of aqueous and organic diffusion layers.

It is here estimated as 0.001 based on realistic assumption of equality of aqueous and organic diffusion layers.[23, 32] $logc_{I,LOD}$ is the concentration of I^- at the detection limit taken for this case to be 0.16 µmol/ L.

However, given the wide variation of concentrations of chloride and iodide in urine, the smaller $\log K_{I,Cl}^{pot}$, the better. Between MC3-DOS and MC3-NPOE membranes, the latter indeed demonstrates better selectivity coefficient. It is noteworthy that it shows significant response to ClO_4^- ion. However perchlorate ions are not generally present in physiological sample; therefore MC3-NPOE membrane is chosen for further studies.

4.3.2 Sensitivity

Upon evaluating selectivity, it is important to establish whether an electrode satisfies sensitivity criteria. In other words, does it demonstrate Nernstian slope and whether the limit of detection can be successfully predicted if electrodes are calibrated in a lab-controlled sample that resembles the real-life sample as closely as possible?

To test for the electrode characteristic of the iodide ISEs in standard solution, three fabricated MC3-NPOE paper ISEs were calibrated by standard addition of series of iodide standards.

Results in figure 4.4 shows the consistency of the electrode fabrication. From this figure, it shows that the average lower limit of detection for the MC3-NPOE electrodes in water without the presence of interfering ions is around $\log_{I} = -6.7$.

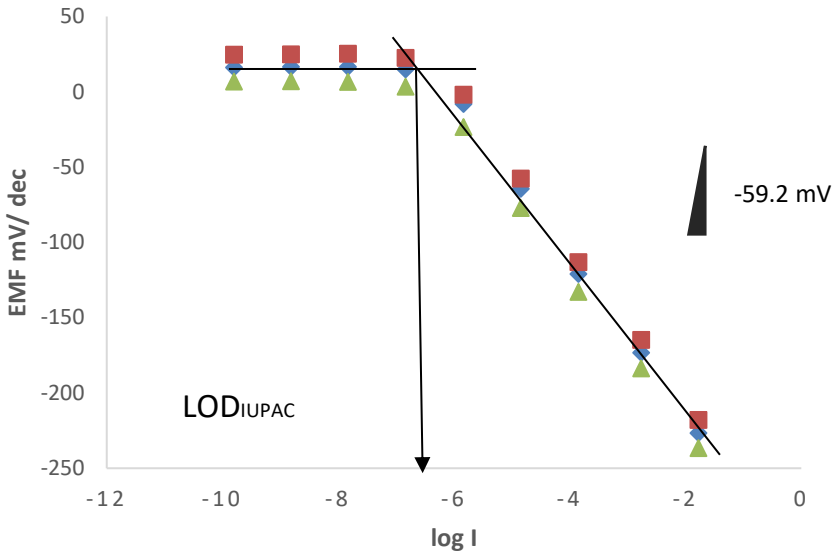

Figure 4.4 The response of three MC3-NPOE electrodes for the calibration of iodide standards in water.

The limit of detection (LOD) for an ion I ($logc_{I,DL}$) can be predicted based on Eq 4.2. Given that AU prepared and used in this work contains 0.29 mol/l of Cl^- and with obtained selectivity coefficient as $\log K_{I,Cl}^{pot}$ = -4.85, expected detection limit is $\log_I$ = -5.1. Figure 4.5 depicts the calibration curve of MC3-NPOE electrode in AU. For clarity reasons, response of only one electrode (ISE#1 from table 4.3) is shown. Experimental data are depicted using points while the line was obtained using Nicolskii-Eisenman equation in equation 4.3 shown below:

$$E_M = E_I^0 + \frac{RT}{z_I F} ln\left(a_I + \sum K_{I,J}^{pot} a_J^{\frac{z_I}{z_J}}\right) \quad (4.3)$$

Where slope obtained using traditionally defined protocol (linear fit of calibration points estimated to be on the Nernstian linear segment of the response curve) was 48

mV/ dec, selectivity coefficient of $\log K_{I,Cl}^{pot}$ = -4.85 and c_J = 0.29 mol/ L. Note that further in the text all calculation based on IUPAC definition of LOD and slope will be referred to as 'point estimate by ISE'.

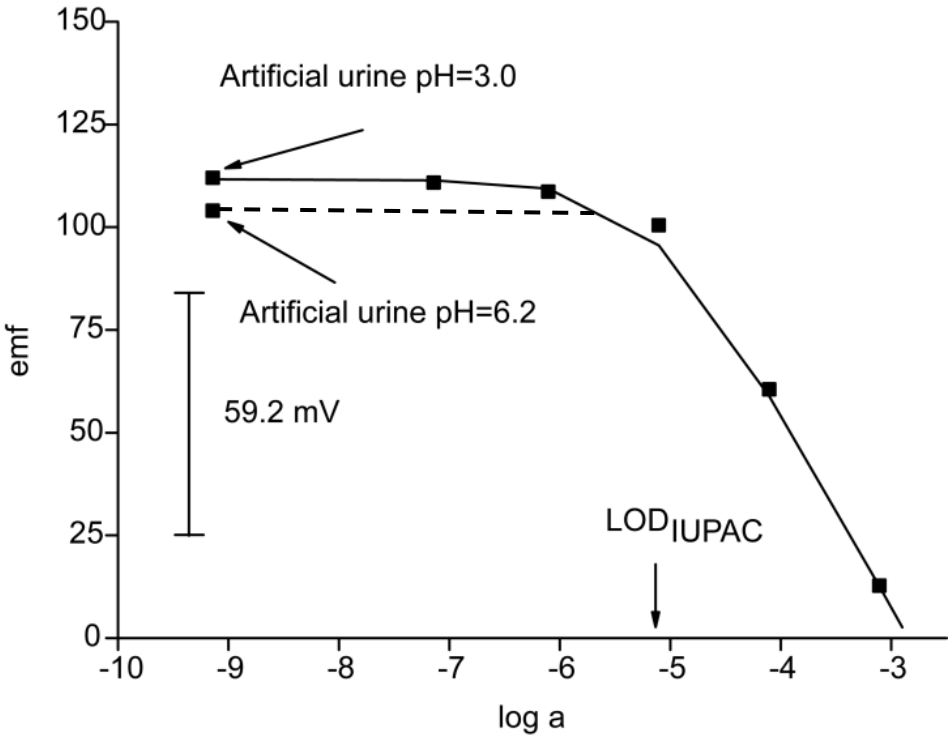

Figure 4.5 Response curve of iodide-selective electrode based on MC3-NPOE as ionophore-plasticizer combination, and 75 mol % of ion exchanger in artificial urine (AU). Acidification of the AU leads to the suppression of the influence of OH^- illustrated by increasing the signal at the base line denoted as ~10^{-9} M iodide.

Table 4.3 shows the slopes and LODs obtained using traditional potentiometric methodology and the Bayesian method. It is interesting to observe that all slopes obtained are sub-Nernstian, with ISE#4 at almost half of theoretical slope of 59.2 mV/ dec; however, the Bayesian model estimates all slopes at almost Nernstian value (more acceptable). The most important benefit of the Bayesian model is that it provides the range of slopes with upper and lower limits. This allows the determination of calibration interval and as a consequence obtaining precisely defined concentration range in which the unknown concentration will fall.[28]

It is worth noting that sub-Nernstian slopes cause bias towards the determination of LOD and provide its unrealistically low value. On the other hand, the Bayesian method by nature returns $LOD_{S/N=3}$. In all cases in table 4.3, the LOD obtained by the Bayesian method is lower by up to half order of magnitude than the ones obtained by IUPAC definition of LOD. This improvement was lower than anticipated. According to figure 4.1 and figure 4.4, improvement of >1.5 orders of magnitude is expected for the iodide electrodes to be able to sense iodide in the urine samples due to selectivity coefficients and the estimated interfering ions deemed present. In summary, the bias due to sub-Nernstian slopes is in part responsible for lower than expected LOD improvements.

More importantly, unrealistically low prediction of noise (<0.1 mV) plays a significant role in the discrepancy of expected and achieved improvement of LOD. Such a low prediction of noise neglects the so called 'ISE noise'. This type of noise and its influence on the LOD is discussed in the section 'Implications'.

Table 4.3. Slopes (in mV/ dec) and limits of detections (mol/ L) obtained using IUPAC's potentiometric definition (point estimate) and the Bayesian method.

ISE#	Slope (mv/ dec)				LOD (mol/ L)	
	Point estimate by ISE (IUPAC)	Bayesian model			Point estimates by ISE (IUPAC)	Bayesian model (S/N=3)
		Estimates	Lower limits	Upper limits		
1	-48.02	-54.0	-66.8	-45.7	-5.1	-5.24
2	-45.51	-52.1	-65.5	-43.5	-5.0	-5.12
3	-44.61	-49.5	-65.1	-42.5	-4.9	-5.20
4	-33.68	-41.0	-65.9	-33.9	-4.8	-4.94
5	-46.78	-51.7	-62.6	-44.6	-4.9	-5.39

4.4 Application in artificial urine

In order to test the integrity of the MC3-NPOE electrode, it was tested in solutions that contained a predetermined concentration of iodide ions. These samples were treated as 'unknown'. The concentrations were chosen to cover both the linear (Nernstian) part of the response curve and curvilinear response around the LOD_{IUPAC}, however, samples #1, #2, and #3 were prepared to be slightly below or just at the LOD_{IUPAC}. For the potentiometric analysis, the method of standard addition was used to determine these concentrations and to determine the error of measurement. In the standard, IUPAC defined approach the EMF values of 'unknown' samples were applied to Equation 4.4[39] and used to determine the concentration of the unknown solutions:

$$C_x = \frac{C_S * \left[\frac{V_S}{V_x + V_S}\right]}{\left[10^{\frac{E_2 - E_1}{m}} - \frac{V_x}{V_x + V_S}\right]} \qquad (4.4)$$

Here, C_x and C_S are concentrations of the unknown sample and the standard respectively, V_x and V_S are volumes of sample and standard solutions, E_1 and E_2 are electrode potentials (mV) of the sample and after the addition of the standard and m is the slope.

In addition, the Bayesian model was used as described by Dillingham et al.[28] Briefly, a non-linear regression based on Bayes' theorem was used to calculate prediction over the entire activity range. The model uses multiple ISEs and poor performing ISEs with wide calibration intervals are automatically down-weighted. Asymmetry in calibration intervals is incorporated into the final calibration interval. All simulations and analyses were based on 4 chains of 75,000 iterations with the first 25,000 iterations discarded, with good convergence diagnostics and low Monte Carlo error throughout. Results

obtained using the two approaches are presented in Table 4.4 and illustrated in figure 4.6.

Table 4.4 Iodide content in artificial urine samples prepared to contain prescribed amount of iodide (actual values). Iodide concentration is measured experimentally and calculated using 'point estimate by ISE' and the Bayesian method.

Sample #	Actual or "unknown" values (mol/ L)	ISE	Bayesian Model		
		Point estimates by ISE (mol/ L)	Estimates (mol/ L)	Lower limits (mol/ L)	Upper limits (mol/ L)
1	-5.30	-4.70±0.14	-4.91	-5.40	-4.57
2	-5.92	-4.63±0.51	-5.09	-8.62	-4.18
3	-4.70	-4.63±0.51	-5.13	-8.65	-4.19
4	-3.30	-3.56±0.33	-3.33	-3.66	-3.07
5	-3.10	-3.07±0.15	-2.95	-3.15	-2.80

As explained in section 4.1, the values obtained here using the 'point estimates by potentiometry' are clearly biased, which is also illustrated in the figure 4.1. Instead of using the actual response curve, the potentiometric measurements are projected at straight line modelled according to Nernstian slope. Consequently, positive bias is introduced and the samples appear to contain higher than real concentration of iodide. However, the Bayesian method returns $LOD_{S/N=3}$ and utilizes the entire response curve. As a consequence, concentrations of iodide in the samples that are at or lower than LOD_{IUPAC} are closer to the true values.

As shown in figure 4.6, the large asymmetry in samples #2 and #3 indicate precision that is generally unacceptable especially in environmental and/or health measurements. This indicates that the definition of LOD should contain the requirement of precision rather than just an arbitrary number. Samples #4 and #5 are in the region defined with Nernstian response and above $LOQ_{traditional}$. While both 'point estimates' and the Bayesian method for samples #4 and #5 return similar values, the Bayesian method returns confidence intervals rather than error bars.

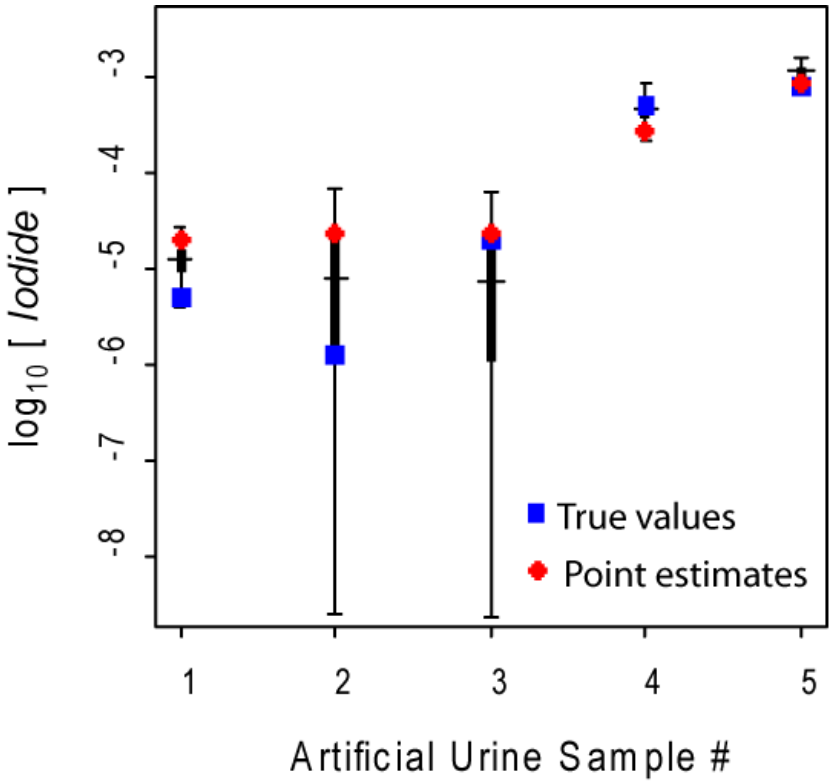

Figure 4.6 Comparison of iodide concentrations in prepared artificial urine samples (blue squares represent the true "unknown" values), experimental results obtained with 'point estimate by ISE' (red diamonds), and midpoints of intervals represent the Bayesian estimates. Error bars indicate 95 % confidence intervals; lower and upper limits are indicated by thick bars.

4.5 Application in human urine

To further test the utility of MCs/NPOE-based electrodes, and test for the closeness of the Bayesian method to standard reference method (ICP-MS), fabricated electrodes were applied for measuring iodide in samples of human urine volunteered by fifteen anonymous individuals that was not pre-treated in any way. The ICP-MS analysis was performed as described above in section 4.2.6. The results obtained from the ICP-MS and the Bayesian method are shown in table 4.5. The results for point estimates by ISE for the samples are excluded from the table as they show similar values are the Bayesian estimates (see figure 4.7). For each sample, the Bayesian model shows estimate derived from its upper limit and lower limit.

Table 4.5 Iodide content in human urine samples determined with MC3/NPOE-based ISEs calculated using 'point estimate by ISE' and the Bayesian method.

Sample #	True values by ICP-MS (mol/ L)	Bayesian model (mol/ L)		
		Estimate	Lower limit	Upper limit
1	-6.48	-4.30	-4.48	-4.10
2	-6.54	-4.45	-4.62	-4.28
3	-6.45	-4.05	-4.25	-3.77
4	-6.44	-4.06	-4.27	-3.81
5	-6.58	-3.88	-4.11	-3.53
6	-6.56	-4.06	-4.29	-3.76
7	-6.70	-4.61	-4.77	-4.43
8	-6.67	-4.19	-4.49	-3.77

9	-6.25	-4.05	-4.26	-3.77
10	-6.70	-4.56	-4.73	-4.38
11	-6.72	-4.42	-4.66	-4.14
12	-6.74	-4.73	-4.88	-4.57
13	-6.33	-4.75	-4.64	-4.22
14	-6.28	-4.74	-5.06	-4.36
15	-6.44	-4.11	-4.30	-3.87

Based on the concentration ranges of iodide and chloride in urine, Zhang et al calculated the required selectivity coefficient to obtain reliable clinical assay results as $\log K_{I,Cl}^{pot} = -6.0$.[19] Reliability here infers values that are above $LOQ_{traditional}$. This immediately excludes any of the electrodes we examined in this work as results in table 4.5 clearly shows almost a difference of two orders of magnitude in the concentrations of iodide measured by the standard reference method (ICP-MS) and the Bayesian estimates. This discrepancy which is majorly as a result of interfering ions present in samples could further be complicated by individual's dietary intake as consumptions of ions, especially chloride vary in different individuals.

However, it was demonstrated here that electrodes with selectivity coefficients inferior to this requirement were still capable of estimating iodide concentration levels that are slightly below $LOQ_{traditional}$ with reasonable reliability. Therefore, the application of Bayesian method can partly, make use of ionophores demonstrating selectivity that were previously considered unacceptable. Rather than going through a significantly huge (and sometimes very expensive) effort to develop new more selective ionophores,

the Bayesian method may still provide opportunity to extend the use of existing ionophores, especially if more studies on improvement of the model are carried out.

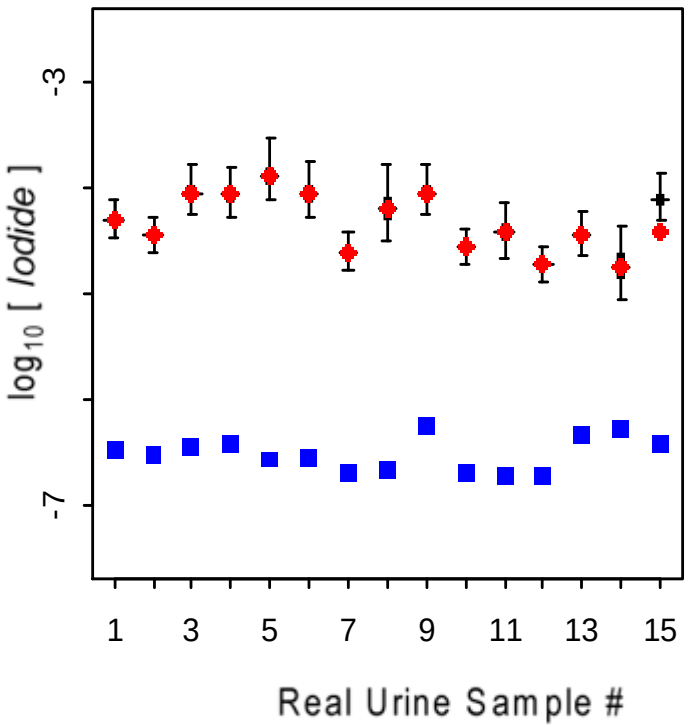

Figure 4.7 Estimations of iodide concentration in human urine samples. Point estimates by ISE are indicated by red diamonds, true values obtained by ICP-MS reference method are represented by blue square, the lower and upper limits are indicated by thick bars, and midpoints of intervals represent the Bayesian estimates. Error bars indicate 95 % confidence intervals.

4.6 Implications of the Bayesian modelling in UI analysis

Large improvements in detection limits of ISEs were expected to lead to their application in a greater spectrum of application fields. While there are certainly interesting examples of penetration in the various application fields in the literature, commercialization of this success is still lagging. We are still waiting for a commercially available device based on ISEs with a significant impact in a field that is outside of clinical analysis of blood electrolytes. Simple and cheap yet very sensitive devices like ISEs would be perfectly suitable in fields requiring routine monitoring and early warning systems such as for example environmental analysis. However, ISEs are still waiting for their big break.

Part of the answer for this problem is perhaps overly optimistic LODs reported so far. While the LOD_{IUPAC} of modern ISEs are certainly very impressive it should not be forgotten that they have been reported for the most optimal samples. Trace level analysis in complex matrixes implies significant interference by other ions ultimately leading to increase of the LOD. Fortunately, the great advances in understanding of the mechanism of response of ISEs equip the experimentator with a tool to correctly estimate the potential utility of ISEs in that matrix.

The more important part of the answer can perhaps be found in the shape of the response curve. The curvature in the response is quite elongated and spans about 2.5 orders of magnitude from the base line to Nernstian segment and $LOQ_{traditional}$ (please see Figure 4.1). IUPAC definition clearly introduces significant bias in this entire section and renders the sensor response for such a large concentration span practically useless. Please note that the LOD and the LOQ are also defined for other instrumental techniques, however they are defined in terms of signal-to-noise ratio which is typically S/N=3 and S/N=10 respectively. According to FDA's guidance for method

validation,[40] deviation from the nominal concentration are not to be larger than 15 % (20 % in the case of standard at the LOQ). Given the logarithmic nature of the ISEs response and the deviations from Nernstian straight line around LOD_{IUPAC}, ISEs can satisfy such requirements only in the region above $LOQ_{traditional}$. Fortunately for ISEs, concentration of blood electrolytes is at least two orders of magnitude higher than LODs of old (non-optimized) ISEs (ppm levels). This offered a chance to overcome issues with the matrix and LOD and still satisfy FDA recommendations. Relying on $LOQ_{traditional}$ as the limit for practical application is quite wasteful of a significant portion of the signal above the baseline and presents a big and costly information loss. If ISEs are to make a significant penetration into new application fields (and markets) it is of utmost importance to utilize the entire response range.

The relative simplicity and self-learning ability of Bayesian method as opposed to traditional nonlinear square fit equations offers fantastic opportunity to address many of the shortcomings of ISEs mentioned here: Benefits of Bayesian method for ISEs can be summarized as, but not limited to, as follows:

1) Allows the use of full calibration curve.

It inherently models the entire response curve and therefore eliminates the bias as introduced with the current IUPAC definition. Consequently, the signal between base line and $LOQ_{traditional}$ is not neglected.

2) Returns LOD as signal-to-noise ratio.

With $LOD_{S/N=3}$ the performance of ISEs can be compared with another instrumental techniques on like-for-like basis.

3) Provides information on precision.

The ability to determine likelihood of concentration of the analyte in the sample being above (or below) previously determined acceptable level is very important for industrial applications and adherence to FDA guidelines for method validation.

What next?

So far we have demonstrated that Bayesian method introduces lots of strength into calibration of ISEs and determination of unknown concentration. However, a keen reader may notice that improvement of LOD from LOD_{IUPAC} to $LOD_{S/N=3}$ are not as great as expected. Instead of improvement of LOD of approximately 1.5 orders of magnitude, improvements of only up to 0.5 orders are observed (table 4.3). The origin of such a discrepancy is most likely in unrealistically low estimate of noise. The noise estimated as ~0.1 mV^1 includes random variations in the potentiometric signal (instrumental noise) but neglects noise originating from random process of ion diffusing through membrane, leaching of membrane components etc (ISE noise). These processes contribute to much larger signal variations (>1 mV).[26] It is therefore imperative to understand and model these processes with a greater degree of understanding.

Another important consequence of defining the ISE noise would be the ability to successfully assign a prescribed acceptable deviation from calibration curve. This will enable the definition of LOD and LOQ that includes the information on precision and ensure the compliance with FDA guidelines.[40]

The attempt to utilize iodide-selective ISE in urine highlighted another important issue. Complex matrixes may contain a large variation of interfering ions. Expectation to develop ISEs with selectivity coefficients that could address the highest possible

concentration of interfering ion may be unrealistic. It would be rather more practical to have an array of ISEs capable of measuring primary and the most significant interfering ion in ‘artificial tongue’ setting. Bayesian method allows excellent possibility to model responses of ISEs in such an array and to thereby greatly improve the utility of ISEs especially in complex matrixes.

4.7 Conclusions

Modern ISEs are an excellent tool for routine monitoring and as early warning system. Diagnosing IDD is dependent on measuring large amount of samples of a population in question. The simplicity, low production cost, large sensing span, and excellent sensitivity of ISEs make them very good candidates as a diagnostic tool for IDD. However, due to the curvilinear response a large section of response curve above the base line is neglected resulting in the requirement for an excellent selectivity coefficient for iodide vs major interfering ions present in urine (e.g. chloride).

The selectivity of two ionophores (MC3 and MC4) in combination with two plasticizers (DOS, NPOE) has been determined in order to find optimal combination with sufficient iodide vs chloride selectivity for the determination of iodide in urine. The membrane with optimal composition has been utilized in the determination of iodide in artificial and real urine.

Bayesian method has been used in order to model and utilize the entire response curve and therefore to reduce the bias in the determination introduced in the currently used methodology defined by IUPAC. The ability of the method to return signal-to-noise ratio resulted in lowering the LOD for up to half order of magnitude compared to classical IUPAC definition. This enabled the determination of iodide at or near the LOD_{IUPAC} with reasonable precision.

References

(1) Bakker, E.; Pretsch, E. Potentiometric Sensors for Trace-Level Analysis. *Trends Analyt Chem* **2005**, *24* (3), 199–207.

(2) Bakker, E.; Pretsch, E. Modern Potentiometry. *Angew Chem Int Ed Engl* **2007**, *46* (30), 5660–5668.

(3) Chumbimuni-Torres, K. Y.; Dai, Z.; Rubinova, N.; Xiang, Y.; Pretsch, E.; Wang, J.; Bakker, E. Potentiometric Biosensing of Proteins with Ultrasensitive Ion-Selective Microelectrodes and Nanoparticle Labels. *J Am Chem Soc* **2006**, *128* (42), 13676–13677.

(4) Chumbimuni-Torres, K. Y.; Wu, J.; Clawson, C.; Galik, M.; Walter, A.; Flechsig, G.-U.; Bakker, E.; Zhang, L.; Wang, J. Amplified Potentiometric Transduction of DNA Hybridization Using Ion-Loaded Liposomes. *Analyst* **2010**, *135* (7), 1618–1623.

(5) De Marco, R.; Clarke, G.; Pejcic, B. Ion-Selective Electrode Potentiometry in Environmental Analysis. *Electroanalysis* **2007**, *19* (19–20), 1987–2001.

(6) Radu, A.; Radu, T.; McGraw, C.; Dillingham, P.; Anastasova, S.; Diamond, D. Ion Selective Electrodes in Environmental Analysis. *Journal of the Serbian Chemical Society* **2013**, *78*, 1729–1761.

(7) Michalska, A. All-Solid-State Ion Selective and All-Solid-State Reference Electrodes. *Electroanalysis* **2012**, *24* (6), 1253–1265.

(8) Cho, H.; Ash) Parameswaran, M.; Yu, H.-Z. Fabrication of Microsensors Using Unmodified Office Inkjet Printers. *Sensors and Actuators B: Chemical* **2007**, *123*, 749–756.

(9) Li, Y.; Li, P. C. H.; Parameswaran, M. (Ash); Yu, H.-Z. Inkjet Printed Electrode Arrays for Potential Modulation of DNA Self-Assembled Monolayers on Gold. *Anal. Chem.* **2008**, *80* (22), 8814–8821.

(10) Diamond, D.; Coyle, S.; Scarmagnani, S.; Hayes, J. Wireless Sensor Networks and Chemo-/Biosensing. *Chem. Rev.* **2008**, *108* (2), 652–679.

(11) Diamond, D.; Lau, K. T.; Brady, S.; Cleary, J. Integration of Analytical Measurements and Wireless Communications--Current Issues and Future Strategies. *Talanta* **2008**, *75* (3), 606–612.

(12) Zuliani, C.; Diamond, D. Opportunities and Challenges of Using Ion-Selective Electrodes in Environmental Monitoring and Wearable Sensors. *Electrochimica Acta* **2012**, *84*, 29–34.

(13) Delange, F.; de Benoist, B.; Pretell, E.; Dunn, J. T. Iodine Deficiency in the World: Where Do We Stand at the Turn of the Century? *Thyroid* **2001**, *11* (5), 437–447.

(14) Hetzel, B. S.; Dunn, J. T. The Iodine Deficiency Disorders: Their Nature and Prevention. *Annual Review of Nutrition* **1989**, *9* (1), 21–38.

(15) Dunn, J. T. What's Happening to Our Iodine? *J Clin Endocrinol Metab* **1998**, *83* (10), 3398–3400.

(16) Sandell, E. B.; Kolthoff, I. M. CHRONOMETRIC CATALYTIC METHOD FOR THE DETERMINATION OF MICRO QUANTITIES OF IODINE. *J. Am. Chem. Soc.* **1934**, *56* (6), 1426–1426.

(17) Dunn, J. T.; Crutchfield, H. E.; Gutekunst, R.; Dunn, A. D. Two Simple Methods for Measuring Iodine in Urine. *Thyroid* **1993**, *3* (2), 119–123.

(18) Mantel, M. Improved Method for the Determination of Iodine in Urine. *Clinica Chimica Acta* **1971**, *33* (1), 39–44.

(19) Zhang, W.; Mnatsakanov, A.; Hower, R.; Cantor, H.; Wang, Y. Urinary Iodine Assays and Ionophore Based Potentiometric Iodide Sensors. *Front Biosci* **2005**, *10*, 88–93.

(20) Nägele, M.; Bakker, E.; Pretsch, E. General Description of the Simultaneous Response of Potentiometric Ionophore-Based Sensors to Ions of Different Charge. *Anal. Chem.* **1999**, *71* (5), 1041–1048.

(21) Ceresa, A.; Radu, A.; Peper, S.; Bakker, E.; Pretsch, E. Rational Design of Potentiometric Trace Level Ion Sensors. A Ag+-Selective Electrode with a 100 Ppt Detection Limit. *Anal. Chem.* **2002**, *74* (16), 4027–4036.

(22) Radu, A.; Meir, A. J.; Bakker, E. Dynamic Diffusion Model for Tracing the Real-Time Potential Response of Polymeric Membrane Ion-Selective Electrodes. *Anal. Chem.* **2004**, *76* (21), 6402–6409.

(23) Duarte, L. T.; Jutten, C.; Moussaoui, S. Ion-Selective Electrode Array Based on a Bayesian Nonlinear Source Separation Method. In *Independent Component Analysis and Signal Separation*; Adali, T., Jutten, C., Romano, J. M. T., Barros, A. K., Eds.; Lecture Notes in Computer Science; Springer Berlin Heidelberg, 2009; pp 662–669.

(24) Hibbert, D. B.; Armstrong, N. An Introduction to Bayesian Methods for Analyzing Chemistry Data. *Chemometrics and Intelligent Laboratory Systems* **2009**, *2* (97), 211–220.

(25) Lau, K.-T.; Guo, W.; Kiernan, B.; Slater, C.; Diamond, D. Non-Linear Carbon Dioxide Determination Using Infrared Gas Sensors and Neural Networks with Bayesian Regularization. *Sensors and Actuators B: Chemical* **2009**, *136* (1), 242–247.

(26) Dillingham, P. W.; Radu, T.; Diamond, D.; Radu, A.; McGraw, C. M. Bayesian Methods for Ion Selective Electrodes. *Electroanalysis 24*, 316–324.

(27) Dillingham, P. Ion selective electrodes | Calibration | Bayesian http://turing.une.edu.au/~pdilling/calibration.html (accessed Oct 9, 2018).

(28) T. Nham, *Analysis of urine and seawater samples by ultrasonic nebulization with a high resolution ICP spectrometer*, Agilent Technologies, 1992.

(29) Radu, A.; Peper, S.; Bakker, E.; Diamond, D. Guidelines for Improving the Lower Detection Limit of Ion-Selective Electrodes: A Systematic Approach. *Electroanalysis* **2007**, *19* (2–3), 144–154.

(30) Badr, I. H. A.; Diaz, M.; Hawthorne, M. F.; Bachas, L. G. Mercuracarborand "Anti-Crown Ether"-Based Chloride-Sensitive Liquid/Polymeric Membrane Electrodes. *Anal. Chem.* **1999**, *71* (7), 1371–1377.

(31) Yang, X.; Knobler, C. B.; Hawthorne, M. F. "[12]Mercuracarborand-4", the First Representative of a New Class of Rigid Macrocyclic Electrophiles: The Chloride Ion Complex of a Charge-Reversed Analogue of [12]Crown-4. *Angewandte Chemie International Edition in English* **1991**, *30* (11), 1507–1508.

(32) Ceresa, A.; Qin, Y.; Peper, S.; Bakker, E. Mechanistic Insights into the Development of Optical Chloride Sensors Based on the [9]Mercuracarborand-3 Ionophore. *Analytical chemistry* **2003**, *75*, 133–140.

(33) Malon, A.; Radu, A.; Qin, W.; Qin, Y.; Ceresa, A.; Maj-Zurawska, M.; Bakker, E.; Pretsch, E. Improving the Detection Limit of Anion-Selective Electrodes: An Iodide-Selective Membrane with a Nanomolar Detection Limit. *Anal. Chem.* **2003**, *75* (15), 3865–3871.

(34) Bakker, E. Determination of Unbiased Selectivity Coefficients of Neutral Carrier-Based Cation-Selective Electrodes. *Anal. Chem.* **1997**, *69* (6), 1061–1069.

(35) Bayer, M. J.; Jalisatgi, S. S.; Smart, B.; Herzog, A.; Knobler, C. B.; Hawthorne, M. F. B-Octamethyl-[12]Mercuracarborand-4 as Host for "Naked" Fluoride Ions. *Angewandte Chemie* **2004**, *116* (14), 1890–1893.

(36) Gethke, K.; Herbst, H.; Montag, D.; Bruszies, D.; Pinnekamp, J. Phosphorus Recovery from Human Urine. *Water Practice and Technology* **2006**, *1* (4).

(37) Yabu, Y.; Miyai, K.; Hayashizaki, S.; Endo, Y.; Hata, N.; Iijima, Y.; Fushimi, R. Measurement of Iodide in Urine Using the Iodide -Selective Ion Electrode. *Endocrinol Japon* **1986**, *33* (6), 905–911.

(38) Yabu, Y.; Miyai, K.; Endo, Y.; Hata, N.; Iijima, Y.; Hayashizaki, S.; Fushimi, R.; Harada, T.; Nose, O.; Kobayashi, A. Urinary Iodide Excretion Measured with an Iodide-Selective Ion Electrode: Studies on Normal Subjects of Varying Ages and Patients with Thyroid Diseases. *Endocrinol. Jpn.* **1988**, *35* (3), 391–398.

(39) NICO2000. Standard & Sample Addition Methods for Ion Selective Electrodes http://www.nico2000.net/datasheets/staddl.html (accessed Oct 9, 2017).

(40) Tiwari, G.; Tiwari, R. Bioanalytical Method Validation: An Updated Review. *Pharm Methods* **2010**, *1* (1), 25–38.

Chapter 5 Concluding remarks and future suggestions

Even though solid contact electrodes were suggested, and has successfully utilized as replacement for liquid-contact electrodes with the view to minimising transmembrane fluxes, early days solid-contact ISEs still suffered from poor potential stabilities, giving rise to loads of transduction mechanism. Simple and low cost polymeric ion-selective electrode fabricated herein in this thesis using household materials have proved to be robust for routine measurements of analytes in different samples. Surprisingly, paper electrodes based on graphite, mechanically drawn unto acetate papers using household pencils showed great potential stability even without the use of any transducer layer. This has opened the door to for its uses in routine monitoring of important nutrients in the environment which could prove dangerous to public health.

With the cost of fabrication significantly down to small proportion compared to most standard techniques, it is even more imperative to encourage non-science personnel to show interest in electrode designing, so they can utilise these cheap sensors for even more day-to-day easy analysis, like monitoring level of physiological species.

The concept of minimising per sample or analysis cost was further evaluated by attempts to utilize the traditional electrode (ISE) response, which mostly carries a caveat of impractical IUPAC limit of detection, especially when used in most real life measurement of trace ions. Improvements in accuracy of estimated ammonium and nitrate measured in soil and water samples, showed promising application of the Bayesian method.

However, due to averagely acceptable results from the non-linear Bayesian approach tested for iodide in human samples, it was concluded more advanced improvements in

materials/ components designing, and synthesis can only complement non-classical approach.